CHALMERS

Development of a 3-cylinder Gasoline Engine Concept

Master's Thesis in Automotive Engineering

BJÖRN JONSSON

DANIEL LUNDAHL

Department of Applied Mechanics
Division of Combustion

CHALMERS UNIVERSITY OF TECHNOLOGY
Göteborg, Sweden 2013

Master's thesis 2013:38

MASTER’S THESIS IN AUTOMOTIVE ENGINEERING

Development of a 3-cylinder Gasoline Engine Concept

BJÖRN JONSSON

DANIEL LUNDAHL

Department of Applied Mechanics
Division of Combustion

CHALMERS UNIVERSITY OF TECHNOLOGY

Göteborg, Sweden 2013

Development of a 3-cylinder Gasoline Engine Concept

BJÖRN JONSSON

DANIEL LUNDAHL

© BJÖRN JONSSON, DANIEL LUNDAHL, 2013

Master's Thesis 2013:38
ISSN 1652-8557
Department of Applied Mechanics
Division of Combustion

Chalmers University of Technology
SE-412 96 Göteborg
Sweden
Telephone: + 46 (0)31-772 1000

Cover:
Picture showing crankshaft and pistons of a 3-cylinder engine. (Reulein, C., Schünemann, E., Schwarz, C., Wetzel, M., (2013), *Thermodynamics of the BMW Three-cylinder Engine*, MTZ worldwide Edition: 2013-05 [Note: Edited by Authors]

Department of Applied Mechanics
Göteborg, Sweden 2013

Development of a 3-cylinder Gasoline Engine Concept

Master's Thesis in *Automotive Engineering*
BJÖRN JONSSON
DANIEL LUNDAHL
Department of Applied Mechanics
Division of Combustion

Chalmers University of Technology

ABSTRACT

The master thesis is performed on request by Volvo Car Corporation (VCC) with focus on evaluating if a 3-cylinder engine could replace a mid- to high performance 4-cylinder engine. The developed 3-cylinder engine concept is compared to a benchmark 4-cylinder engine provided by VCC with respect to steady state performance and fuel consumption as well as transient response (Time-To-Torque). The 3-cylinder engine model is developed, tested and evaluated with GT-Power but it has not been fully validated with test-rig data. The engine concept is developed from a 2.0 litre 4-cylinder SI engine where one cylinder has been removed to create a 1.5 litre 3-cylinder SI engine, which is boosted with a single-scroll turbocharger. Several technologies are investigated based on a literature study with the aim of reducing the fuel consumption and utilize synergistic effects, i.e. the investigated technologies are meant to have the possibility of being combined. Technologies that are evaluated are different turbocharger set-ups, Fully Variable Valve Train (FVVT), Two-Stage Valve Lift (TSVL), Dual Individual Cam Phasing (DICP), Integrated Exhaust Manifold (IEM) and Cylinder Deactivation.

A comparison of the 4-cylinder engine with the 3-cylinder concept engine at different part load points reduced the fuel consumption of the 3-cylinder engine by 6-14%. The 3-cylinder engine was evaluated at 3bar IMEP at 2000rpm with TSVL and FVVT for early intake valve closing. The reduction in fuel consumption was 4.6% and 6% respectively. At the same part load point, cylinder deactivation on the 3-cylinder engine reduced the fuel consumption by 17.7% and 23.5% compared to the 3- and 4-cylinder engine respectively, only equipped with DICP.

Two different turbines for the single-scroll turbocharger have been evaluated which both fulfils the performance targets. The smaller turbine showed high levels of backpressure, and therefore an alternative with limited backpressure was presented. The turbine with limited backpressure resulted in 1.6% lower peak power compared to the benchmark 4-cylinder engine and the 50mm turbine was able to produce 3.1% higher peak power. Both turbines reached the torque knee 300rpm later compared to the benchmark engine. The 45mm turbine has the best transient response and matches the benchmark engine if the engine speed is increased by 300rpm.

An Integrated Exhaust Manifold (IEM), which particularly suits a 3-cylinder engine, has been evaluated on the concept engine. The IEM shows improvements in decreasing the exhaust gas temperature which reduces the need of mixture enrichment to decrease the temperatures at full load.

Key words: Downsizing, 3-cylinder engine, technology evaluation, GT-Power

Utveckling av ett 3-cylindrigt bensinmotorkoncept

Examensarbete inom *Automotive Engineering*
BJÖRN JONSSON
DANIEL LUNDAHL
Institutionen för tillämpad mekanik
Avdelningen för Förbränning

Chalmers tekniska högskola

SAMMANFATTNING

Examensarbetet är utfört på begäran av Volvo Personvagnar med fokus på att utvärdera om en 3-cylindrig motor kan ersätta en medel- till högprestanda 4-cylindrig motor. Den 3-cylindriga konceptmotorn är jämförd med den 4-cylindriga referensmotorn tillhandahållen av Volvo Personvagnar med avseende på stationär prestanda och bränsleförbrukning samt transient respons. Den 3-cylindriga motormodellen är utvecklad, testad och utvärderad med GT-Power, dock är modellen är inte fullt validerad gentemot test-rigg data. Motorkonceptet är utvecklat från en 2.0 liters 4-cylindrig bensinmotor varav en cylinder har tagits bort för att skapa en 1.5 liters 3-cylindrig motor som är överladdad med en single-scroll turbo. Flera tekniker har undersökts som är baserade på en litteraturstudie med målet att minska bränsleförbrukningen och utnyttja synergieffekter, d.v.s. att teknikerna skall fördelaktigt kunna kombineras. De tekniker som är utvärderade är olika turbokonfigurationer, fullvariabel ventilstyrning av insugskam, två-stegs profillyft av insugskam, kamfasning på insug- och avgaskam, integrerat grenrör i topplocket samt cylinderdeaktivering.

Vid jämförelse av den 4-cylindriga motorn och det 3-cylindriga motorkonceptet för olika dellastpunkter var bränsleförbrukningen för den 3-cylindriga motorn reducerad från 6% till 14%. Den 3-cylindriga motorn var utvärderad för 3 bar IMEP vid 2000 rpm med två-stegs profillyft av insugskammen och fullvariabelt ventilsystem för tidig stängning av insugsventilerna. Minskningen av bränsleförbrukningen var 4.6% respektive 6%. För samma dellastpunkt är även cylinderdeaktivering genomförd för den 3-cylindriga motorn. Bränsleförbrukningen minskade med 17.7% och 23.5% relativt den 3- och 4-cylindriga motorn.

Ett integrerat grenrör i topplocket utvärderades på konceptmotorn vilket är speciellt fördelaktigt på en 3-cylindrig motor då avgaspulserna inte stör varandra. Med det integrerade grenröret sänks avgastemperaturen vilket leder till att luft/bränsleblandningen kan vara närmare stökiometrisk blandning vid maximal effekt.

Nyckelord: Downsizing, 3-cylindrar, teknikevaluering, GT-Power

Contents

Preface

In this study, a 3-cylinder concept engine has been developed with the aim of replacing a mid- to high performance 4-cylinder engine. The project is a master thesis carried out by Björn Jonsson and Daniel Lundahl. Professor Ingemar Denbratt has been the examiner of the thesis work who works at the Division of Combustion at Chalmers University of Technology. We like to thank Ingemar Denbratt for his advices and thoughts during the project.

All simulation work has been carried out at Volvo Car Corporation (VCC), located in Torslanda, Göteborg. The master thesis was carried out at the Engine CAE department.

We would like to specially thank Stefan Bohatsch who was our supervisor at VCC, who learned us a lot about engine development and helped us through the project. We would also like to thank Ragnar Burenius (VCC), David Willermark (AVL), Karl Wågman (AVL) and Joel Ohlsson (AVL) for their guidance during the project.

Göteborg, June 2013

Björn Jonsson and Daniel Lundahl

Notations

ABDC	After Bottom Dead Center
ATDC	After Top Dead Center
BBDC	Before Bottom Dead Center
BDC	Bottom Dead Center
BMEP	Brake Mean Effective Pressure
BSFC	Brake Specific Fuel Consumption
BTDC	Before Top Dead Center
CAD	Crank Angle Degree
CE	Combustion Efficiency
CI	Compression Ignition
CR	Compression Ratio
DI	Direct Injection
DICP	Dual Individual Cam Phasing
EGR	Exhaust Gas Recirculation
EIVC	Early Intake Valve Closing
EVC	Exhaust Valve Closing
EVO	Exhaust Valve Opening
FVVT	Fully Variable Valve Train
GDI	Gasoline Direct Injection
HLC	High Lift Cam
iEGR	internal Exhaust Gas Recirculation
IEM	Integrated Exhaust Manifold
IMEP	Indicated Mean Effective Pressure
ISFC	Indicated Specific Fuel Consumption
IVC	Intake Valve Closing
IVO	Intake Valve Opening
LIVC	Late Intake Valve Closing
LLC	Low Lift Cam
NEDC	New European Driving Cycle
NMEP	Net Mean Effective Pressure
NVH	Noise, Vibration and Harshness
PLP	Part Load Point
PMEP	Pumping Mean Effective Pressure
SI	Spark Ignition
TDC	Top Dead Center
TTT	Time-To-Torque
VCC	Volvo Car Corporation
WOT	Wide Open Throttle
WOW	Wide Open Wastegate

1 Introduction

This report investigates if it is beneficial to replace a 4-cylinder mid-high performance engine with a 3-cylinder engine, regarding fuel consumption and performance.

1.1 Background

In order to meet the future legislations regarding fuel consumption, the car manufacturers are developing supercharged, downsized engines in order to reduce fuel consumption and maintain performance.

Volvo Car Corporation (VCC) has stated that they only will use 4-cylinder engines from the Volvo Environmental Architecture (VEA) in the near future. The trend of downsizing has resulted in that OEMs have extended their engine line-up, offering 3-cylinder engines for small- to medium-sized passenger cars that have proven to be a successful concept. The 3-cylinder engines are often developed in order to replace the entry-level performance 4-cylinder engines, i.e. further downsizing. This is made due to the potential of improvements in e.g. fuel consumption, weight, cost and packaging. BMW are launching a new 3-cylinder engine that is able to replace the mid-high performance 4-cylinder engines of today.

Recently a new legislation has been approved on the Chinese market meaning that engines with a swept volume below 1.6 litre receives a tax reduction (Xinhua News Agency - CEIS, 2012), which is another reason for VCC to develop a 3-cylinder engine. With respect to manufacture aspects, there is an advantage of using the same cylinder geometry as the existing 2.0 litre engine architecture. Then it is possible to eliminate one cylinder and create a 1.5 litre engine and use many carry-over parts.

2 Objectives

VCC is interested in knowing of how to best achieve the same performance and driveability with a 3-cylinder gasoline engine as their mid/high performance 4-cylinder gasoline engine. The investigation shall also include a comparison of the fuel consumption and a recommendation of design parameters and a technology proposal with synergy effects. The investigation of this thesis will focus on:

- Creating GT-Power models of possible engine configurations
- Investigate where the “line” between a high-tech, rather expensive 3-cylinder engine is compared to a cheap, low-tech 4-cylinder engine
- Investigate if there are synergies between different technologies that are advantageous for a 3-cylinder engine versus a 4-cylinder engine

2.1 Tasks and Questions

To achieve a thorough investigation of the objectives, these have been broken down into three areas; Background, Simulation and analysis and Results.

2.1.1 Background

- Which technologies are commonly combined in 3-cylinder engines?
- Are there any technologies especially suited for 3-cylinder engines?
- Which are the main differences of 3- and 4-cylinder engines regarding technologies and characteristics?
- Which are the challenges and advantages of a 3-cylinder engine?
- Investigate methods of deciding a suitable turbocharger

2.1.2 Simulation and Analysis

- Which simplifications are made in the GT-Power model?
- How does the FKFS combustion model work and why is it used?
- How well do the GT-Power model correspond to the real system?

2.1.3 Results

- How is the driveability and performance of the 3-cylinder engine compared to the benchmark 4-cylinder engine?
- Are there any obvious synergies of technologies in the 3-cylinder engine concept?

2.2 Aim

The aim of this thesis is to deliver a 3-cylinder engine concept with proposed technologies that has the same performance and driveability as the benchmarked 4-cylinder engine.

2.3 Scope

A GT-Power model is provided to the thesis based on a turbocharged 4-cylinder gasoline engine from VCC of which one cylinder has been removed in order to create a basis for the 3-cylinder engine concept.

The GT-Power model will be modified in order to optimise the performance and driveability. Further, a new turbocharger has to be adapted to the engine as well as adding and evaluating different technologies that are of interest. The result will be based on computer simulations in GT-Power and no prototypes will be made.

The combustion model that is used is developed by Forschungsinstitut für Kraftfahrwesen und Fahrzeugmotoren Stuttgart (FKFS) and shall not be changed or modified since it is validated by VCC. The thesis will be limited to only investigate 3- and 4-cylinder inline spark-ignited (SI) 4-stroke gasoline engines.

3 Theory

This chapter is written in order to give a basic theory background of the subjects focused on in the report.

3.1 Downsizing

Downsizing means that the swept volume is reduced in order to make the engine operate at a higher load. The displacement is highly affecting the maximum work per cycle and thereby the torque output of an internal combustion engine (Heywood, 1988). In order to obtain the same performance from a downsized engine as from a full-size engine the Brake Mean Effective Pressure (BMEP) can be increased by for example supercharging. The corresponding BMEP for an engine with the same output is calculated by equation (3.1).

$$BMEP = \frac{2\pi T_e}{V_d}\ [bar] \rightarrow T_e = \frac{BMEP \cdot V_d}{2\pi}\ [Nm]$$

$$Since\ T_{e,1} = T_{e,2} \rightarrow \quad \frac{BMEP_1 \cdot V_{d,1}}{2\pi} = \frac{BMEP_2 \cdot V_{d,2}}{2\pi}$$

$$\rightarrow \quad BMEP_2 = \frac{BMEP_1 \cdot V_{d,1}}{V_{d,2}}\ [bar] \tag{3.1}$$

This results in higher engine efficiency due to lower pumping losses from throttling, and lower friction losses due to smaller in-cylinder area. A smaller engine also has a lower weight on its internal parts and block, which reduces the inertia of the engine as well as lowering the overall weight of the vehicle. If the engine is downsized to a very small volume, more supercharging is needed. Knocking issues might also appear due to high cylinder pressures. This requires stronger engine components and larger intercoolers, which will add cost and weight. It is therefore truly that the reduction will slow down in the future (Stephenson, 2009).

3.1.1 Engine Load

Recent advances in gasoline engine development have shown that a downsizing of more than 35% gives a fuel consumption reduction of more than 20%. This was established by Mahle (2012), on their 3-cylinder 1.2 l turbocharged engine, producing 163 hp. They have also an experimental project engine downsized by 50% that has reduced the CO_2 emissions by more than 30% (Mahle, 2012).

3.2 3- vs. 4-Cylinder Engines

A major advantage of a 3-cylinder engine is that it reduces over all weight and size compared to engines with the same performance with more cylinders. The obvious alternative to a 3-cylinder engine for a normal sized passenger car would be a 4-cylinder engine. According to Kirwan (2009), there are some areas of which a 3-cylinder engine is particularly beneficial compared to a 4-cylinder engine with the same power output. These are for example improved engine breathing at full load (improved scavenging), reduced heat transfer area, reduced quench layer and crevices as well as reduced friction. The downside of a 3-cylinder engine is increased NVH and balancing problems.

3.2.1 Synergistic Technologies of 3-Cylinder Engines

In order to develop a successful engine, the technologies chosen have to interact well together in a way that maximizes the output. Coltman et al (2011) started a project named “Project Sabre” of which the aim was to find synergistic technologies for a 3-cylinder engine to achieve low fuel consumption. The technology content was following:

- Switchable Valvetrain System on the intake camshaft
- Twin Cam Phasers
- Direct Injection with homogeneous air/fuel mixture
- Single-stage turbocharger
- Cylinder head with Integrated Exhaust Manifold (IEM)

In the Sabre project, stratified operation was discussed which could be an alternative to a switchable valvetrain system in order to decrease the throttling losses. Though, stratified operation requires expensive aftertreatment systems and piezo-fuel injectors and was therefore not prioritized. According to Coltman et al (2011), an IEM is especially suited for a 3-cylinder engine due to the 240 CAD firing interval (see Chapter 3.7)

3.2.2 Scavenging

In Direct Injected (DI) turbocharged engines, scavenging is used to improve low-end-toque. At low engine speed and high load, it is advantageous to utilize large valve overlap to let fresh air from the intake manifold blow through the cylinder in order to speed up the turbine wheel. The turbocharger is then able to increase the boost pressure at low engine speed more quickly. The amount of scavenging available is highly improved on DI engines compared to port-injected engines. On DI engines, the fuel is injected into the cylinder after the exhaust valves closes and no unburned fuel will enter the exhaust system. At high load and engine speed, the pressure difference will increase between the intake and exhaust system, which is affecting the scavenging efficiency. A 3-cylinder engine ignites every 240 CAD, i.e. the exhaust valves are only open for one cylinder at the same time during the gas-exchange process. A 4-cylinder engine ignites every 180 CAD and when the exhaust valves opens near TDC for one cylinder, the exhaust valves opens at BDC for another cylinder. A 3-cylinder engine is therefore more advantageous regarding scavenging efficiency (Kirwan, 2009).

On boosted engines with three or less cylinders, the benefits of valve overlap also means that even if the average back pressure is higher (moderately) than the boost pressure, the engine could still have scavenging benefits. This means that the scavenging process of removing residuals from the combustions chamber is improved which reduces the knock propensity and increases torque output since the knock limit is increased (Schernus, Dieterich, Nebbia, Sehr et al, 2011). Further, the 3-cylinder engine has the advantage of not need a pulse-divided exhaust manifold to separate the exhaust pulses which mean that the manifold design could be kept short. This improves throttle response since the turbine could be located closer to the exhaust port (Coltman, 2011).

3.2.3 Balancing problem

According to Heisler (1999), both the primary and secondary forces so called dynamic shake are completely balanced out. The problem with an inline 3-cylinder engine is instead rocking forces which cannot be balanced out. Heisler (1999) claims that the cyclic torque is sufficiently smooth on an inline 3-cylinder engine to be a competitor to the 4-cylinder engines in terms of balancing. These advantages of the 3-cylinder engine are savings in engine weight and length, reduced reciprocating and rotational drag and hence better fuel consumption (Heisler, 1999). According to Coltman et al (2011), the rocking forces could be addressed by using a counter-rotating balance shaft. The 3-cylinder engine could have a firing order of either 1-3-2 or 1-2-3 with 240 degrees apart. The basic design of an inline 3-cylinder engine is seen below in *Figure 1* (AutoZine, 2013).

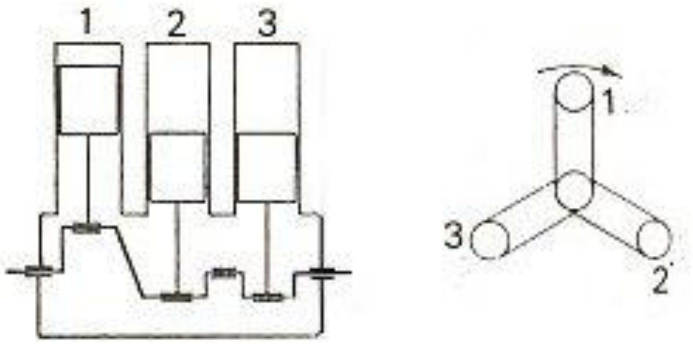

Figure 1 - Layout of a 3-cylinder engine (AutoZine, 2013)

3.3 Three Cylinder Engines Today

There are two three cylinder engine configurations today that have similar size and performance as the targets for this project. These are the BMW B38 1.5liter and Mahle 1.2liter technology demonstrator.

3.3.1 The BMW B38

BMW are developing a three cylinder engine based on their 500cc design commitment (Davis, 2013). According to Davis (2013) BMW has confirmed that the 500cc cylinder has the ideal balance at the given performance level with respect to the better acoustics and vibrations of a smaller displacement and the higher efficiency and reduced friction of a larger cylinder. The geometry will be used on the future 3-, 4- and 6-cylinder engines and this means that production cost are reduced since the same tools and production lines can be used for all engines. The engine uses BWMs fully variable valve-lift system (Valvetronic) on the intake side together with dual individual cam phasers (double VANOS) and turbocharging. The engine tested by Davis (2013) was equipped with a single twin-scroll turbocharger, but according to BWM the B38 engine will have a variable geometry turbine which will produce boost pressures between 1.5-2.0bar. With this setup the B38 engines will produce between 40 and 75PS per cylinder, hence 120-225PS in total for the engine. The tested engine produced 270Nm at 1500rpm and 175PS at 5000rpm with a boost pressure of 14.5psi (1bar). BMW will not utilize cylinder deactivation because they do not believe that the on/off strategy will produce the same fuel efficiency as with their sophisticated Valvetronic-system. The use of stratified direct fuel injection is also something that they have rejected because the engines according to them must be able to use a wide range of fuel blends around the world. Since stratified injection demands highly refined fuel blends this limits the possible market of sales and the technology was therefore rejected (Davis, 2013).

3.3.2 The Mahle Technology Demonstrator

Mahle has developed a 3-cylinder engine to demonstrate the possibilities of downsizing and suitable technologies according to Korte, Lumsden, Fraser and Hall (2010). The engine has a displaced volume of 1.2liter and was developed to match a naturally aspirated 2.4liter engine, hence demonstrating a 50% downsizing. Mahle has equipped the engine with gasoline direct injection (GDI) and a two-stage turbocharger system with one low-pressure and one high-pressure turbocharger. According to Korte et al (2010), this turbocharger configuration is used for improved transient response and enabling low and high engine speed torque. The engines peak cylinder pressure is 140bar and 286Nm (30bar BMEP) at 3000rpm with a maximum boost pressure of 2.7bar which results in a peak power of 144kW (196PS) at 6000rpm. The engine is developed to run at high levels of EGR and can achieve up to 15% EGR at the high power conditions. The engine uses switchable followers design to actuate the variable valve lift. It also has high tumble inlet ports to create the charge motion necessary for running at high BMEP. To avoid knocking the ignition is moved forward to reduce the cylinder pressure, but this leads to large pulsating exhaust gases which in combination with large valve overlaps used, the maximum temperature of the exhaust gases is limited to 1020^{o}C. The engine Brake Specific Fuel Consumption (BSFC) at the part load point 2000rpm and 4bar BMEP is 285g/kWh. This resulted in a total fuel consumption reduction of 30% in the NEDC compared to the 50% larger engine (Korte et al, 2010).

3.4 Residual Gas Fraction

The residual gas fraction in the cylinder is affecting the engine performance, emissions and efficiency. According to Heywood (1988), the residual gas fraction is a function of inlet and exhaust manifold pressure, engine speed, compression ratio and valve timing. The residual gas fraction (x_r) is defined as the residual mass that is left from the previous cycle (m_r) divided by the fresh charge trapped in the cylinder (m_c), see equation (3.2).

$$x_r = \frac{m_r}{m_c}\ [-] \tag{3.2}$$

According to Heywood (1988), common levels of residual fraction in a SI engine is about 20% at part load to 7% at full load.

In SI engines, it is usual to dilute the fresh mixture by enable internal Exhaust Gas Recirculation (iEGR) in order to decrease the oxygen content in the air-fuel mixture, which results in decreased BSFC and reduced exhaust gas temperatures. This is thanks to lower pumping work, reduced heat losses to the cylinder walls and reduced high-temperature dissociation, i.e. more of the chemical energy of the fuel can be converted to sensible energy. Though, a result of the decreased combustion rate and temperature, the combustion will become more instable (with increasing EGR), therefore an SI engine can only tolerate between 15-30% EGR during part-load throttle conditions (Heywood, 1988).

3.5 Modelling

This chapter explains the combustion model used.

3.5.1 Predictive Combustion Models

The advantage of predictive engine models is they are able to simulate an entire operating map with often only a single set of parameters. If using a non-predictive model, a high number of measurement points is needed due to their limitation of estimate the surroundings around a measurement point (Operating instructions for the GT-Power expansion, 2013).

3.5.2 Quasi-Dimensional Model (QDM)

The FKFS combustion model is a Quasi-Dimensional Model (QDM) which is a thermodynamic model, based on the equations of energy conservation. The QDM divides the combustion chamber in two zones of burned- and unburned gases. The unburned zone consists of a homogeneous mixture of air, fuel and residual gases. During combustion, the flame front is described between the two zones of burned- and unburned gases where new unburned gas constantly is captured by the flame front which is referred to as the penetration zone. When describing the penetration zone, a simplification is made in the FKFS combustion model by assuming homogeneous isotropic turbulence. This means that the flow field has an equal statistic distribution and the average turbulence fluctuation velocity is equal in all coordinate directions (Operating instructions for the GT-Power expansion, 2013). In the flame propagation model, the flame front is added to the unburned zone, hence the two-zone computation. In the simulation, the spark plug should not be located exactly in the middle of the combustion chamber but instead use an offset of about 3-4 mm. Due to the hemispherical flame propagation, the flame will increase fast until it hits the cylinder walls and without using an offset for the spark plug the flame speed would decrease very rapidly. In the case of no offset, sharp, unrealistic burn rates will appear which not correspond to the reality where the flame propagation never is spherical (M.Grill, T. Billinger, M. Bargende, 2006).

3.5.3 Turbulence Model

In a QDM, the turbulence is one of the most important variables to be calibrated correctly. A difficulty when creating a turbulence model is how to represent the turbulence in the cylinder after Inlet Valve Closing (IVC), referred to as the tumble breakdown. Today, there has been no successful method of representing the tumble breakdown and therefore the turbulence differential equation is solved from 20 CAD before firing TDC and before that, the turbulence is given a fixed value. The tumble breakdown is not solved with differential equations that instead are given a starting value. The subsequent values that the zero-dimensional turbulence model is compared with are based on turbulence gradients from CFD calculations (Operating instructions for the GT-Power expansion, 2013).

3.5.4 Knock Models

Knock is an undesired combustion phenomena which is influenced by several parameters such as; compression ratio, ignition timing, charging pressure, temperature etc. The appearance of knock is necessary to control because it can cause severe engine damage due to high local pressures caused by rapid release of chemical energy (Heywood, 1988).

Within the GT-Power model provided by VCC, three different knock models are available; *Franzke*, *Worret* and *FKFS* own developed knock model. The Franzke knock model was developed in the 1980's and is considered as a rather simplified knock model compared to Worret and FKFS. The Franzke knock model was later refined by Worret in year 2002, which is an alternative knock model to FKFS (Operating instructions for the GT-Power expansion, 2013).

The knock model developed by Franzke is based on the "Franzke integral" that estimates the probability if knock will occur. The Franzke model does not use any parameters that are calibrated with a test engine. The Worret knock model is simulated in parallel to the Franzke knock model which is based on two variables. As Franzke, Worret uses an integral that predicts knock but only integrates up to 75% burn point. The second variable used by the Worret knock model is called the "critical pre-reaction state", which is referred to as the limit when knocking starts. The model is calibrated to the test-bench engine that the model is created for. The test engine is operated on the knock limit at engine loads where the probability of knock is likely to occur at between 10-15%, which is used as a reference point. The Worret knock model is calibrated to the reference operating point in terms of knock frequency and knock angle (the knock angle is the same as the crankshaft angle when knocking starts). When the calibration is made, the knock model can variate the critical pre-reaction state as a function of the 75% burn point and compare it with the reference operating point (Operating instructions for the GT-Power expansion, 2013).

The knock model developed by FKFS predicts the knock tendency with a pre-reaction integral that uses the temperature and pressure history as well. The model also accounts for hot-spots and turbulence in the end gas area (Operating instructions for the GT-Power expansion, 2013).

3.6 Boosting the Engine

According to Hiereth and Prenninger (2007), the objective of supercharging is to increase the density of the working medium (air or air-fuel mixture) with the help of a suitable system before entering the cylinder i.e. pre-compressing it. This should be done without significantly raising the temperature of the working medium since it would adversely influence the temperature profile of the high-pressure work cycle. The two relationships equation (3.3) and (3.4) are according to them valid for combustion engines (Hiereth and Prenninger, 2007).

.

$$IMEP \sim \rho_{Air,cyl} \tag{3.3}$$

$$P_i \sim \dot{m}_{Air,cyl} \tag{3.4}$$

From equation (3.3) it seen that the Indicated Mean Effective Pressure (IMEP) is proportional to the charge density in the cylinder at the beginning of the compression stroke and from equation (3.4) is seen that the power output of the engine to be proportional to the air mass flow through the engine. This means that increased charge density produces more torque (Hiereth and Prenninger, 2007).

The air density relates to pressure and temperature and to achieve high power density, the charge air needs cooling. In fact, the lower temperature for a specific constant pressure the smaller the volume of the air, hence more charge can enter the cylinder. If no charge air cooling is added on a supercharged engine, measures as fuel enrichment and retarded ignition timing will be necessary in a larger extent to avoid knock and indirectly increase the fuel consumption (Bosch Automotive Handbook, 2011).

3.6.1 Turbocharging

Turbocharging is designed to utilize the exhaust gas energy which otherwise would be lost at the end of each engine operating cycle (Hiereth and Prenninger, 2007). It consists of a compressor and a turbine which are connected by a common shaft shown in *Figure 2*.

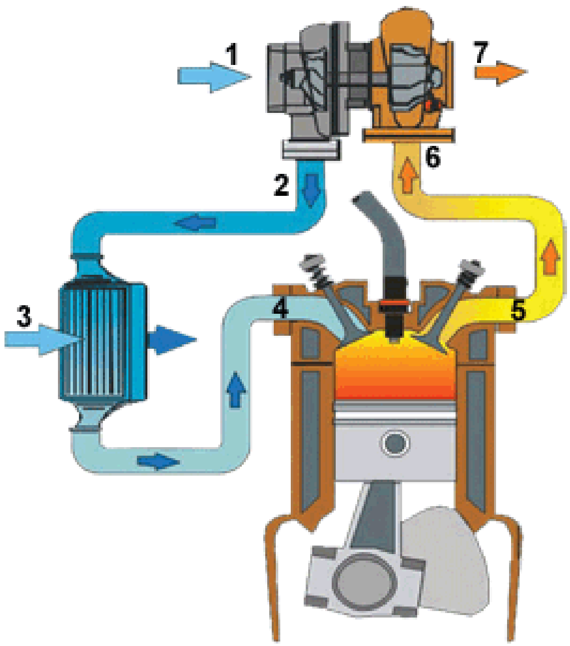

Figure 2 - Layout of a turbocharger configuration and its gas flow (Garrett-4, 2013)

3.6.1.1 The Turbine

The turbine essentially utilizes the exhaust gas energy and converts it to mechanical energy, which drives the compressor via the connecting shaft. The exhaust gases are restricted by the turbine flow sectional area, which results in a pressure and temperature drop between the inlet and outlet of the turbine. This means that energy from the exhaust gases has been removed from the gas flow and instead been converted into kinetic energy which drives the turbine wheel (3K-Warner-1, 2013).

There are two main types of turbines, categorised by the direction of the inflow which could be either axial or radial. On axial-flow turbines the flow is directed through the turbine in the axial direction, and can be designed to have several stages and they are used for aircraft or stationary gas turbines (Hiereth and Prenninger, 2007). Radial turbines have a centripetal in-flow from outside and inwards in a radial direction and the outflow in the axial direction. Radial type turbines are the most common type used on automotive applications and have the layout seen in Figure 3. The turbine wheel is designed to convert the kinetic energy from the exhaust gases to mechanical energy by the time the gases reach the wheel outlet of the turbine (3K-Warner-1, 2013).

The performance of the turbine increases as the pressure difference between the inlet and outlet increases according to 3K-Warner (2013). This occurs when the engine speed is increased resulting in higher gas flow speed as well as higher temperatures due to higher energy in the exhaust gases.

According to Garrett-1 (2013), the turbine performance is greatly affected by the A/R ratio. The A/R ratio describes the ratio between the turbine entry cross-sectional area A [cm^2] at the point of transition from the inlet area into the volute and the radius R [cm], which is the distance from the turbo shaft centreline to the mean flow path at the point where the mass flow has been reduced to half (Hiereth and Prenninger, 2007). This means that the A/R ratio is a measure of the flow capacity of the turbine housing. A smaller A/R turbine has a faster boost rise and increases the exhaust gas velocity faster which increases transient response. But due to the fact that the air enters the wheel more tangentially this results in a reduced flow capacity of the turbine which will tend to increase the exhaust backpressure, which limits the turbine at high engine speeds hence affecting (reducing) the peak power. A turbine with a larger A/R ratio will have lower increasing exhaust gas velocity which delays boost rise. Since the air enters the turbine wheel more radially this increases the wheels effective flow capacity causing a lower back pressure at high engine speed resulting in higher peak power. This means that lower A/R are suitable for engine applications used in normal daily driving since it has better transient response and low engine speed performance compared to the high A/R turbines which are more suited for racing applications since they deliver high engine speed performance (Garrett-1, 2013).

Another parameter that describes the turbine is *Trim*, see equation (3.5) which refers to a geometry ratio of the turbine and the compressor wheel regarding the difference between the inducer and exducer diameter.

$$Trim = 100 \cdot \left(\frac{Inducer^2}{Exducer^2}\right) \tag{3.5}$$

The inducer diameter is defined as the diameter where the working fluid enters the wheel, whereas the exducer diameter is defined as the diameter where the working fluid exits the wheel (see *Figure 3*). Together, the A/R and the Trim fully characterises the swallowing capacity of the turbine for a constant turbine rotor diameter (Garrett-1, 2013).

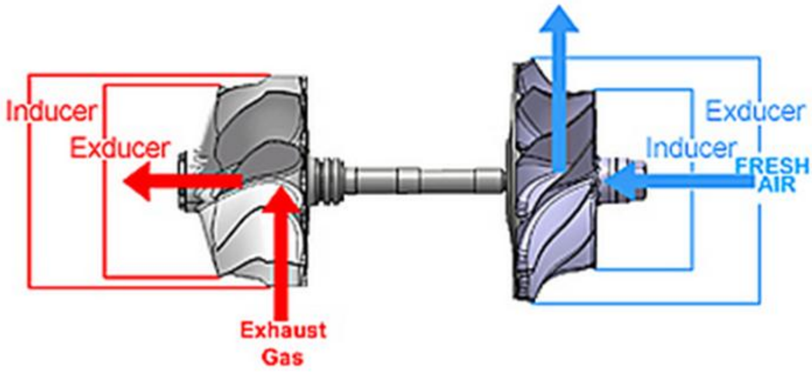

Figure 3 - Layout of how trim is defined on a turbocharger (Garrett-1, 2013)

Turbine maps are a way of describing the operating characteristics of the turbine by displaying the flow parameters plotted against the turbine pressure ratio as seen in *Figure 4*. In figure YY provided by Garrett-1 (2013) these flow parameters are mass flow and turbine efficiency curves plotted against the pressure ratio P_{3t}/P_{4st} which is the ratio between the turbine inlet pressure (P_3) and the static turbine outlet pressure (P_{4st}) (Hiereth and Prenninger, 2007).

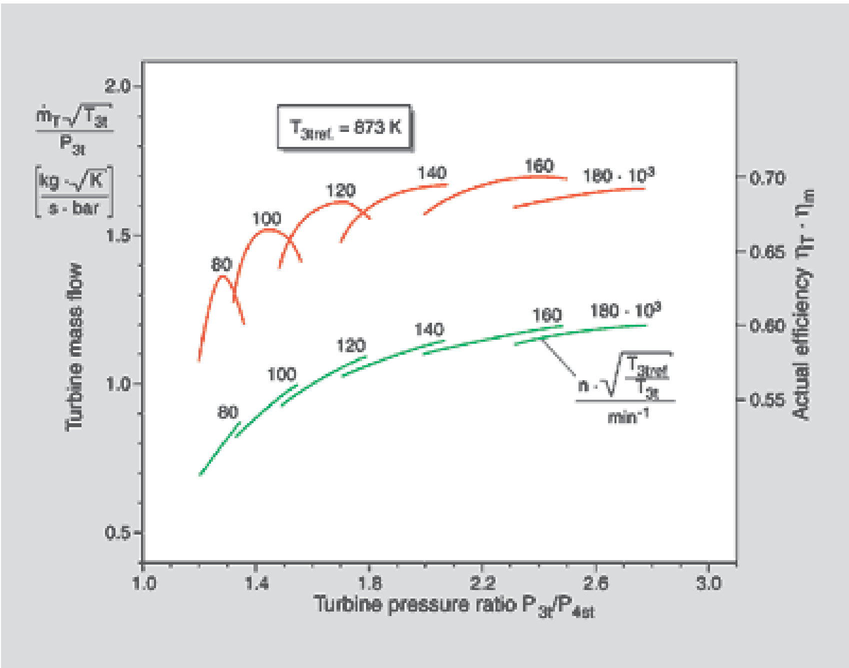

Figure 4 - A turbocharger turbine map (BorgWarner-1, 2013)

3.6.1.2 The Compressor

The compressor of the turbocharger is generally of radial centrifugal type which draws the inlet air into the housing axially by the rotational speed of the compressor wheel. The air is accelerated and released radially into a diffusor which formed by the compressor back-plate as a part of the volute housing. The diffusor slows down the air and compresses it as it travels through the diffusor until it reaches the compressor outlet (3K-Warner-2, 2013).

The operation characteristics of radial compressors are defined by maps which show how the pressure ratio between the outlet (P_2) and the inlet (P_1) depends on either mass- or volume flow. Such a compressor map is seen in *Figure 5*. The dashed lines represent different constant compressor wheel speeds with the maximum speed seen at the top right corner which is the maximum permissible compressor wheel speed (Hiereth and Prenninger, 2007).

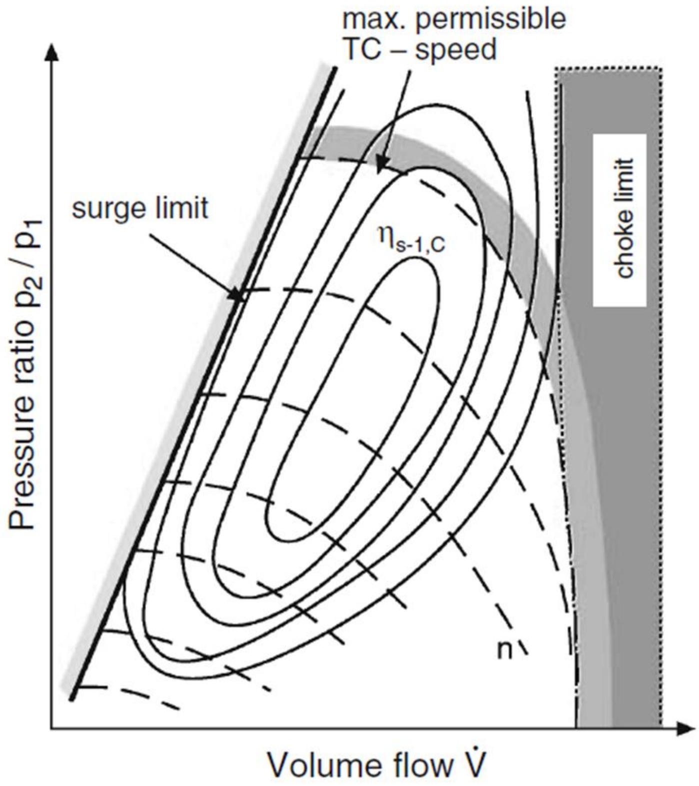

Figure 5 - Layout of a turbocharger compressor map (Hiereth and Prenninger, 2007)

3.6.1.3 The Surge and Choke Lines

There are two limits which are of interest on the compressor map; they are the surge limit and the choke limit. At the left side of the map, the surge line is located and indicates that the pressure ratio between the outlet and inlet is so high that the flow basically stalls at the inlet causing the compressor wheel to be unable to draw air into the compressor. This results in a revers air flow through the compressor until lower and more stable levels of pressure ratios are reached and the compressor can start building up pressure again (Hiereth and Prenninger, 2007). The process of stabilising the air flow in the compressor occurs at a constant frequency which results in a noise known as surging (3K-Warner-2, 2013). Continuous operation at the surge region will lead to heavy trust loading on the compressor leading to premature failure which is most damaging during load. Surge can also occur when the throttle is quickly closed when boost pressure is built up which causes the mass flow do decrease drastically while the compressor is still generating boost since it is still spinning causing the compressor to surge. This effect is reduced if a Blow-off valve or bypass valve is used (Garrett-2, 2013).

The choke limit is located at the right side of the compressor map and it shows where the gas flow reaches sonic speed at the inlet. This is the upper limit of the flow since no further increase in flow rate is possible due to the fact that the limiter of the compressor is the cross-sectional area at the inlet and when the flow reaches sonic speed no more air can enter the compressor even if the compressor wheel speed is increased, thereby limiting the amount of air being able to be compressed and delivered to the engine intake port (Hiereth and Prenninger, 2007).

3.6.2 The Wastegate

On the vast majority of all turbocharged gasoline engines a wastegate is used to control the boost pressure. The wastegate bypasses the exhaust gas flow from the turbine wheel to the exhaust system which results in less energy to run the turbine hence reducing the turbine wheel speed which results in less boost pressure since the compressor rotates at the same speed (Garrett-3, 2013).

3.6.3 Matching the Turbo and Compressor

The matching process of a turbocharger is initiated by estimating the necessary compressor pressure ratio including charged air cooler pressure losses. When this estimation is done an equivalent turbine area is adapted by an iterative process until the compressor reaches the desired pressure ratio while keeping the power equilibrium between the compressor and turbine (Hiereth and Prenninger, 2007).

When matching a turbocharger it is important to know that the charger speed and thus the boost pressure are not directly related to engine speed. Since the power of the compressor and turbine is related, the first step is to accelerate the turbine which increases the power equilibrium and accelerates the compressor wheel hence increasing the boost pressure. Since the turbine is driven by exhaust gases this means that to achieve an increased boost pressure this demands a higher exhaust gas flow (Hiereth and Prenninger, 2007).

There are two different turbocharging methods, Constant-pressure turbocharging and Pulse turbocharging. The method of constant pressure turbocharging means that the exhaust gas pressure is maintained constant by having the gases sent through a plenum located after each exhaust port seen in *Figure 6*. The system is designed to dampen out exhaust gas pulses which occur when the exhaust valve is opening; hence the exhaust gas pressure and temperature are kept as constant as possible. This results in higher turbine efficiencies since the turbine is feed with a constant gas flow. This method however has a serious disadvantage on automotive applications where transient response is important due to the fact that the system has to achieve a new pressure equilibrium in order for it to work properly which drastically decrease the transient response. This means that Constant-pressure turbocharging is suited for steady state operation on stationary engines where transient response is modest or not relevant (Hiereth and Prenninger, 2007).

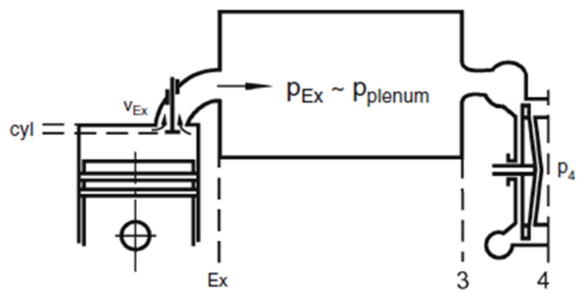

Figure 6 - Layout of constant pressure turbocharging (Hiereth and Prenninger, 2007)

Pulse turbocharging utilises the kinetic energy exhaust gas pulses caused by the pressure waves created from the engine blow-down pulses. Compared to constant-pressure turbocharging this represents a gain since the volume flow of the exhaust gases can be kept, which is crucial for increasing boost pressure in a faster way since the flow do not have to be evened out. The method is seen in *Figure 7* since it has the advantage of having increased transient response which is important for automotive applications (Hiereth and Prenninger, 2007).

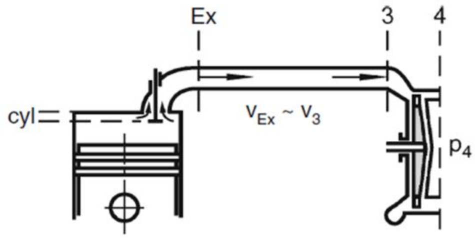

Figure 7 - Layout of pulse turbocharging (Hiereth and Prenninger, 2007)

3.7 Integrated Exhaust Manifold

By integrating the exhaust manifold in the cylinder head, there are advantages regarding cost, fuel economy and performance (Coltman, Turner, Curtis, Blake, et al, 2008).

An inline 3-cylinder engine does not have conflicting exhaust gas pulses; this means that there is no need for separating the exhaust gases from the different exhaust ports. According to Friedfeldt, Zenner, Ernst and Fraser (2012) the exhaust gas manifold volume could be small since there is no risk of backflow into neighbouring cylinders. Therefore an Integrated Exhaust Manifold (IEM) could be utilized on an inline 3-cylinder engine, since there is no need for the manifold piping from each exhaust port to be crossed before the turbocharger, i.e. there is no inter-cylinder exhaust pulse interaction (Coltman, Turner, Curtis, Blake, et al, 2008).

There are two key benefits of using an IEM according to Friedfeldt et al (2012) which are improved fuel economy and complexity at an affordable cost. The improved fuel economy is establish by two advantages of the IEM which is that there is a faster heating process of the engine resulting in reducing parasitic losses. The second advantage is faster warm up of the catalyst which reduces the need for fuel consuming catalyst heating since there is less surface area that dissipates heat between the exhaust port and the catalyst. This means that the engine could operate more often at $\lambda = 1$ since there is less need for more fuel to feed of the sole purpose of heating the catalyst which reduces the fuel consumption. By using an IEM the cost can be reduced since there is no need for an expensive separate manifold which has high Nickel content. Nickel is an expansive material compared to the cylinder head material in i.e. Aluminium (Friedfeldt et al, 2012).

By using an IEM the number of parts can be reduced. According to Coltman et al (2008) the number of components could be reduced from 28 parts to 10 parts because the manifold and the gaskets, studs and nuts that were required for its assembly could be removed. This reduces both component and assembly cost since complexity can be reduced (Coltman et al, 2008).

With an IEM, the cooling channels are made around the exhaust manifold. By using a split water cooling system with two thermostats controlling the engine cooling and the exhaust manifold cooling, they can be heated and cooled separately since each thermostat could be set at different shut-off temperatures (Friedfeldt et al, 2012). This means that not only can the engine and catalyst be heated to optimum temperature faster; it means that the exhaust gases can be cooled since the manifold can be cooled through the cooling channels. This results in that the engine can work more often at stoichiometric conditions since there is no need to run rich to cool the exhaust gases and hence reducing the fuel consumption (Becker, 2011).

According to Coltman et al (2008), an IEM reduces the pre-turbine volume which increases the throttle-response that utilizes the exhaust gas pulses better. They also point out that an IEM has disadvantages. At low engine speed, a reduction in exhaust gas thermal energy occurs which is cooled of instead of driving the turbine which reduces low speed performance. This is also the problem at high engine speed but since the cooler exhaust gases reduces the need to run richer this helps towards achieving stoichiometric conditions all over the engine map which results in better fuel economy and reduced CO_2 emissions. (Coltman et al, 2008).

3.8 Pumping Losses

The main part of the spark ignited engines today is throttle load controlled which causes pumping losses. The pumping losses can be decreased by varying the lift and duration of the valves as well as by using cam phasing. The optimal settings for the lift, duration and cam phasing are changing with load and engine speed. At part load, the lift and duration should be relatively small and vice versa at high load- and engine speed.

Kuberczyk et al (2009) made an investigation of the fractional losses of a naturally aspirated SI engine and a CI engine for the urban driving cycle. A large difference in fractional losses between the SI and diesel engine were seen in the gas-exchange process which is clearly higher for the SI engine. *Figure 8* shows that there are great potentials in reducing the fuel consumption of an SI engine by decreasing the losses caused in the gas-exchange process.

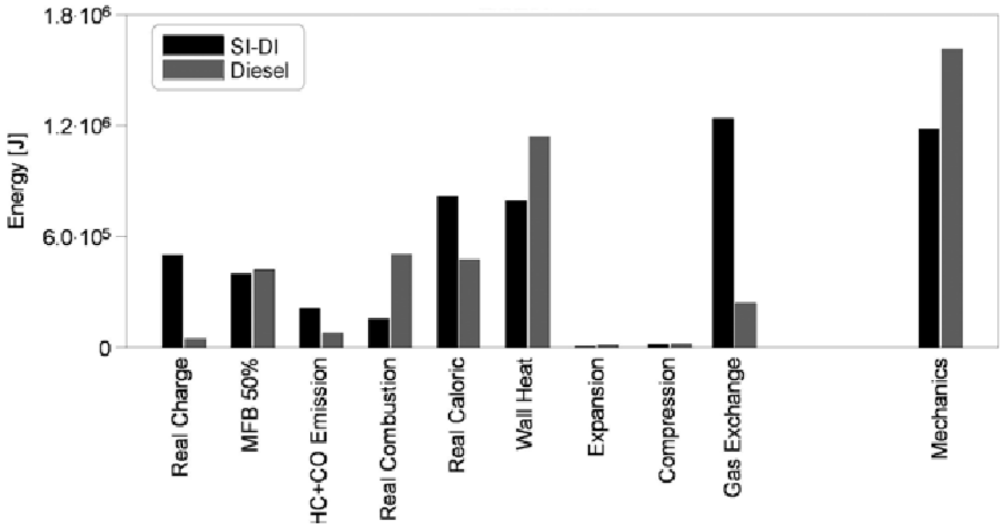

Figure 8 –Fractions of losses in the urban driving cycle (Kuberczyk et al, 2009)

By using Fully Variable Valve Train (FVVT) or two-stage valve lift design, the pumping losses can be highly reduced. With a FVVT system in combination with cam phasing, the valves can be fully controlled to deliver the correct amount of air into the cylinders without using the throttle (Oswaldo Mendes França Junior, 2009).

3.9 Early and Late IVC

The principle of Early Intake Valve Closing (EIVC) and Late Inlet Valve Closing (LIVC) is to draw air into the cylinders as close to atmospheric pressure as possible. With EIVC, the air is drawn into the cylinder in from the beginning of the induction stroke and the intake valves closes before the piston reaches Bottom Dead Center (BDC). By closing the intake valve before BDC, the air mass drawn into the cylinder is restricted. After the intake valve closes, the pressure is decreasing in the cylinder but the extra work that is lost is almost regained during the beginning of the compression stroke. By enable LIVC, the air mass is also restricted but instead by closing the intake valve After Top Dead Center (ATDC), which allows the air drawn into the cylinder flow back into the intake manifold. *Figure 9* illustrates the differences in pumping losses between EIVC and LIVC compared to the conventional pumping losses of a throttle controlled engine. The additional pumping loss for LIVC strategy is due to the resistance from the valve head which arise when the air is from the cylinder is pushed back into the intake manifold (Mechadyne, 2012).

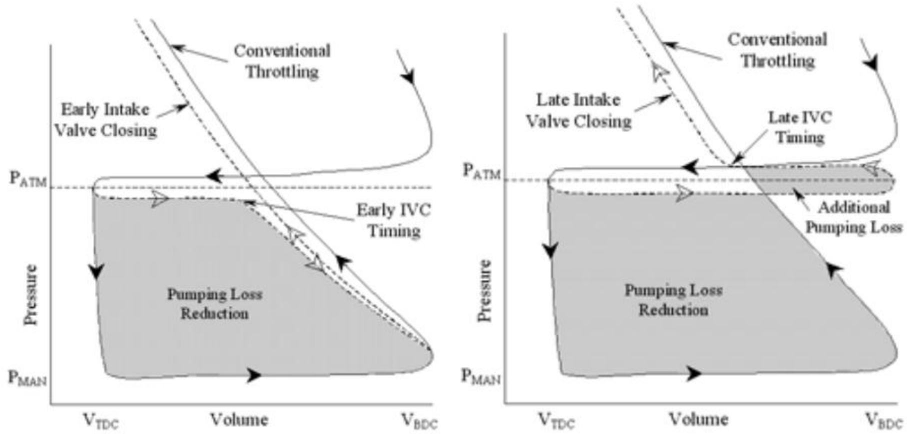

Figure 9 – An ideal Early and Late IVC Strategy (Mechadyne, 2012)

3.10 Pumping Work Analysis

According to Shelby, Stein and Warren (2004) there are two main methods of defining the indicated and pumping work for a conventional four-stroke engine. The first method called "360^{o} integration" is defined so that both the pumping work and indicated work is calculated over a period of 360 CAD respectively. The pumping work at the integral calculated from BDC of the exhaust stroke to BDC of the intake stroke which is seen as Area B and C in *Figure 10*. The indicated work is calculated as the rest of the cycle which is from BDC at the intake stroke until BDC of the exhaust stroke seen as Area A and B in *Figure 10.*

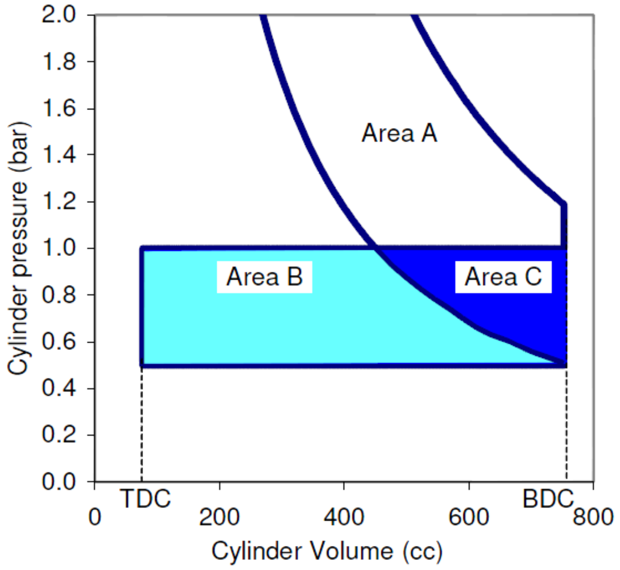

Figure 10 – Layout of the pumping work analysis (Shelby, 2004)

From these two definitions the pumping work (PMEP) and indicated work (IMEP) is calculated by equation (3.6) and (3.7).

$$IMEP = \frac{Area\ A + Area\ C}{V_D} \quad (3.6) \qquad PMEP = \frac{Area\ B + Area\ C}{V_D} \quad (3.7)$$

$$V_D = Displacement\ Volume\ of\ the\ cylinder$$

According to Shelby et al (2004) this method implicitly assumes that the work associated with gas exchange occurs during the exhaust and intake stroke, which means that it will have a major inaccuracy when changing the timing angles for LIVC or Early Exhaust Valve Closing (EEVC).

The second method does not include Area C in the pumping work and instead regards it when calculating the indicated work. This means that Area C will give a zero contribution since the area is positive during one stroke and negative during another, which results in a total of zero when integrating the cycle, hence only Area A will have a contribution to the indicated work and Area B contributes to the pumping work. According to Shelby et al (2004) there are a number of significant disadvantages of using this method. Although the calculation of Area B is useful, it does not include the complete work done during the intake stroke which means that it cannot represent the total reduction of pumping work related to inlet valve timing. The second disadvantage is the fact that it does regard the full exhaust stroke and the factors which affects the first part of the exhaust stroke. One factor of this is if the exhaust blow-down is completed after BDC which causes an increased pumping work in reality since the final expelling of the exhaust gases are done during the first part of the exhaust stroke. The increased pumping work is not accounted for since it is not included in Area B. This additional work is seen in *Figure 11*.

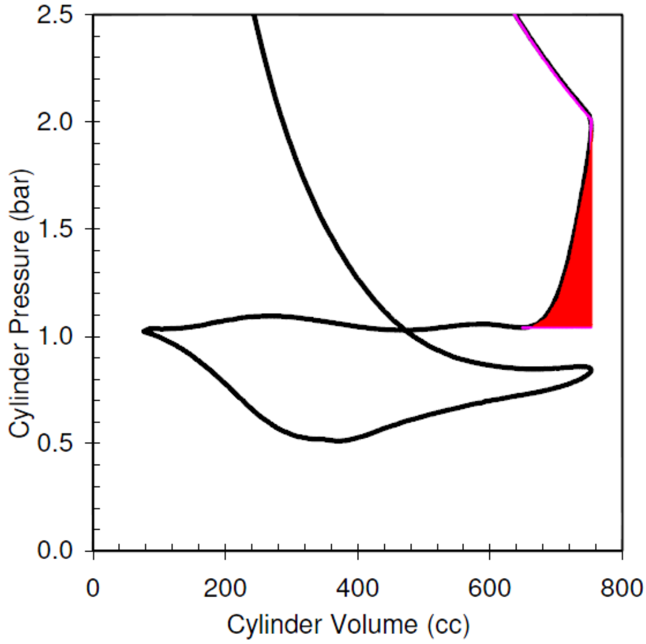

Figure 11 – Losses caused by Early Exhaust Valve Opening (Shelby, 2004)

3.10.1 Shelby´s Method of Analysing the Pumping Work

Shelby et al (2004) has created their own adjusted method of calculating the indicated and pumping work which overcomes the limitations of the two earlier methods with the basis from the "360^o integration" method. Their new method introduces adjustments to both PMEP and IMEP with respect to the effects of inlet and exhaust valve timing and summons all affecting factors for these two into $PMEP_{adjusted}$ and $IMEP_{adjusted}$ which are the actual pumping and indicated work.

The trade-off between which Exhaust Valve Opening (EVO) timing which is to be used is high speed exhaust stroke pumping work and low speed expansion work. The EVO is according to Shelby usually chosen to allow sufficient flow during the exhaust blow-down near BDC at peak power which results in EVO well before BDC. This causes losses of expansion work which is seen as the red in *Figure 12*. This affects the results since the amount of work lost by opening early traditionally will appear as a reduction in IMEP while it actually should be considered as a contribution to PMEP since it is a pumping work loss. The expansion work lost is calculated by extrapolation the expansion pressure from EVO to BDC and is called EVO loss and normalised by engine displacement to MEP.

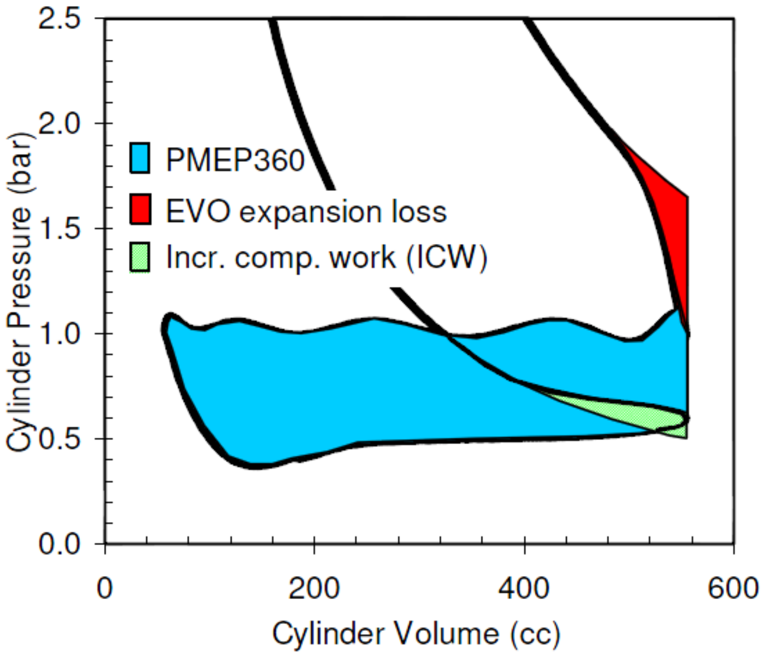

Figure 12 – Layout of the pumping losses during the pumping loop (Shelby, 2004)

The trade-off when choosing IVC timing is low speed torque or high speed power. To reduce the pumping losses at low speed the timing could be adjusted in two ways, either it is advanced well before BDC during the intake stroke (EIVC). By using EIVC the reduction of Area B is very large but it is limited by the pumping work performed after IVC. The second option is to retard IVC into the compression stroke (LIVC). Since there is no pumping work after IVC this result in an almost complete elimination of pumping losses, but there are still losses. Since IVC occurs during the compression stroke, the charge is pushed back into the intake manifold which results in a large increase of compression work during the first part of the compression stroke. This contribution to the compression work is called Incremental Compression Work (ICW) and is expressed in MEP and seen as the green area in *Figure 12*. According to Shelby et al (2004), the total area of the remaining pumping work of EIVC and the area of ICW with LIVC is approximately equal which mean that the upper limit to the reduction of pumping work is the same as the calculated Area B with either EIVC or LIVC.

According to Shelby et al (2004) it is useful to group all terms related to the gas exchange regarding and another term based on IMEP calculations which is only affected by high pressure region during combustion. By using Shelby's methodology the improvements in fuel consumption can be broken down into two key components, a pumping work component and an indicated efficient or ISFC component. Since both the PMEP and IMEP are affected by the effects of ICW and EVO losses they are adjusted by their contributions in order for them to solely be associated with pumping work and indicated efficiency respectively. These two components are referred to as adjusted PMEP and IMEP and are seen as equation (3.8) and (3.9).

$$PMEP_{adj} = PMEP_{360} + ICW + EVO_{exp\_loss} \tag{3.8}$$

$$IMEP_{adj} = IMEP_{360} + ICW + EVO_{exp\_loss} \tag{3.9}$$

Shelby et al (2004) also states that NMEP is the integral $\int PdV$ over the full cycle of 720 CAD it is also equal to the adjusted components hence the actual NMEP is the same regardless of method of calculation seen in equation (3.10).

$$NMEP = IMEP_{360} - PMEP_{360} = IMEP_{adjusted} - PMEP_{adjusted} \tag{3.10}$$

3.11 Variable Valve Timing

Variable valve timing is used for several reasons, e.g. de-throttling, control the amount of residuals at different load points, at cold start conditions, low end torque for turbocharged engines as well as to increase the power and torque (T. Leroy et al, 2008).

With Dual Individual Cam Phasers (DICP), the overlap period can be controlled (when both the inlet and exhaust cam are open at the same time). By controlling the valve overlap, the amount of burned residuals is also controlled (internal EGR) and thus the in-cylinder mixture temperature. With increasing mixing temperature, the charge will become more homogenous before ignited which is beneficial regarding fuel consumption. The diluted mixture (internal EGR) slows down the flame propagation and lowers the cylinder pressure and temperature during the combustion, which also decreases NO_x emissions. Another advantage with increasing amount of residuals at part load is that higher intake pressure is necessary to maintain the same torque which reduces the pumping losses (T. Leroy et al, 2008).

Kramer and Philips (2002) made an investigation on a 1.6l SI engine, equipped with DICP in order to create a phasing strategy. The recommended phasing strategy is shown in *Figure 13* and *14.* According to the phasing strategy, the exhaust cam should be fully advanced at idle and retarded continuously up to medium engine speed and load. At full load and low engine speed, the exhaust cam should be retarded and advanced with increasing engine speed. The recommended phasing strategy of the intake cam is to fully advance the cam for low engine speed and high torque and retard the cam with increasing engine speed and load (Kramer and Philips, 2002).

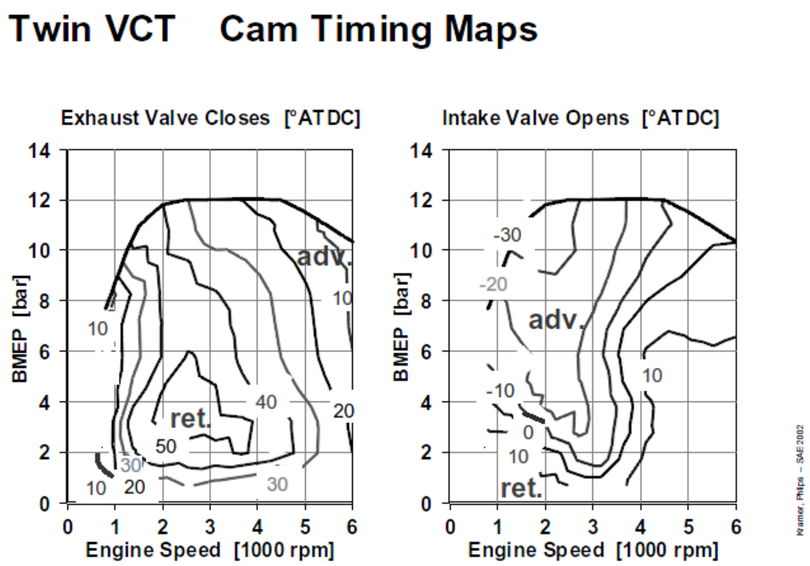

Figure 13 - Cam Timing Maps (Kramer and Philips, 2002)

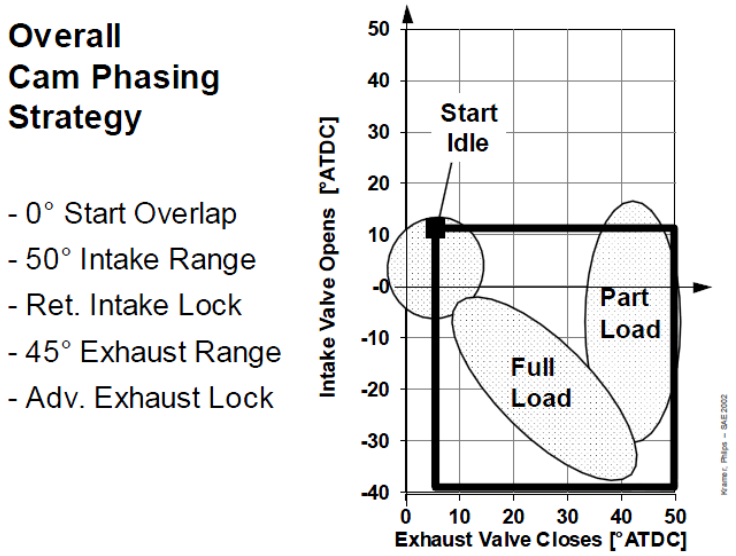

Figure 14 - Overall Cam Phasing Strategy (Kramer and Philips, 2002)

3.12 Fully Variable Valve Train (FVVT)

A FVVT utilizes a large number of lift curves in order to decrease the pumping losses for a wide spread of engine speed and load. With a FVVT system, the lift and duration is optimised optimized for various load points (Flierl et al, 2011).

At the technical university of Kaiserslautern, a FVVT system called Univalve has been developed. The Univalve system was tested on a 1.6 l, NA SI engine with direct injection, equipped with start/stop technology. Besides the 1.6 l NA SI engine, the Univalve system was also fitted to a turbocharged SI engine with reduced displacement, producing the same power output as the 1.6 l engine. In *Figure 15*, the lift curves and cam phasing system is shown that the engines were equipped with (Flierl et al, 2011).

When running the engines in the NEDC, a reduction in fuel consumption was obtained of 8.5% for the 1.6 l NA engine and 5% for the downsized turbocharged engine (Flierl et al, 2011).

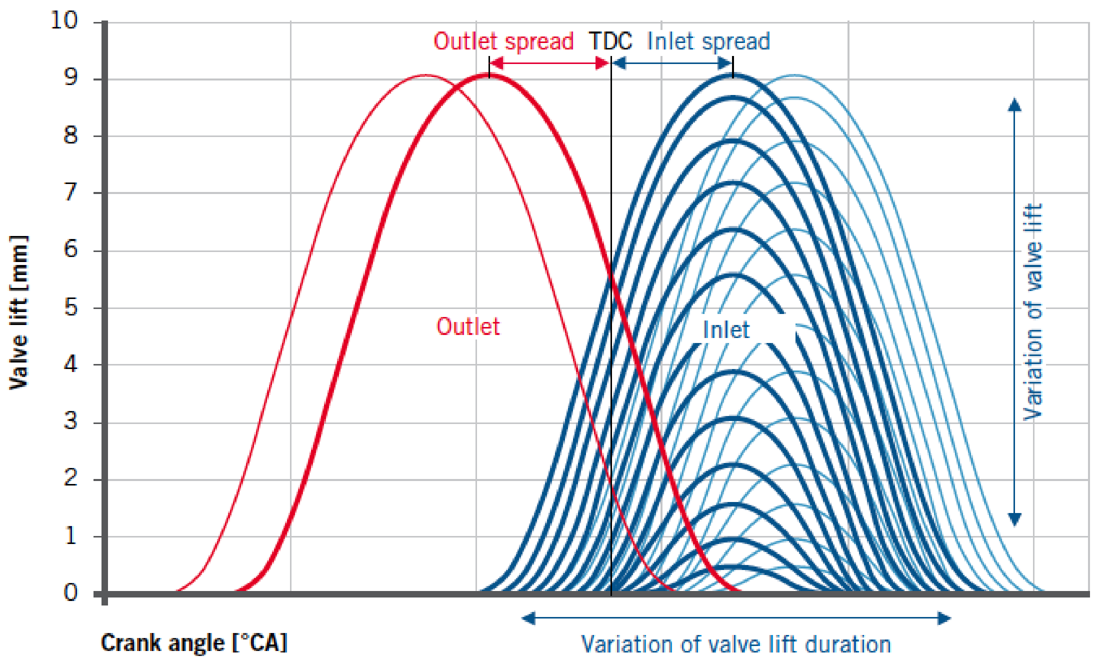

Figure 15 - Valve lift duration curves of the Univalve system (Flierl et al, 2011)

3.13 Two-Stage Valve Lift

The two-stage valve lift system uses two different valve lift profiles, one with smaller lift and duration for low load and engine speed and one profile optimized for high flow speed and charge volumes for full load (Huber, Klumpp and Ulbrich, 2010). Audi has developed a two-stage valvelift system which they call the Audi Valve lift System (AVS). According to Huber et al (2010), Audi claims that the AVS is 80% as efficient compared with a FVVT system to only 20% of the cost. The slightly degraded efficiency of the AVS compared to a FVVT system is caused by using the throttle to some extent, but the pumping losses are still highly reduced compared to a conventional throttle-load controlled engine (Huber et al, 2010).

3.14 Switching Cam

When switching cams, there are two driving scenarios that have to be considered. The first scenario is when the driver is requesting a rapid increase of torque (i.e. a large change of the acceleration pedal position) when the engine operates in the part load area. The load will increase instantly and the Low Lift Cam (LLC) is switched to the High Lift Cam (HLC). The second scenario is when the driver slowly accelerates to the point when the HLC has to be actuated. A smooth cam shift is then required which is critical to accomplish (Brüstle and Schwarzenthal, 2001).

In order to success with a smooth cam shift, the volumetric efficiency has to be the same when switching cams, which is accomplished by cam phasing. In order to optimize the efficiency of the system, the switch of cams should occur at the optimal point of BSFC for the LLC, to the cam phasing settings of the HLC with corresponding volumetric efficiency (Brüstle and Schwarzenthal, 2001).

3.15 Cylinder Deactivation

Cylinder deactivation is a technology for reducing the fuel consumption on throttle load controlled engines (Flierl & Lauer, 2013). By cutting of the fuel supply to some cylinders and at the same time keep the valves closed, the engine will run with reduced effective displacement (Green Car Congress, 2012). Since the displacement reduction requires less throttling for a certain amount of power output compared to full displacement operation of the same engine, the pumping work and the fuel consumption is reduced. According to Flierl & Lauer (2013), cylinder deactivation also reduces the pumping work since the charge losses associated with the otherwise running cylinders will be removed during deactivation which also improves the total efficiency, hence reduces fuel consumption. Mitsubishi claimed a 10-20% improvement in fuel economy for their version of cylinder deactivation called Modulated Displacement that operates during low engine load (Knowling, 2005).

3.16 Time-To-Torque Definition

The aim of turbocharging is to improve the fuel economy of the engine by downsizing. By turbocharging, the same power output of a NA engine can be reached with a turbocharged engine with reduced displacement. One of the challenges of a downsized turbocharged engine is to maintain the same performance as a NA engine regarding transient response. The phenomenon of "turbo-lag" is critical for the transient response which becomes worse with decreasing displacement with increasing size of turbocharger. During accelerating conditions, the turbine wheel transfers energy to the compressor in order to raise the intake manifold pressure. Initially, only a part of the energy is transferred to the compressor wheel and the rest is used to overcome the inertia of the rotating parts of the turbocharger. The boost pressure during acceleration is therefore expected to be lower compared to steady state conditions for the same engine speed (Lefebvre and Guilain, 2005).

The transient response of an engine could be measured according to *Figure 16*, which is an example of how to define the response time criterion. The definition of the response time is starting from when the throttle position changes from part load to full load and up till 90% of when the maximum torque target is reached.

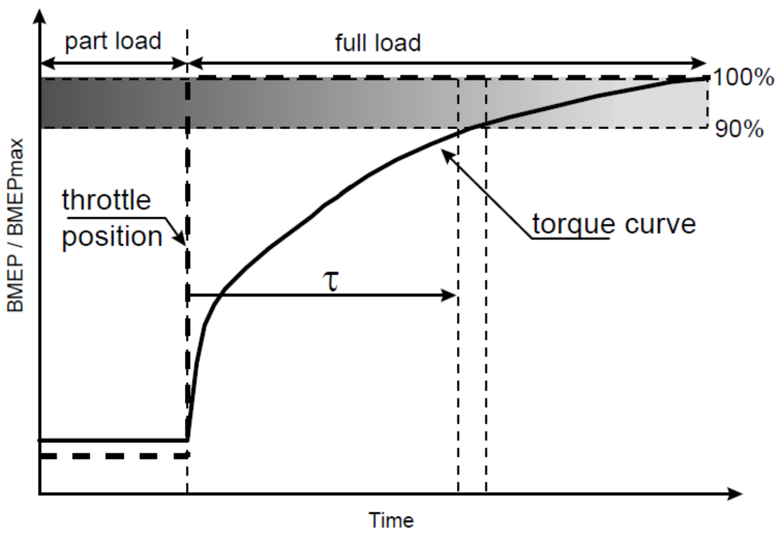

Figure 16 - Response time τ definition for a tip-in at constant speed (Lefebvre and Guilain, 2005)

4 Methodology

In order to create a solid foundation for the thesis regarding 3-cylinder engines, a literature study will be made with focus on the questions in the background. From the literature study, the 3-cylinder engines that exist today and the technologies used will be investigated as well as other feasible technologies. Next step is to create engine concept models in GT-Power. When creating the GT-Power models, the initial step is to create a base-engine from the model provided by VCC. This is done by removing the turbocharger and tune the engine in order to embody the characteristics of a 3-cylinder engine. When the characteristics of the base-engine are satisfying, a suitable method of deciding turbocharger is developed, in order for the turbocharger to provide desirable engine characteristics regarding performance and driveability.

When a suitable turbocharged base-engine has been developed, the technologies that are of interest will be added, modelled and evaluated. From these added technologies, new concepts will be made and possible synergy effects will be investigated. During this stage, a comparison between the developed concept and the benchmarked 4-cylinder engine will be done to investigate how the engine-concept fulfils the requirements. If not, further refinements have to be investigated in order to match the benchmarked engine.

The final step is to analyse the models and results in order to choose a 3-cylinder engine concept and give recommendations to VCC.

4.1 General Modeling

The general model parameters such as the ambient temperature and pressure of the model are seen in *Table 1*.

Table 1 - Initial parameters for the model regarding pressure and temperature

Engine model parameters		
Ambient Temperature	293	[K]
Ambient Pressure	100	[kPa]
Compression Ratio	9.8	[-]
Combustion Efficiency	95	[%]

4.1.1 VCC Cam Phasing Definition

VCC uses a definition for Cam Phasing with respect to the Camshafts maximum lift point. This point is referred to as the Cam Top Angle (CTA) [1] and is measured from Top Dead Center (TDC). The CTA is from the beginning used to define how different camshafts are related to TDC when installing them in the engine. The possible cam phasing angles available is referred to as the actual change of the CTA. In *Figure 17* the definition and the available cam phasing is shown for both the intake and exhaust cams. The Cam Phasing used during this project is mainly focused on using the cam phasing settings seen in *Table 2*. The exhaust camshaft can be retarded 30^o towards TDC and the intake camshaft can be advanced 50^o towards TDC. Maximum

[1] Translation from the Swedish definintion “Kamtoppvinkel” (KTV)

scavenging is obtained at maximum overlap, i.e. with the phasing of 30/-50 (EV/IV). With the initial settings with no phasing, maximum trapping is obtained.

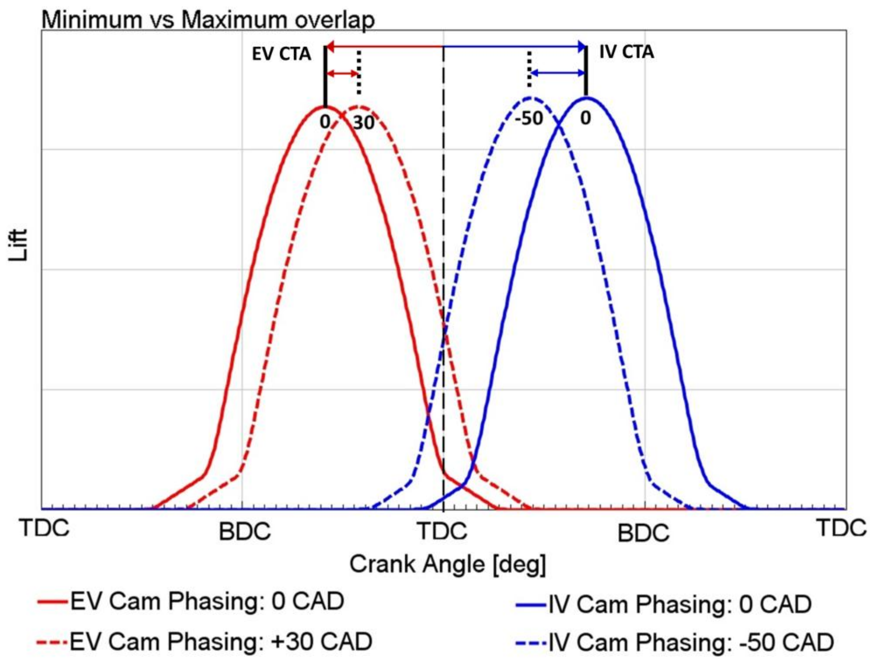

Figure 17 - VCC Cam phasing definition

When different VVT settings where evaluated on the engine concept the settings most often used are seen in *Table 2*.

Table 2 - VVT settings used when running GT-Power simulations

VVT settings with respect to EV CTA and IV CTA						
Case:	**1**	**2**	**3**	**4**	**5**	**6**
IV:	-50	-50	-50	-50	-40	-40
EV:	0	10	20	30	0	10
Case:	**7**	**8**	**9**	**10**	**11**	**12**
IV:	-40	-40	-30	-30	-30	-30
EV:	20	30	0	10	20	30
Case:	**13**	**14**	**15**	**16**	**17**	**18**
IV:	-20	-20	-20	-20	-10	-10
EV:	0	10	20	30	0	10
Case:	**19**	**20**	**21**	**22**	**23**	**24**
IV:	-10	-10	0	0	0	0
EV:	20	30	0	10	20	30

4.1.2 Residuals

When choosing the cam phasing settings for the best possible BSFC, the amount of residuals in the cylinder is important to keep at realistic values. According to Heywood (1988), the maximum limit of residuals is 30% in order to maintain a stable combustion which is also recommended by VCC. The 30% limit is kept for all results presented.

4.1.3 Ignition Timing to Prevent Knock

The 3-cylinder concept engine is designed to match a 4-cylinder high performance engine of the VEA architecture in terms of performance, which results in high BMEP. For the max load curve, knock becomes a critical factor.

In the 3-cylinder engine model, the knock probability data from the max load curve of the 4-cylinder benchmark engine is stored (there is no measurement available of the max load curve of the 3-cylinder concept engine). The output signal for knock probability of the FKFS knock model is compared in *Figure 18*. When the knock probability of the 3-cylinder engine is the same as the test data measured based on the 4-cylinder engine, the 50% burn point is retarded from MBT at 8 CAD. *Figure 18* shows that the FKFS knock model is detecting very low probability of knock below 1800 rpm; hence the 50% burn point is not retarded. From 1800 rpm up to maximum engine speed, the output signal from the knock model of the 3-cylinder engine model is limited by the stored knock probability data from the 4-cylinder engine. The control system retards the 50% burn point (tb50) in the range of 18.5 to 25 degrees above 1800 rpm see *Figure 19.*

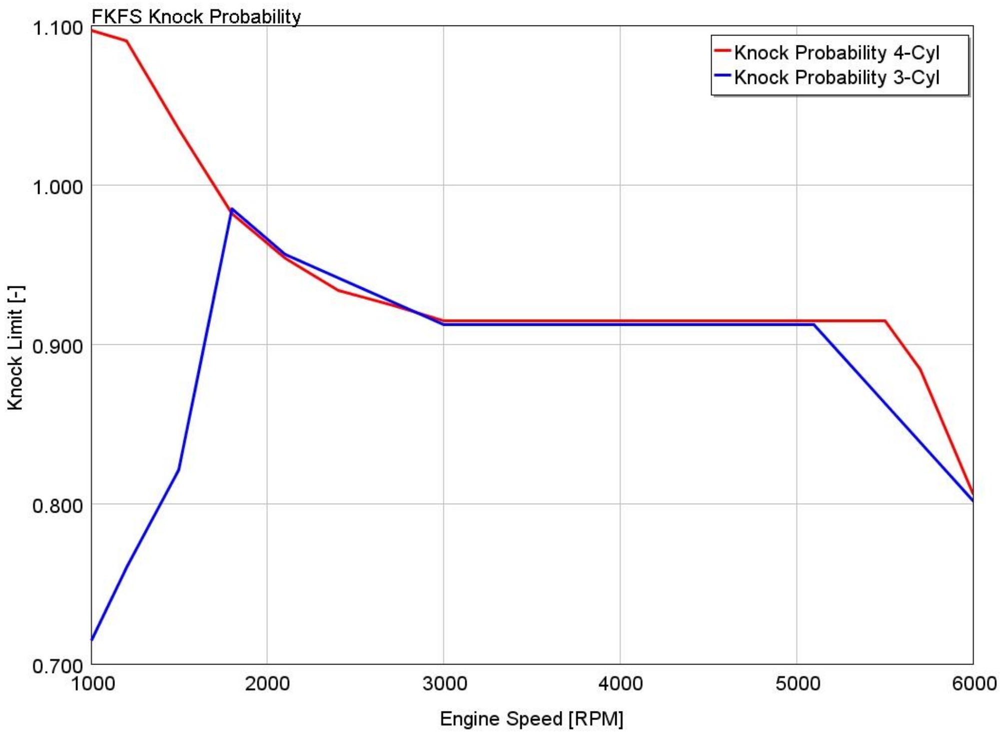

Figure 18 - FKFS Knock Probability vs. Engine Speed for the 3- and 4-cylinder engines

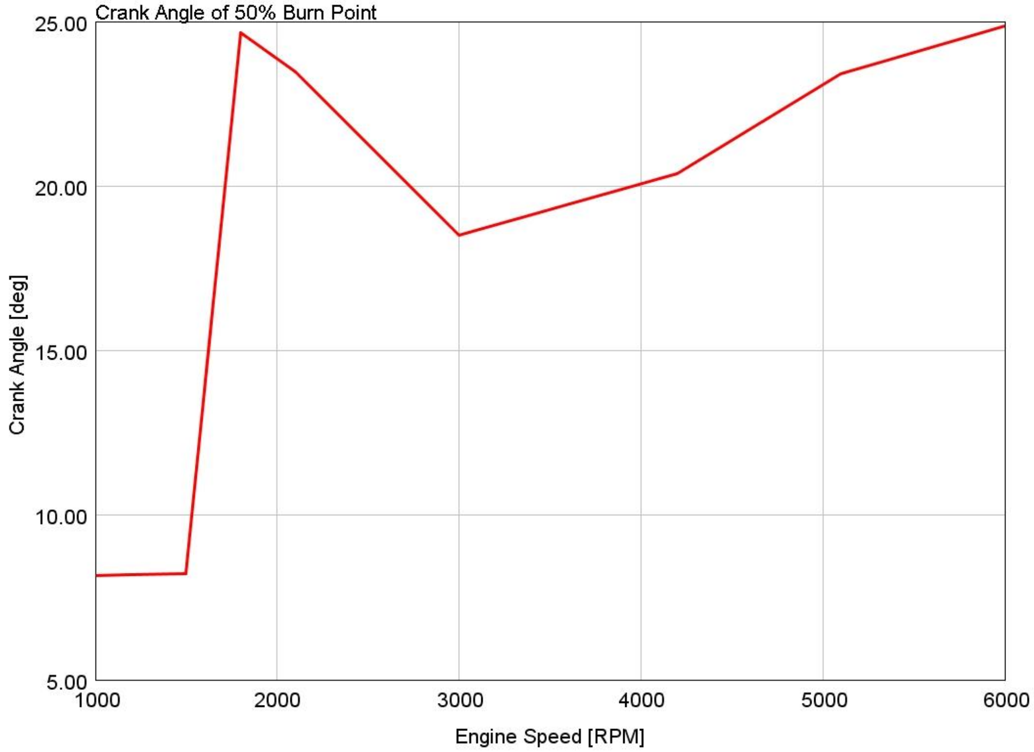

Figure 19 – tb50 vs. Engine Speed for the 3-cylinder engine when using the FKFS knock model

Due to the lack of knock probability data for the max load curve of the 3-cylinder concept engine, the control system in the GT-Power model which automatically adjusts the 50% burn point cannot be used. Instead the timing is retarded manually according to *Table 3*. The 50% burn point is retarded to 25 CAD After Top Dead Centre (ATDC) up till 4200 rpm and then gradually decreased with increasing engine speed, which is based on recommendations from VCC. At part load, the 50% burn point is set to MBT.

Table 3 - 50% burn point vs. Engine Speed for the maximum curve

Engine speed [rpm]	50% Burn Point ATDC [CAD]
1000	25
1200	25
1500	25
1800	25
2100	25
3000	25
4200	25
5100	22
5700	20
6000	19
6900	16

4.1.4 Temperature Controller

The maximum temperature of the engine is regulated by the thermocouple temperature of the exhaust manifold depending on the engine speed, which is seen in *Table 4*. The points in-between are interpolated between the closest point above and below. Points outside the table are limited to the first or last value; hence below 1000rpm the maximum temperature will be 736^{o}C and 970^{o}C above 6000rpm.

Table 4 - Maximum allowed Thermocouple Temperature vs. Engine Speed for the maximum curve

Engine speed [rpm]	Temp [^{o}C]
1000	736
1200	792
1500	863
1800	903
2100	934
2400	952
2700	970
6000	970

If the temperature reaches above the maximum allowed temperature, it is limited by the lambda controller which causes the model to inject more fuel since an enriched air/fuel mixture lowers the temperature. The controller is allowed to enrich the mixture from the standard setting of $\lambda = 1.0$ to $\lambda = 0.75$. If this limit is reached, the wastegate will be used to limit the temperature by opening up more and slow down the turbocharger shaft speed which reduces the power output hence reduces the temperature. This is also done if the air temperature at the compressor outlet reaches 230 ^{o}C.

4.2 Method Turbocharging

The chosen turbocharger configuration was identified by running the engine towards the specified performance targets. The first step was to find a suitable turbine since it is correlated with both the power needed to run the compressor as well as the amount of unburned residual gases at each cycle end. A smaller turbine enables an easier pressure build up at low engine speed, but it also increases unburned residuals as well as the backpressure which limit the performance on higher engine speeds. By using a larger turbine the residuals are lower as well as the exhaust runner backpressure which enables a higher output, but it reduces the low-end drivability of the engine. A suitable turbine was decided by the tradeoff between residuals and the engine speed range performance.

To reach the requested power demand, different compressors were tested with the chosen turbine. The initial target was to meet a mid-performance target where the torque-knee was met at low engine speed and peak power is reached at the upper end of the mid-engine speed range. When this target was met the next step was to meet a high-performance target where the torque-knee could be met later and instead results in a higher peak power and high engine speed performance.

The key parameters to identify when choosing the turbocharger configuration is mass flow through the engine, which is important for choosing the turbine, since it is driven by the exhaust gases. The exhaust gas pressure before and after the turbine is used to establish the amount of energy that can be used to run the turbine as well reducing the amount residuals. The compressor parameters are mainly mass flow and pressure ratio since it indicates the amount of air being delivered to the engine and the boost pressure.

To find an optimum turbocharger configuration these parameters was sent to Borg Warner since VCC only has configurations regarding more evenly pulsed engines which meant that none of the turbines/compressors was a perfect match for the 3-cylinder engine.

The turbocharger recommended by Borg Warner, had a new configuration of turbine/compressor which was implemented in the model and tested against the performance target of the benchmark 4-cylinder. The new configuration resulted in higher levels of backpressure. A limit of 4bar was set as a maximum level of allowed backpressure during maximum power output. Transient response and peak power are two parameters that are of great importance and were considered together with back pressure when the final turbine was chosen between two turbines with inducer diameters of 45mm and 50mm respectively.

4.3 Time-To-Torque

In order to analyse the drivability of the engine, a Time-To-Torque (TTT) investigation is carried out. The aim is to build up torque as quickly as possible by finding the optimal cam phasing settings for different engine speeds. By changing the cam phasing settings, the amount of fresh air blown through the cylinder is controlled.

The turbocharger of the 3-cylinder concept engine is sized to deliver enough boost pressure in order to get the same torque and power output as the 4-cylinder benchmark engine. With increasing size of turbocharger, the inertia increases as well. It is therefore important to investigate the response of the engine, i.e. simulate how long time it takes the engine to deliver a certain amount of torque for various engine speeds for respective turbocharger considered.

The TTT is investigated for several different engine speeds in the range of 1000 to 2400 rpm for all possible cam phasing settings according to *Table 2*. By investigating the cam phasing settings, the optimal cam phasing is identified for each time step with increasing torque. Further, the optimal cam phasing settings are combined for the best turbo response of each configuration considered. The TTT is compared with the benchmarked 4-cylinder engine in order to choose the best compromise of turbo configuration.

The inertia of the turbine and compressor wheel has a large influence on the TTT response of the engine. The inertia is included in the shaft between the turbine and compressor wheel. The large influence of the inertia is affecting the selection of turbine and compressor wheel, which also will affect the maximum power output, backpressure etc.

An investigation is carried out with decreased inertia for the same turbine and compressor wheel in order to investigate the influence of the inertia. Another reason of decreasing the inertia is for future development to see if there could be another suitable choice of turbine and compressor wheel in the near future.

4.3.1 The Cam Phasing Control Sysem During Time-to-Torque

In order to optimize the cam phasing settings during the TTT simulation, a control system is needed which is able to change cam phasing settings during the simulation. The control system shown in *Figure 20* regulates the cam phasing via a signal generator (ScavengeMode) where a "mode" represents each time step according to *Table 5* and *Table 6*. The mode number and engine speed is send to a lookup2D table (IV_VVT and EV_VVT) which controls the phasing of the intake and exhaust cams. In the lookup2D table, mode 1 is corresponding to the maximum valve overlap with the intake cam advanced 50 CAD and the exhaust cam retarded 30 CAD. In mode 2, the exhaust cam phasing is retarded to 10 CAD and the intake cam is the same. The control system also includes a limiter template in order to limit the speed of the cam phasers according to manufacturer data. Further, two signal generators (IV_KTV and EV_KTV) stores a linearized table with values of the phasing angle when maximum lift occurs, which adapts the control system for various durations.

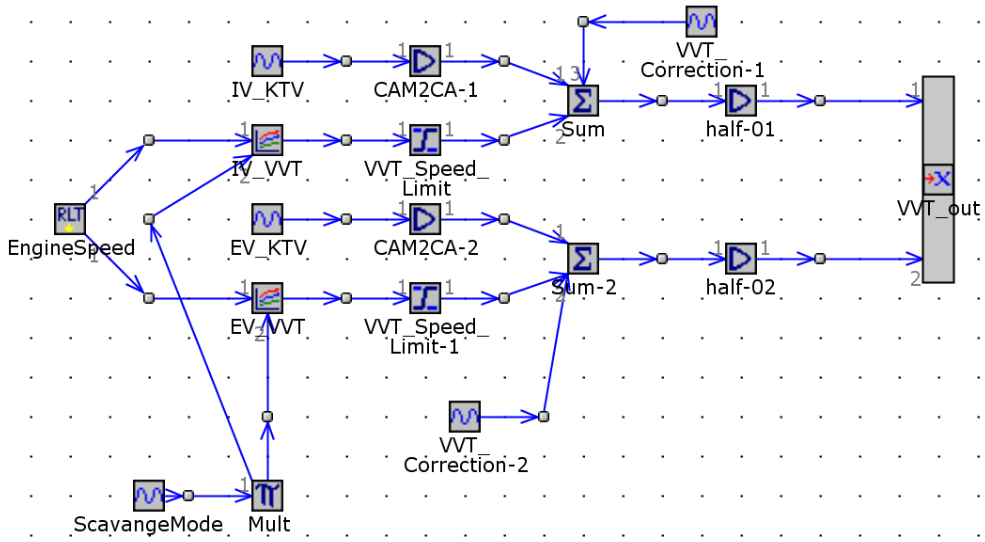

Figure 20 - Layout of the VVT controller in GT-Power during Time-To-Torque

Table 5 - VVT settings vs. TTT- mode

	IV_VVT	EV_VVT
Mode	1800 rpm	1800 rpm
0	5	-5
1	30	-50
2	10	-50

Table 6 - Time vs. TTT-mode

Time [s]	Mode
0	0
5	0
5.01	1
6.16	1
6.17	2
8	2

4.3.2 Efficiency of Compressor Maps

When investigating the TTT for the 3-cylinder concept engine, the compressor map provided by BorgWarner is used, which is simulated with software specialized for generating turbine and compressor maps. In the area of the compressor map where low pressure ratio and low mass flow are present, the compressor map efficiency do not correspond the reality. The efficiency is better in the reality and therefore, VCC has generated a compressor map which has been improved by using refined measurement techniques in the critical area of the compressor map. The improvement of the efficiency is illustrated with *Figure 21* and *Figure 22*. The performance of the concept engine is evaluated for two different turbines with one compressor map provided by BorgWarner. When comparing the 3-cylinder concept engine with the 4-cylinder benchmark engine, the refined compressor map provided by VCC is used in order to compare the 3- and 4-cylinder engines with the same conditions.

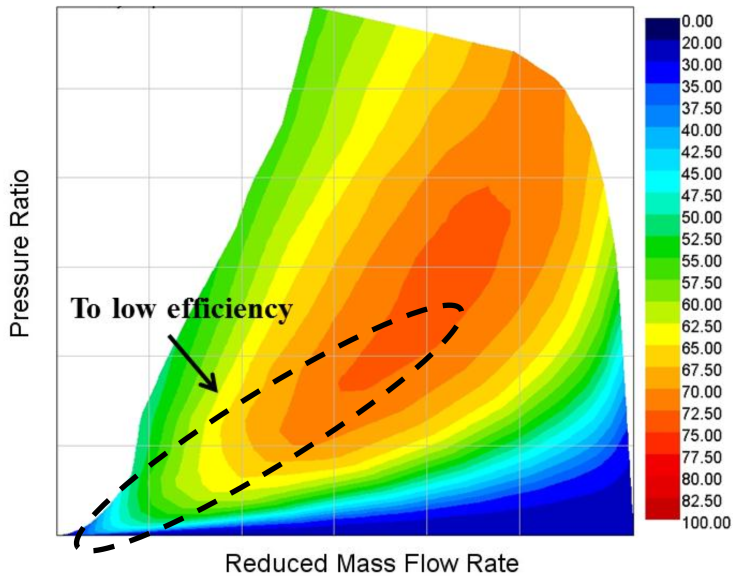

Figure 21 - Compressor Map provided by BorgWarner

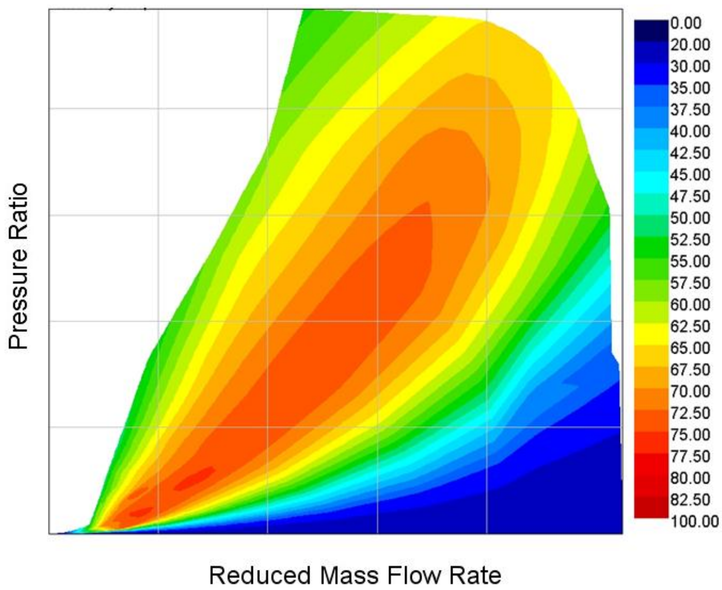

Figure 22 - Refined compressor map provided by VCC

4.4 Two-Stage Valve Lift

In order to decrease the amount of throttling losses in the part-load area and hence the fuel consumption, an investigation of an alternative camshaft for a two-stage valve lift system is performed. The original camshaft on the intake side is changed to a cam with decreased lift and duration. In the GT-Power model, a formula is created that scales the lift profile according to which duration is chosen (based on lift- and duration multipliers). The formula scales the lift profile according to the chosen duration to maintain reasonable lift and accelerations profiles. When changing the duration of the Low Lift Cam (LLC), the maximum lift terms of CAD adjusts after a table stored in the GT-Power model in order to get the same IVO and overlap as the high lift cam (HLC), see *Figure 23*. The investigated interval of duration for the LLC is from 110 to 170 CAD with steps of 20 CAD. The duration interval is estimated to provide the most suitable LLC for the desired part load operating area.

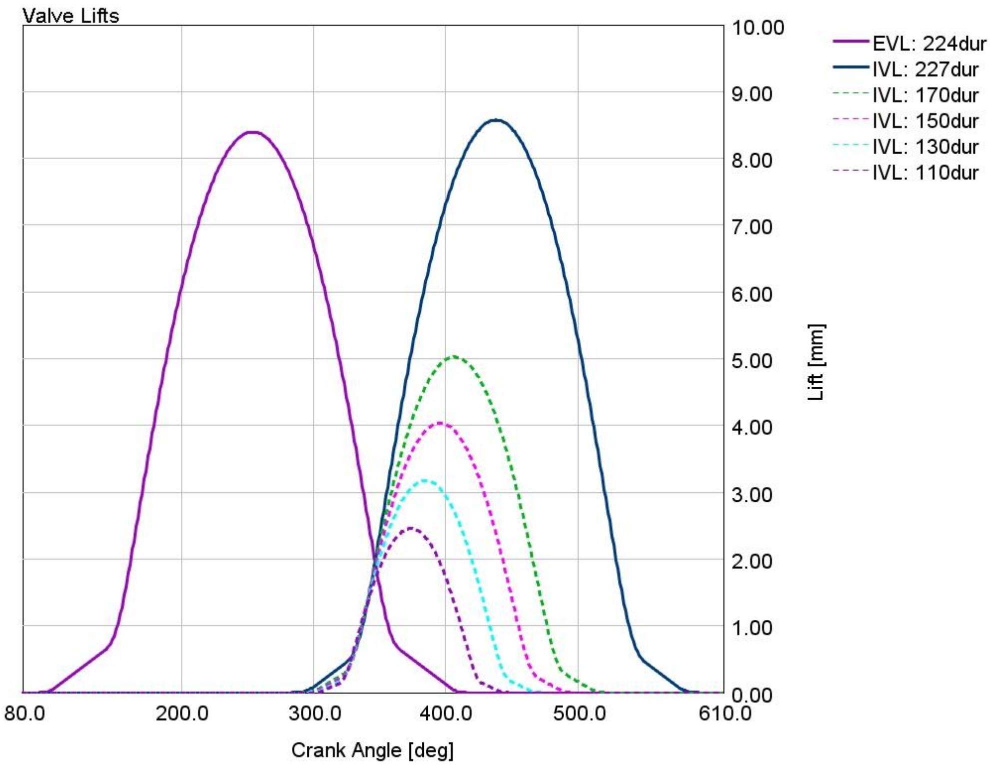

Figure 23 - Valve Lift for different camshaft profiles

In *Figure 24*, the effect on the ramps due to scaling is shown. The ramps of the LLC's are not optimized and have to be refined for production, but when investigating the gas-exchange process, the effect off the ramps due to scaling are negligible.

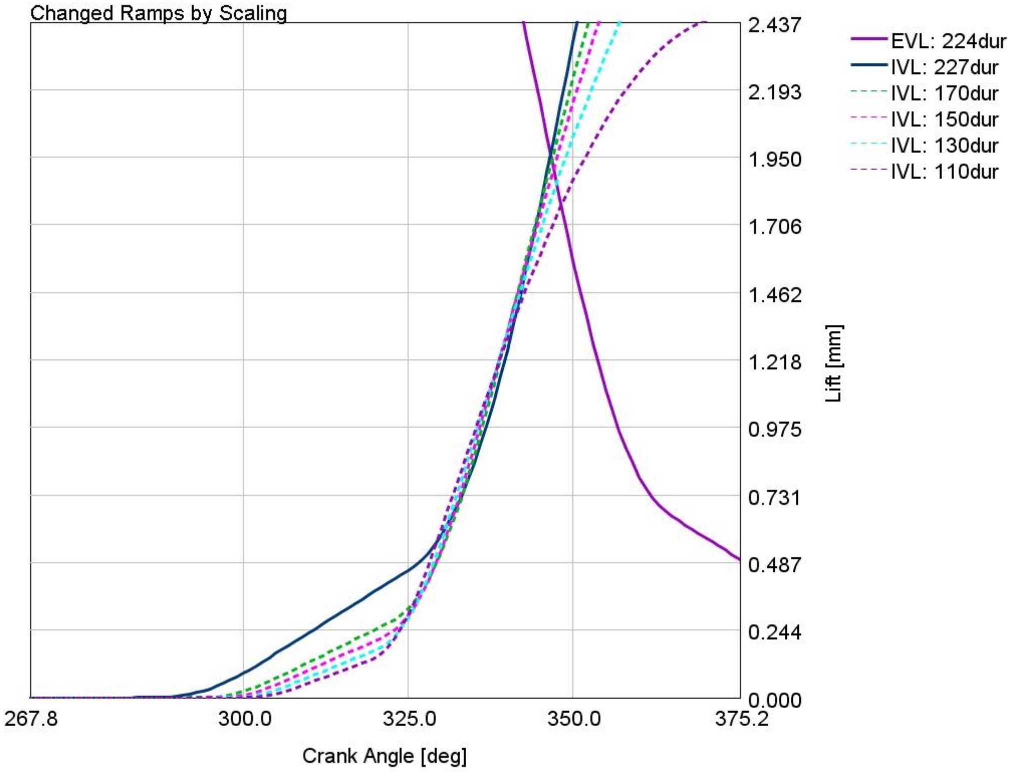

Figure 24 - Valve overlap and ramps for different camshaft profiles

The LLC is chosen based on six load points in the part load area shown in *Table 7*. The engine model is throttle load control with Wide Open Wastegate (WOW); hence the torque is reached without supercharging. The load points are evaluated for all possible cam phasing combinations regarding BSFC, the amount of residuals and if the cam is able to deliver the desired torque (i.e. operating area). When choosing cam phasing settings, the amount of residuals are carefully studied for the part load area of which high amounts of residuals is expected.

Table 7 - Torque vs. Engine Speed for the six load points

	1000 [rpm]	2100 [rpm]	3000 [rpm]
Torque [Nm]	45	45	45
Torque [Nm]	90	90	90

4.5 Switch Cam

In order to switch cam smoothly, the volumetric efficiency has to be the same in the moment of switching cam, which is accomplished by changing the cam phasing settings. Simulations are computed with WOW and Wide Open Throttle (WOT) for both the LLC and the HLC in order to know where the same volumetric efficiency occurs. The switching strategy is to use the LLC up to the load which correspond to the optimal BSFC for the LLC. When the optimal BSFC is reached for the LLC, the control system switches to the HLC with the cam phasing settings that provides the same volumetric efficiency and thereby a smooth shift is fulfilled.

The operating area of where it is possible to perform a smooth cam shift is limited by the engine speed of where the same volumetric efficiency of the LLC and HLC cannot be fulfilled with cam phasing. Therefore, simulations are carried out with increasing engine speed in order to investigate where the limit occurs.

4.6 Fully Variable Valve Train (FVVT)

A FVVT system is an alternative to a two-stage valve lift system of which the lift and duration of the valves could be more optimized over the entire load range. The FVVT enables varying lift and duration on the intake cam shaft with Dual Individual Cam Phasers (DICP) as described in Chapter 3.11. The investigation of the FVVT system is performed at 2000 rpm with increasing load. The load is evaluated at 3 bar IMEP with increasing load with spacing of 4 bar up to full load. The scaling of the original camshaft is performed in the same way as for the two-stage valve lift system; see Chapter 4.4. The range of the duration for each load point is adjusted from minimum duration of which the torque is reached with increasing spacing of 20 CAD, see *Table 8*. The lift curves with decreased duration are compared to the original duration of the HLC (227 CAD) in order to compare the benefits of the FVVT system. Up till 11 bar IMEP, the engine model is throttle load controlled with wide open wastegate. At 15 bar IMEP, the engine model is wastegate controlled with wide open throttle in order to reach the increasing load. The FVVT system is optimized with cam phasing for lowest BSFC and the residuals are limited to 30%.

Table 8 - Load (IMEP) vs. camshaft duration used for modelling

IMEP [bar]		**3**	**7**	**11**	**15**	**19**	**23**	**27**	**31**
Duration [CAD]	**110**	X							
	130	X	X						
	150	X	X	X					
	170		X	X	X	X	X	X	
	190			X	X	X	X	X	X
	207				X	X	X	X	X
	227	X	X	X	X	X	X	X	X

4.7 Part Load Comparison

VCC uses 12 Part Load Points (PLP) for evaluation of different engine concepts. These points are the 12 most used points in the NEDC and hence important to have in mind when selecting the right engine concept. These points where given for the 4-cylinder benchmark engine and by equation (3.1) and the fact that the 3-cylinder engine has 75% of the 4-cylinder displaced volume since a cylinder is removed, the corresponding BMEP is calculated by equation (4.1).

$$(3.1)\ and\ V_{d,3} = \frac{3}{4} V_{d,4} \qquad \rightarrow bmep_3 = \frac{4}{3} \cdot bmep_4 \qquad (4.1)$$

The part load points (PLP) are seen in *Table 8*.

Table 9 - Modelled Part Load Points for the 3- and 4-cylinder engine

Part Load Point (PLP)	RPM	$BMEP_4$ [bar]	$BMEP_3$ [bar]
1	1000	1.5	2.00
2	1000	4	5.33
3	1000	8	10.67
4	1500	1	1.33
5	1500	2.62	3.49
6	1500	5	6.67
7	1500	10	13.33
8	1750	8	10.67
9	2000	2	2.67
10	2000	5	6.67
11	2500	5.5	7.33
12	2500	8	10.67

To enable a better comparison between the 4-cylinder benchmark engine and the 3-cylinder concept, the same heat transfer model and initial parameters were used on both models. These were chosen as same parameters as used on the 3-cylinder model and hence also the same as used for all models during the project. The three main changes to the 4-cylinder model was changing the cylinder heat transfer model, using the same initial temperatures and setting the 50% mass fraction burned (tb50) point to 8 CAD ATDC. Both models was tested with the same valve timing settings and the best setting with respect to ISFC was chosen since fuel consumption is the main focus at part load optimisation. The models are run with WOW as much as possible to decrease the pumping losses due to the fact that less throttling is needed and only if WOT operation was needed, the wastegate was throttled, hence increasing the power output of the engine until the target was met.

Since the 3-cylinder engine is evaluated at the operation point, 3bar IMEP 2000rpm, this point is also compared between the 3- and 4-cylinder engines.

4.7.1 Influence of Gas Exchange

The Gas Exchange process is evaluated at the part load point 3bar IMEP at 2000rpm for VVT settings where the exhaust valve cam phasing is the same as the standard test of 0 to +30 CAD. The intake valve cam phasing is investigated from -50 to +50 CAD to evaluate the influence of ICW at LIVC.

4.8 Integrated Exhaust Manifold

The process of evaluating the possibilities of an IEM was performed on the engine configuration with the T45 turbine with the backpressure limited to 4bar. The evaluation was done on the maximum curve and it was chosen to evaluate the possibilities of running with less enrichment to keep the maximum temperatures below the allowed limit and hence reduce the fuel consumed at maximum power output. The IEM was evaluated by changing the exhaust port lengths from 0 to 100mm, without any other change in the exhaust manifold which results in a longer distance between the exhaust valve and the turbine with increased exhaust port lengths.

4.9 Cylinder Deactivation

The process of cylinder deactivation meaning that not all cylinders are fired during each cycle was initiated by deactivation of cylinder two. This was done by keeping both the intake and exhaust valves closed at all times and not injection any fuel, resulting in that the combustion and gas exchange process was limited to cylinder one and three. The investigation was done on four part load points, the first on 3bar IMEP720 at 2000rpm. The results were compared with both the 3- and 4-cylinder engine. Since this point is calculated for the entire engine this will increase the cylinder IMEP for the case with cylinder deactivation because it will have one less cylinder to produce the same output. This result in that the cylinder deactivated 3-cylinder engine will have a cylinder IMEP720 calculated by equation (4.2).

$$\frac{3\ cylinders \cdot 3bar\ IMEP}{2} = 4.5bar\ IMEP720 = 50\%\ increase \quad (4.2)$$

Three other points were evaluated, which were the point which produced the best improvement in ISFC on the 3-cylinder compared to the benchmark 4-cylinder engine. Due to a problem of not reaching the target BMEP of 5.33bar for PLP2, the lower target (2.0bar) at 1000rpm was chosen instead. These selected points for evaluating are PLP1, PLP5 and PLP9. Both models have the same cylinder heat transfer model, initial temperatures and ignition is set to enable tb50 at 8 CAD ATDC. All runs where done using a throttle controller and wide open wastegate.

5 Results

In this chapter, the results of the obtained performance of the 3-cylinder concept engine are shown with two different configurations of turbochargers, time-to-torque performance and the evaluated technologies for improving the fuel consumption.

5.1 Maximum Load Curve

The maximum torque-curve of the 3-cylinder engine compared with the benchmark 4-cylinder engine is seen in *Figure 25*. The main difference between the 3- and 4-cylinder engines is that the 3-cylinder engine reaches the torque targets 300rpm later than the 4-cylinder engine at 1200rpm and 1500rpm. The torque knee for the 4-cylinder engine is reached at 1500rpm and at 1800rpm for the 3-cylinder engine.

With the T50 turbine, the torque at 5700rpm can be increased by 4.0% which results in an increase of the peak power by 3.1% (see Figure 25).

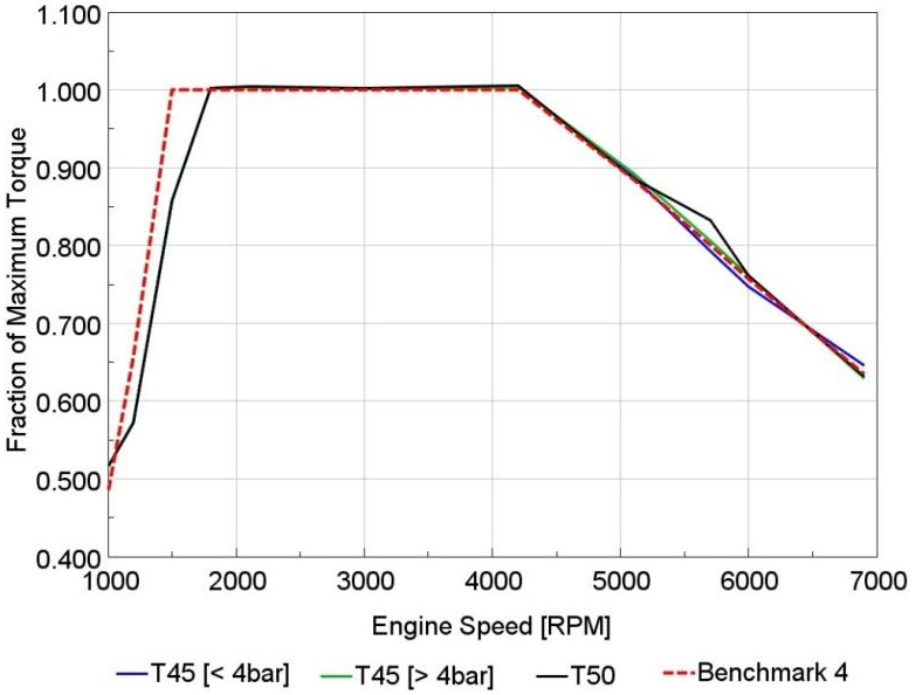

Figure 25 - Maximum torque curve [fraction of maximum target] for the 3- and 4-cylinder engine

In *Figure 26*, the compressor map is shown with the data from the three tested turbo configurations. The configuration with the T45 turbine with limited and not limited backpressure are equal up to 5100rpm were the two alternatives separate since the power output is decreased when the backpressure is limited, hence the required mass flow is not available. The T50 configuration operates at lower boost pressure levels, hence the decreased pressure ratio (seen in *Figure 27*).

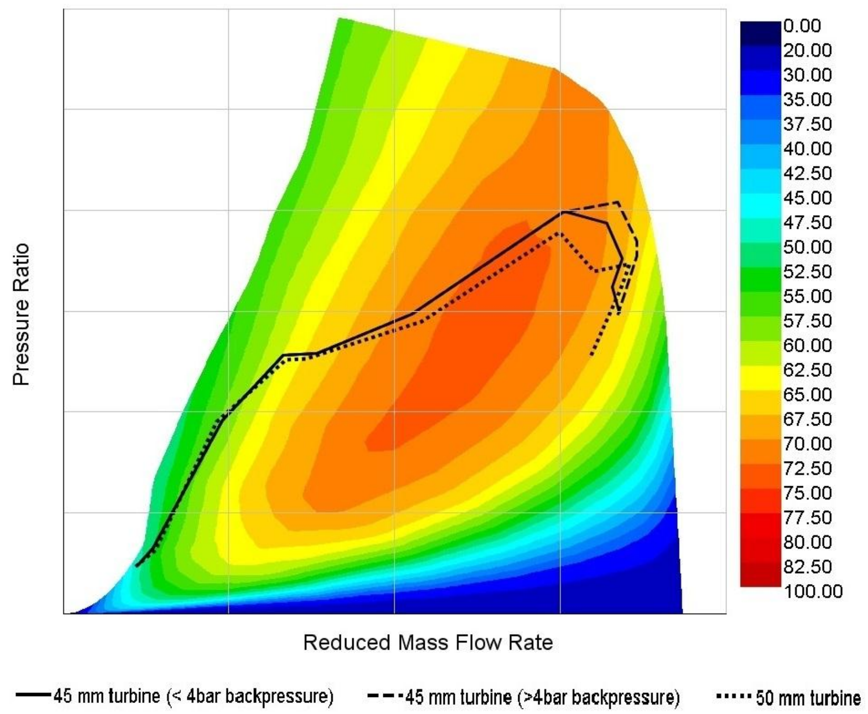

Figure 26 - Compressor map for the three configurations evaluated on the 3-cylinder engine

In *Figure 27* the absolute pressure of the grommet (the pipe between the charged air cooler and the throttle) is shown, which is the absolute boost pressure (ABP). It is seen in *Figure 27* that the ABP is similar up to the torque knee point at 1800rpm and after this point the T50 turbine configuration require less boost.

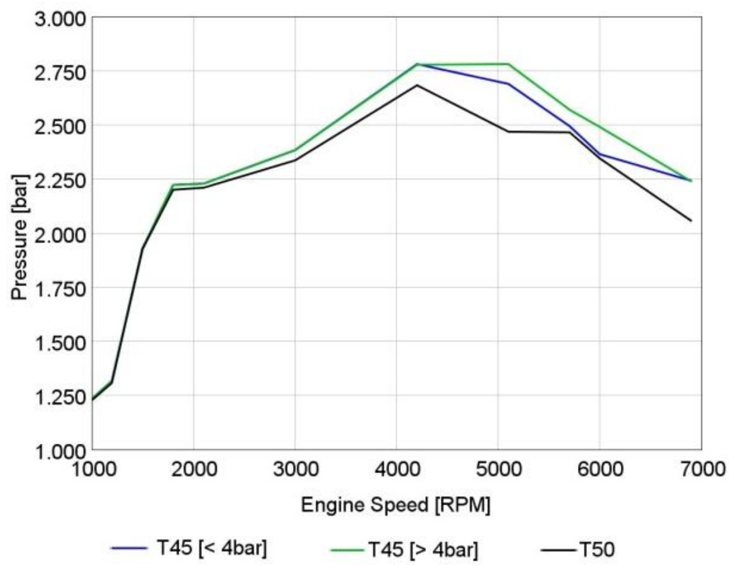

Figure 27 - Boost pressure (absolute) at the Grommet for each turbine configuration

In *Figure 28*, the wastegate diameter is shown, which is lower for the T50 turbine compared to the T45 configurations until 5100rpm where the peak power area is reached.

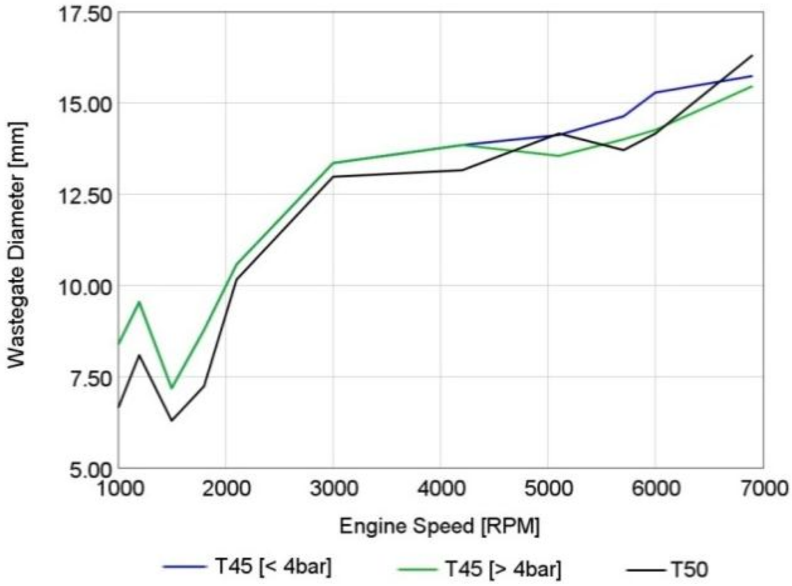

Figure 28 - Wastegate diameter vs. Engine Speed for the three turbine configurations

The exhaust runner pressure (exhaust backpressure) is shown together with the amount of residuals in *Figure 29*. The backpressure is lower for the T50 turbine compared to the T45 configurations. From 3000rpm and above, the amount of residuals are lower for the T50 configuration where the backpressure and the amount of residuals begin to differ at the same point (5100rpm) where the limited backpressure also reduces the residuals.

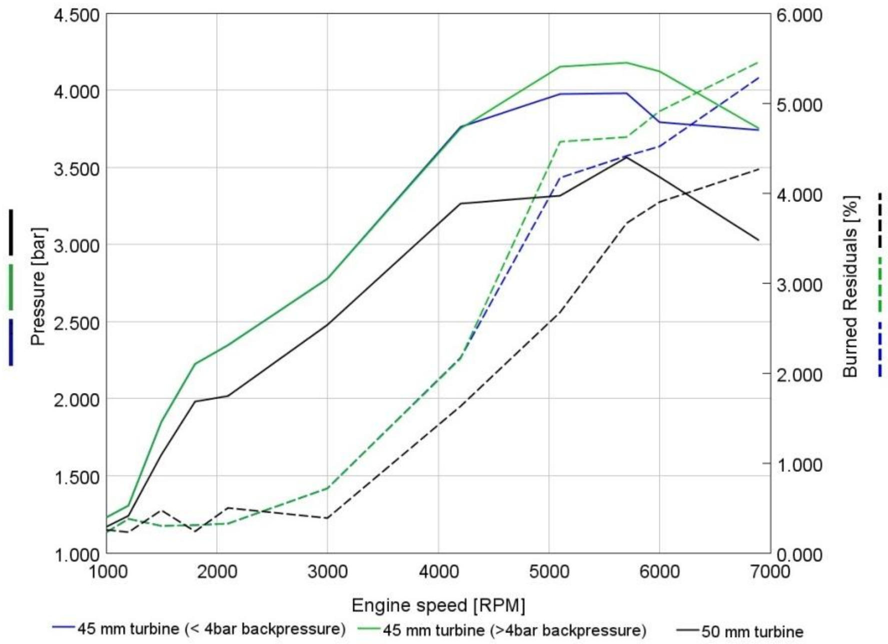

Figure 29 - Backpressure and Residuals for the three turbine configurations

In *Figure 30*, the lambda control output and exhaust manifold thermocouple temperature is shown. The T45 configuration without backpressure limitation reaches the minimum level of λ=0.75 at 5100rpm compared to the two other configurations which only reach the limit at peak power.

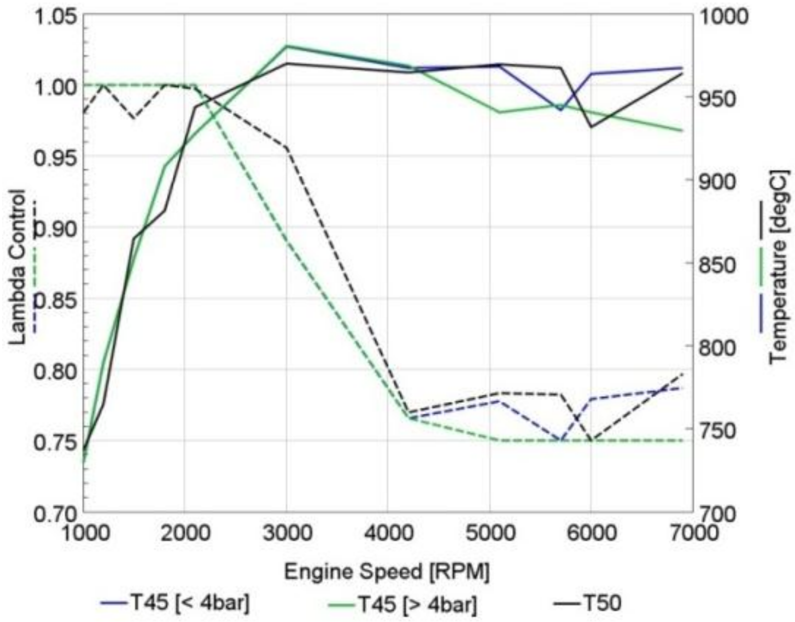

Figure 30 - Lambda controller output and Thermocouple temperature for the three turbine configurations

The shaft speed of the turbocharger is shown in *Figure 31* where the T45 configuration almost reaches the maximum allowed shaft speed of 204000rpm (201238rpm). All configurations are using the wastegate to limit the temperature when lambda reaches the $\lambda = 0.75$ limit.

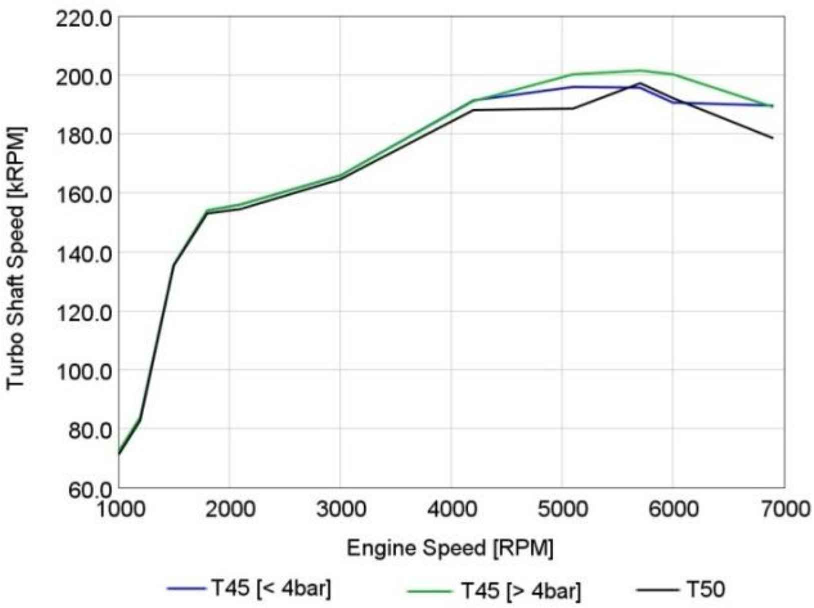

Figure 31 - Turbocharger shaft speed for the three turbine configurations

5.2 Turbocharging

The engine is designed to reach maximum power at 5700 rpm. In *Table 10-12*, the power output of each turbo configuration is compared with the benchmark 4-cylinder engine in terms of power, exhaust runner backpressure and compressor outlet pressure from 5100-6900 rpm.

In *Table 10* the results of the 45mm turbine (T45) without backpressure limitation is shown. This configuration meets all power output targets except at 5700rpm which deviates with 0.2%. The exhaust back pressure without limitation is above 4bar at 5100, 5700 and 6000rpm and has a peak compressor outlet pressure of 2.85bar absolute.

Table 10 - Power, Backpressure and Compressor Outlet Pressure for the T45

Turbine 45mm [>4.0bar]			
Engine speed [RPM]	Power [% of target]	Backpressure Exhaust runner [bar]	Outlet pressure Compressor [bar]
5100	100.7%	4.15	2.85
5700	99.8%	4.18	2.66
6000	100.5%	4.12	2.59
6900	100.6%	3.75	2.32

When limiting the exhaust runner backpressure to 4bar, it results in that the configuration with the T45 turbine does not reach its power output target at 5700 and 6000rpm. The peak compressor outlet pressure is reduced to 2.76bar at 5100rpm *Table 11*.

Table 11 - Power, Backpressure and Compressor Outlet Pressure for the limited T45

Turbine 45mm [<4.0bar]			
Engine speed [RPM]	Power [% of target]	Backpressure Exhaust runner [bar	Outlet pressure Compressor [bar]
5100	100.2%	3.98	2.76
5700	98.2%	3.98	2.58
6000	98.6%	3.79	2.46
6900	103.3%	3.74	2.33

The data from the T50 turbine is shown in *Table 12*. It reaches all power output targets with exhaust runner backpressure below 4bar and a peak compressor outlet pressure of 2.55bar.

Table 12 - Power, Backpressure and Compressor Outlet Pressure for the T50

Turbine 50mm			
Engine speed [RPM]	Power [% of target]	Backpressure Exhaust runner [bar]	Outlet pressure Compressor [bar]
5100	100.1%	3.32	2.54
5700	103.1%	3.57	2.55
6000	100.6%	3.44	2.44
6900	101.0%	3.03	2.14

5.3 Integrated Exhaust Manifold

In *Figure 32*, the results from the maximum curve for three different exhaust port lengths are shown; the original, +70mm and +100mm. The longest port length does not reach the 1500rpm torque target which the other two lengths do.

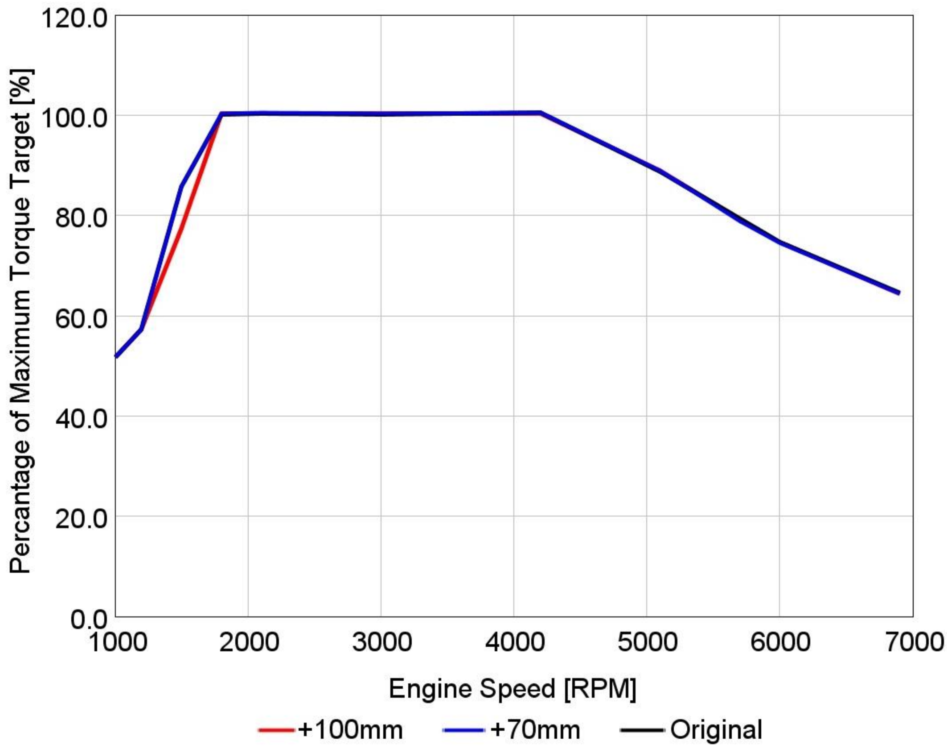

Figure 32- Torque vs. Engine speed for the IEM configurations

A test with different exhaust port lengths at 1500rpm it is seen in *Figure 33*. The figure shows that the maximum increase of the exhaust port length is 70mm with maintained torque output.

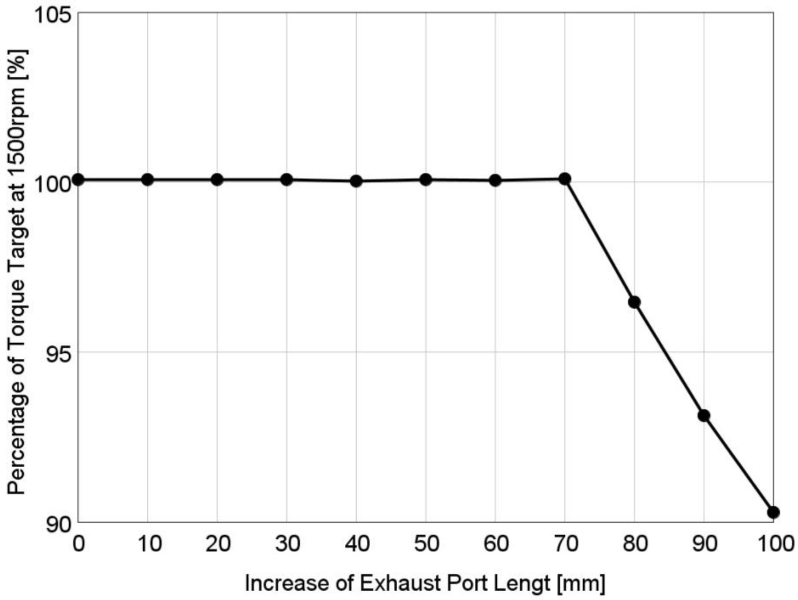

Figure 33 - Analysis of exhaust port length vs. torque at 1500rpm

In *Figure 34* it is seen that the Lambda controller output does not enrich the air/fuel mixture when increasing the exhaust port lengths. At +70mm and +100mm, the limit of 0.75 is not reached and the engine can run closer to $\lambda = 1$ at higher engine speed.

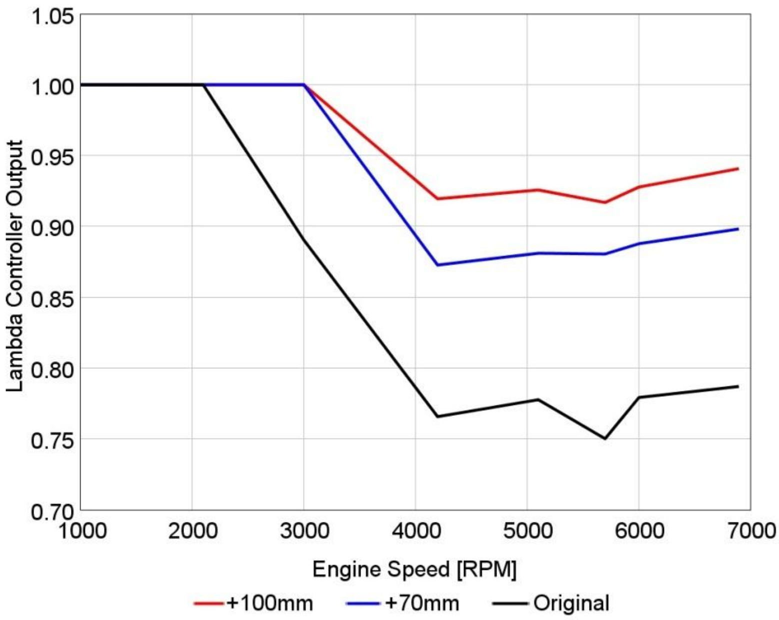

Figure 34 - Lambda controller output for the different IEM configurations

The thermocouple temperature is also reduced at engine speeds below 4200rpm compared to the original length, which is seen in *Figure 35.*

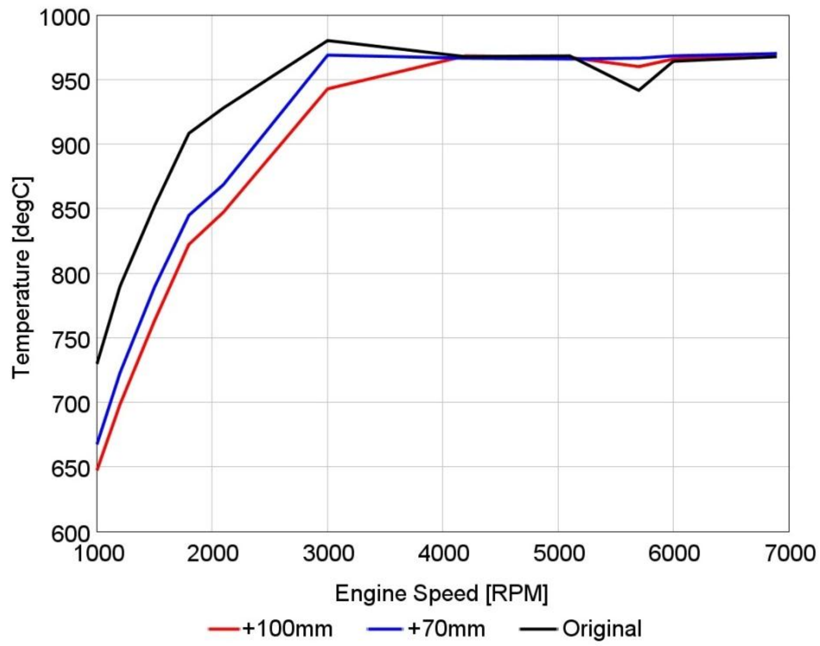

Figure 35 - Thermocouple temperature for the different IEM configurations

The wastegate diameter is decreased until the peak power area (>5100rpm) with increased exhaust port length which is seen in *Figure 36.*

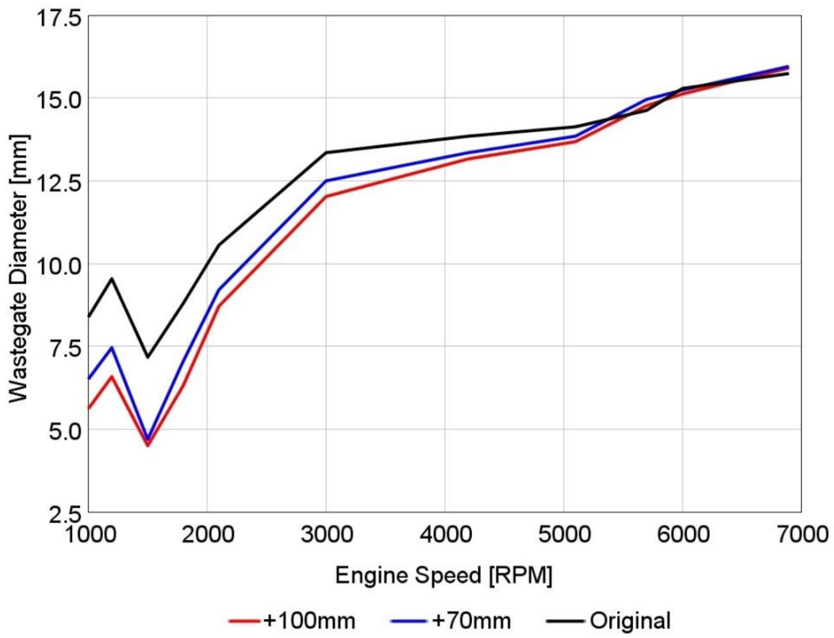

Figure 36 - Wastegate diameter for the different IEM configurations

The boost pressure at the grommet is reduced above 3000rpm with an increased exhaust port length compared to the original, which seen in *Figure 37*.

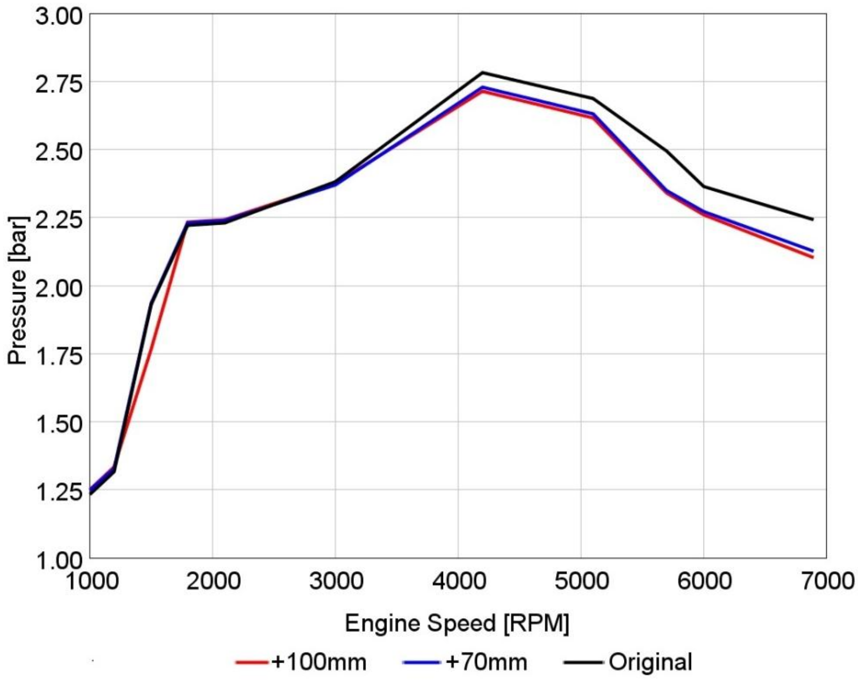

Figure 37 - Boost pressure (absolute) for the different IEM configurations

The same results as the grommet pressure are seen in *Figure 38* which shows that the resulting backpressure in the Exhaust manifold is decreased with increasing exhaust port length.

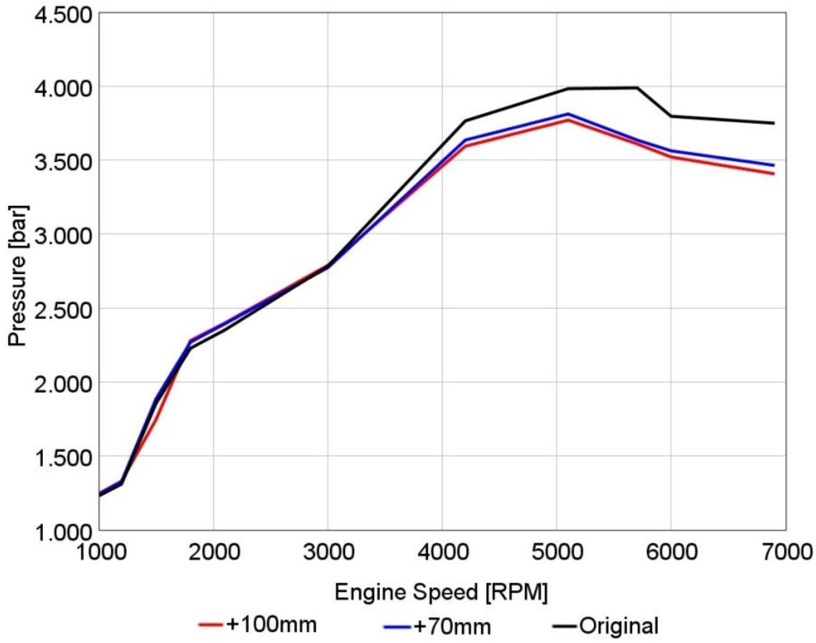

Figure 38 - Backpressure (absolute) for the different IEM configurations

5.4 Time-To-Torque (TTT)

In this section, the TTT is evaluated for the 3-cylinder engine compared to the benchmark 4-cylinder engine. The results of cam phasing strategy, engine speed, size of turbine and the inertia are presented.

5.4.1 Cam Phasing Strategy

The cam phasing strategy that is most efficient for increasing the torque in the investigated range of engine speed is in general to enable maximum overlap. In *Figure 39*, the TTT is shown for the 45 mm turbine at 1300 rpm for different valve overlap. It is shown that maximum valve overlap gives the best response and that the phasing of the intake valve has a larger influence on the TTT compared to the phasing of the exhaust valve.

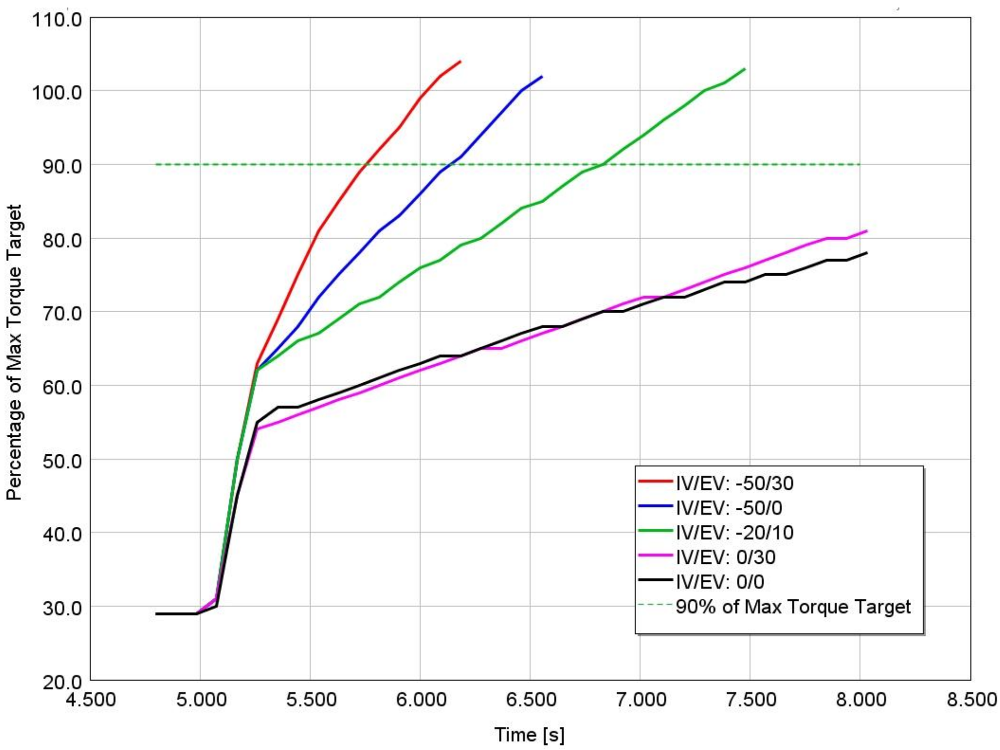

Figure 39 - TTT for the 45 mm turbine at 1300 rpm for different valve overlaps

5.4.2 Time-To-Torque Comparison, 3-Cyl vs. 4-Cyl

In *Figure 40-43*, the TTT of the 4-cylinder engine is compared with the 3-cylinder engine. Three different configurations for the 3-cylinder engine are tested and compared with the 4-cylinder engine which are:

- A 45 mm turbine with the same engine speed as the 4-cylinder engine
- A 45 mm turbine with increased engine (300 rpm relative the 4-cylinder engine)
- A 50 mm turbine with increased engine speed (300 rpm relative the 4-cylinder engine)

Figure 40 shows the TTT comparison of the 3-cylinder engine with the benchmarked 4-cylinder engine at 1000 rpm. The best alternative for the 3-cylinder engine is the 45 mm turbine at 1300 rpm that match the 4-cylinder engine (see *Table 13*). The 50 mm turbine and the 45 mm turbine (1000 rpm) do not match the 4-cylinder engine.

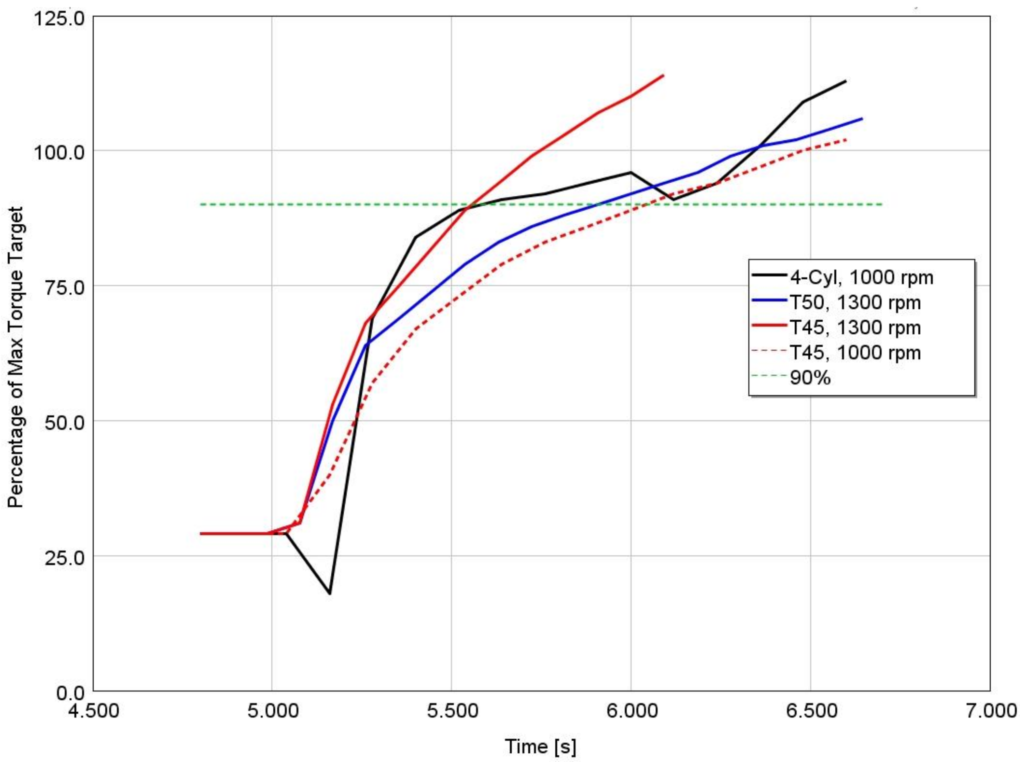

Figure 40 - TTT comparison of the 3- and 4-cylinder engine at 1000 rpm

Table 13 - Table regarding the TTT comparison of the 3- and 4-cylinder engine at 1000 rpm

Engine	Eng. Speed [rpm]	Turbine diameter [mm]	Time [s]	Time [s] 90% of max torque	Time-To-Torque [s]
4-Cyl	1000	-	5.0	5.58	0.58
3-Cyl	1300	T50	5.0	5.908	0.908
3-Cyl	1300	T45	5.0	5.555	0.555
3-Cyl	1000	T45	5.0	6.04	0.1.04

In *Figure 41*, the 4-cylinder engine is compared with the 3-cylinder engine at 1300 rpm. The 45 mm turbine with increased engine speed is marginally better compared to the 4-cylinder engine. The other two configurations do not match the 4-cylinder engine. The difference in TTT is about 0.7 to 0.9 seconds relative to the 4-cylinder engine, see *Table 14*.

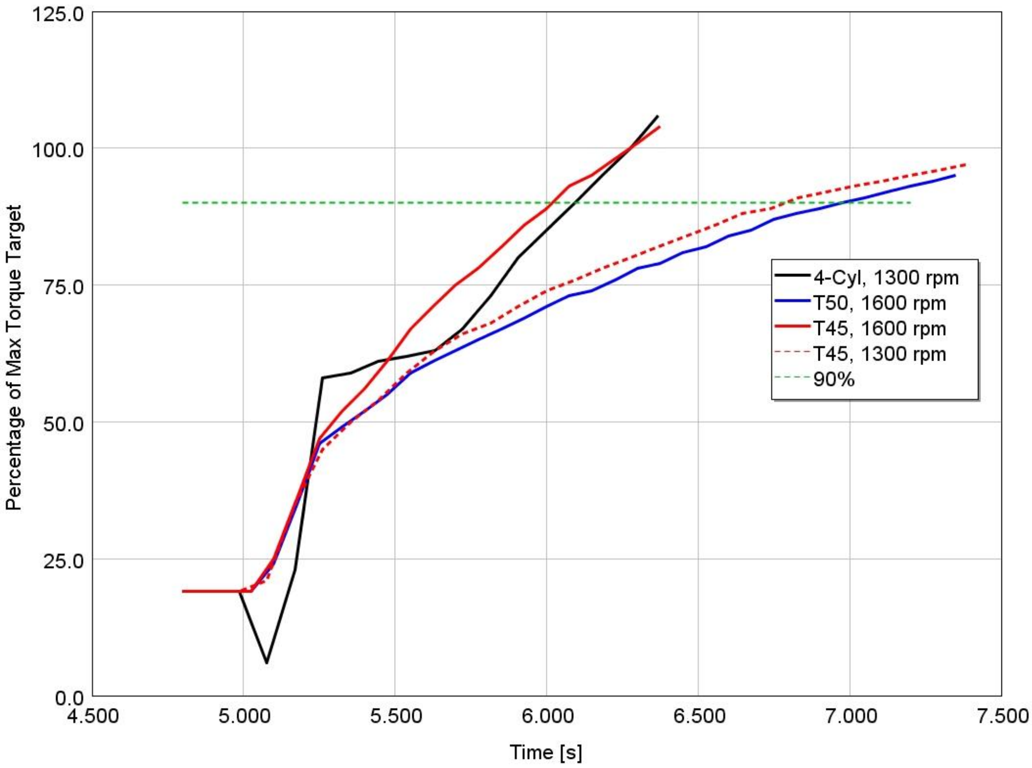

Figure 41 - TTT comparison of the 3- and 4-cylinder engine at 1300 rpm

Table 14 - Table regarding the TTT comparison of the 3- and 4-cylinder engine at 1300 rpm

Engine	Eng. Speed [rpm]	Turbine diameter [mm]	Time [s] 5 bar BMEP	Time [s] 90% of max torque	Time-To-Torque [s]
4-Cyl	1300	-	5.0	6.092	1.092
3-Cyl	1600	T50	5.0	6.975	1.975
3-Cyl	1600	T45	5.0	6.019	1.019
3-Cyl	1300	T45	5.0	6.785	1.785

In *Figure 42*, the 4-cylinder engine is compared at 1500 rpm where the 45 mm turbine of the 3-cylinder at 1800 rpm is the best alternative (see *Table 15*). The TTT is equal between the 45 mm turbine (1500 rpm) and the 50 mm turbine (at 1800 rpm) but they have 0.5 seconds longer response time compared to the 4-cylinder engine.

Regarding the 50 mm turbine, maximum valve overlap is not the best alternative. It is beneficial of starting with maximum overlap and change the phasing of the exhaust valve to 10 CAD after 6 seconds which gives the best response. The trend seen is that the overlap is preferable to decrease with increased engine speed.

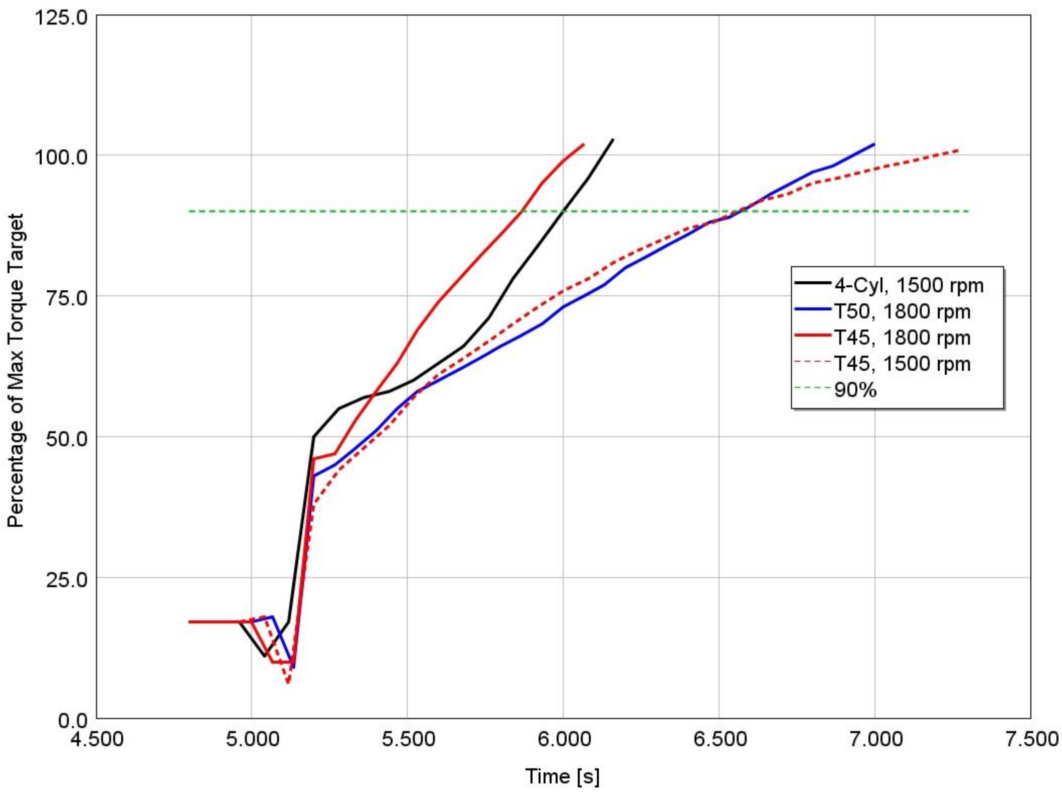

Figure 42 - TTT comparison of the 3- and 4-cylinder engine at 1500 rpm

Table 15 - Table regarding the TTT comparison of the 3- and 4-cylinder engine at 1500 rpm

Engine	Eng. Speed [rpm]	Turbine diameter [mm]	Time [s] 5 bar BMEP	Time [s] 90% of max torque	Time-To-Torque [s]
4-Cyl	1500	-	4.96	6.0	1.04
3-Cyl	1800	T50	5.0	6.567	1.567
3-Cyl	1800	T45	5.0	5.867	0.867
3-Cyl	1500	T45	4.96	6.56	1.60

In *Figure 43*, the 4-cylinder engine is compared at 2100 rpm. At this engine speed, the 45 mm turbine of both 2100 and 2400 rpm matches the 4-cylinder engine. According to *Table 16*, the TTT of the 50 mm turbine is about 0.20 seconds longer. At 2400 rpm with the 45 mm turbine, the intake cam is preferably advanced to -40 CAD instead of enable maximum valve overlap.

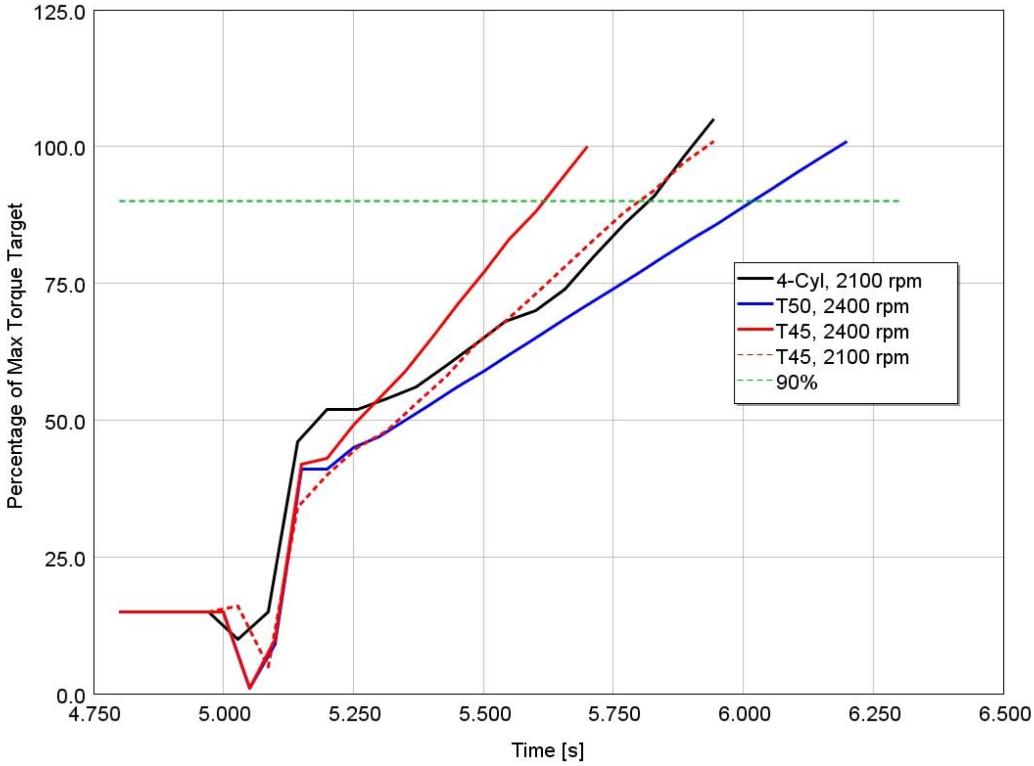

Figure 43 - TTT comparison of the 3- and 4-cylinder engine at 2100 rpm

Table 16 - Table regarding the TTT comparison of the 3- and 4-cylinder engine at 2100 rpm

Engine	Eng. Speed [rpm]	Turbine diameter [mm]	Time [s] 5 bar BMEP	Time [s] 90% of max torque	Time-To-Torque [s]
4-Cyl	2100	-	4.97	5.817	0.82
3-Cyl	2400	T50	5.0	6.017	1.017
3-Cyl	2400	T45	5.0	5.617	0.617
3-Cyl	2100	T45	4.97	5.8	0.83

5.4.3 Influence of Inertia

In *Figure 44*, the TTT is shown for the 3-cylinder engine with the 45 mm turbine at 1000 rpm, compared with the 4-cylinder engine at the same engine speed. A test is performed with different inertia for the 3-cylinder engine. The turbine and compressor configuration with the highest inertia is the same as used in the previous section (Section 5.4.2), which is the standard inertia provided by Borg Warner. The inertia of the standard turbine and compressor wheel is shown by the blue line in *Figure 44* and the configuration with decreased inertia is represented by the purple line. The inertia and TTT response are listed in *Table 17* which shows that the TTT is much improved by decreasing the inertia (0.32 s).

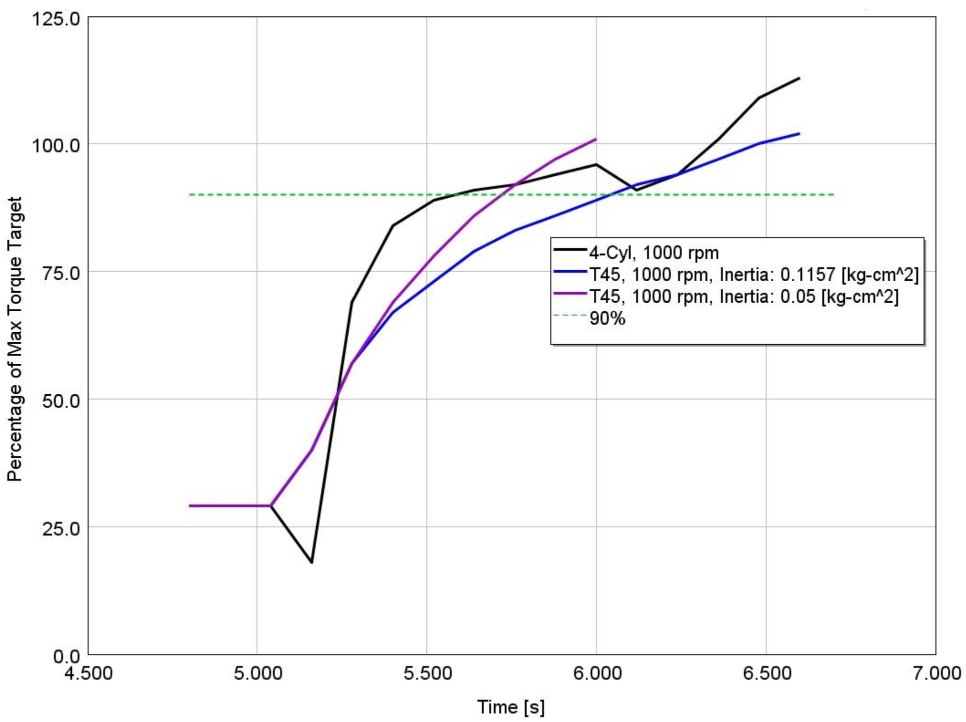

Figure 44 - TTT for different inertias for the T45 at 1000rpm

Table 17 - Table regarding the TTT for different inertias for the T45 at 1000rpm

Engine	Eng. Speed [rpm]	Inertia [kg- cm^2]	Time [s] 5 bar BMEP	Time [s] 90% of max torque	Time-To-Torque [s]
4-Cyl	1000	-	5.04	5.58	0.54
3-Cyl	1000	0.1157	5.04	6.04	1.00
3-Cyl	1000	0.050	5.04	5.72	0.68

In *Figure 45*, a similar investigation of the inertia is performed for the 50 mm turbine. The engine speed of the 3-cylinder engine is increased with 300 rpm compared to the 4-cylinder engine. Three different moments of inertia are tested for the turbine and compressor configuration of which the blue curve in *Figure 45* is representing the one with standard inertia. According to *Table 18*, the turbine and compressor with the inertia of 0.11 kg-cm^2 match the TTT of the 4-cylinder engine which it should.

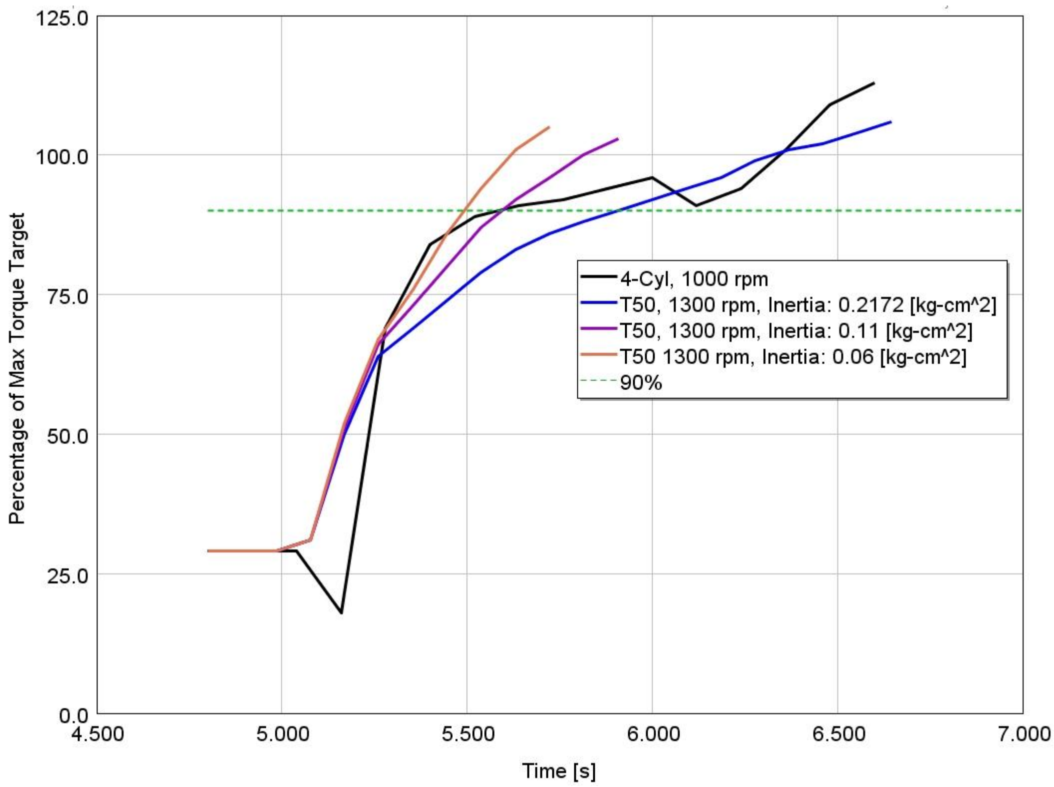

Figure 45 - TTT for different inertias for the T50 at 1300rpm

Table 18 - Table regarding the TTT for different inertias for the T45 at 1300rpm

Engine	Eng. Speed [rpm]	Inertia [kg-cm^2]	Time [s] 5 bar BMEP	Time [s] 90% of max torque	Time-To-Torque [s]
4-Cyl	1000	-	4.98	5.58	0.60
3-Cyl	1300	0.2172	4.98	5.91	0.93
3-Cyl	1300	0.110	4.98	5.59	0.61
3-Cyl	1300	0.060	4.98	5.49	0.51

5.5 Influence of Compression Ratio and Combustion Efficiency

This investigation is made in order to see which influence the compression ratio (CR) and the combustion efficiency (CE) have on the fuel consumption. The standard settings of the engine model which all results are based on are simulated with the CR of 9.8 and the CE of 95%. Since the CR is decreased relative to the benchmark engine (from 10.3 to 9.8) due to uncertainties of knock, the effect on the fuel consumption is investigated as well as the influence of the CE which is presented in *Table 19*. The results are compared relative to the standard settings at the part load of 3 bar IMEP at 2000 rpm. The duration of the intake camshaft used is 150 CAD (same as the LLC of the two-stage valve lift system).

The difference of the CR between 9.5 and 10.3 resulted in a maximum 2% difference in fuel consumption. Comparing the standard CR of 9.8 with the higher and lower CR, the deviation in fuel consumption is 1%. Between the ideal case of 100% CE and the standard case, the deviation in fuel consumption ascended to 2%. The largest potential of improvement in terms of fuel consumption between the standard settings compared to the highest CR and CE is 3%.

Table 19 - Difference of BSFC relative to the standard settings (3bar IMEP 2000rpm)

CR [-] CE [%]	9.5	9.8	10.3
90	-3%	-3%	-2%
95	-1%	**ref**	+1%
100	+1%	+2%	+3%

5.6 Influence of Gas Exchange

The pumping losses comparison between PMEP and adjusted PMEP are seen in *Figure 46* (the pumping losses in Figure AA are negative in reality). The red dotted line in *Figure 46* represents the adjusted PMEP which is obtained by *equation (3.8)*, i.e. it is the sum of the PMEP, EVO losses and ICW. Also seen in *Figure 46* is that the PMEP and the adjusted PMEP are almost equal at intake cam phasing from -50 CAD to -10 CAD, where the ICW is increasing from 0.01bar (IV: -10) to 0.18bar at minimum overlap (IV: 50).

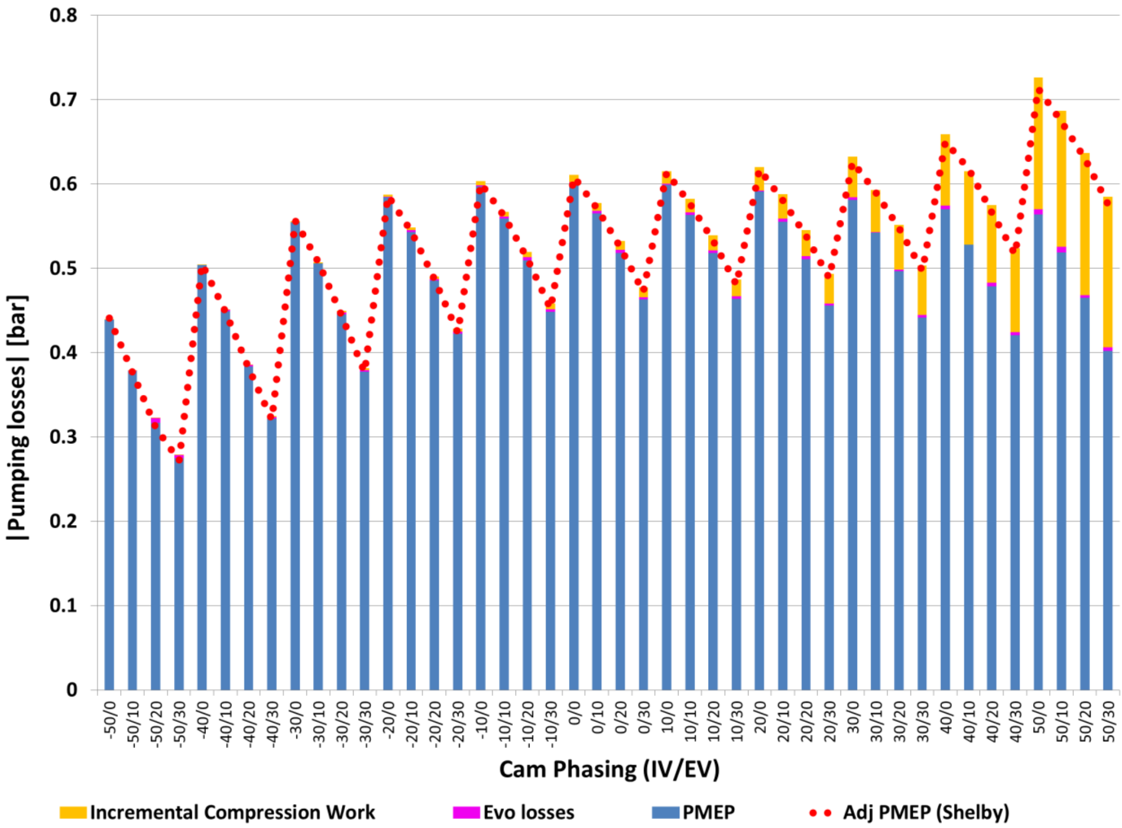

Figure 46 - Pumping losses at 3bar IMEP 2000rpm for different VVT settings

In *Figure 47*, the normalized total pumping losses are shown. It is seen that the ICW increases from the intake cam phasing setting of -10 CAD towards +50 where the maximum is located. It is also seen that the EVO losses are only a few percent of the total pumping losses. The biggest contributions of the total pumping losses are Shelby´s Area B which is the Intersection Pumping Integral and it represents 98% at maximum overlap to 63% at minimum overlap.

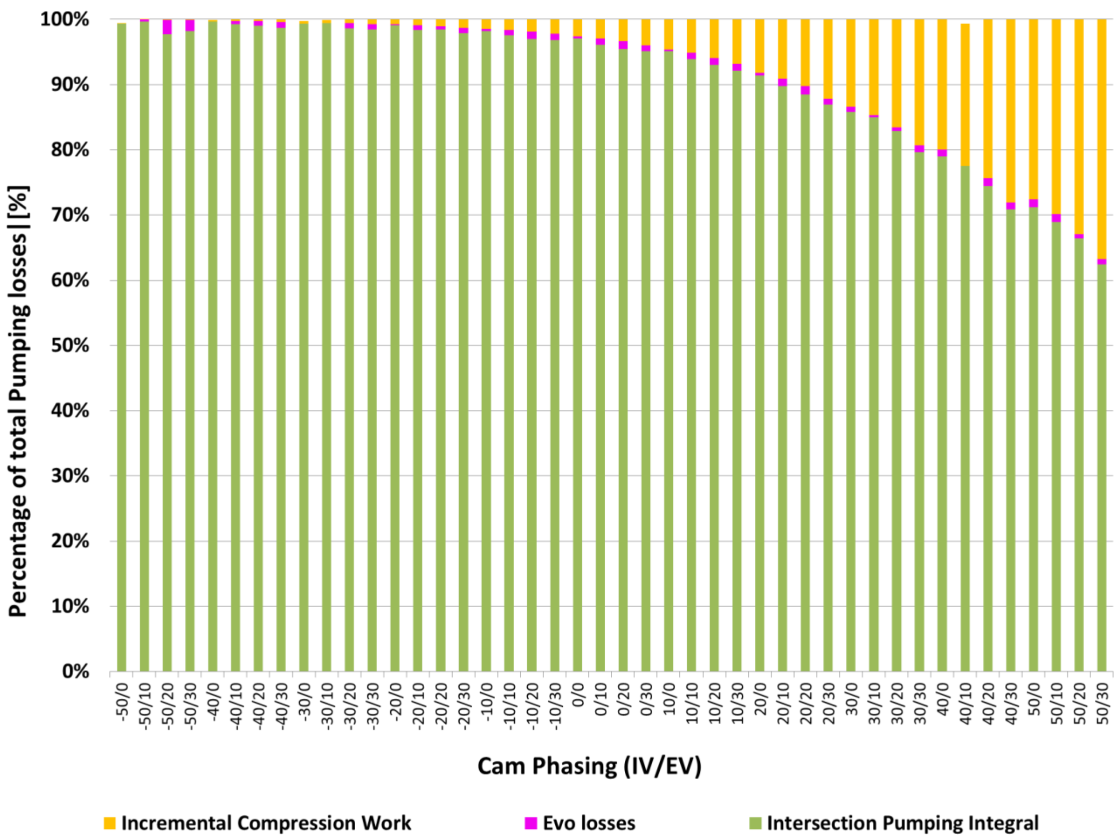

Figure 47 - Percentage of total Pumping losses at 3bar IMEP 2000rpm for different VVT settings

PMEP$_{adj}$ of the four different exhaust cam phasing settings (0, 10, 20, 30 CAD) with respect to the intake cam phasing (x-axis) are seen in *Figure 48*. Two relationships are seen in *Figure 48*. With later cam phasing on either the exhaust or the intake cam results in higher pumping losses. The lowest losses are at maximum valve overlap (-50/30) and the highest losses are at minimum valve overlap (50/0).

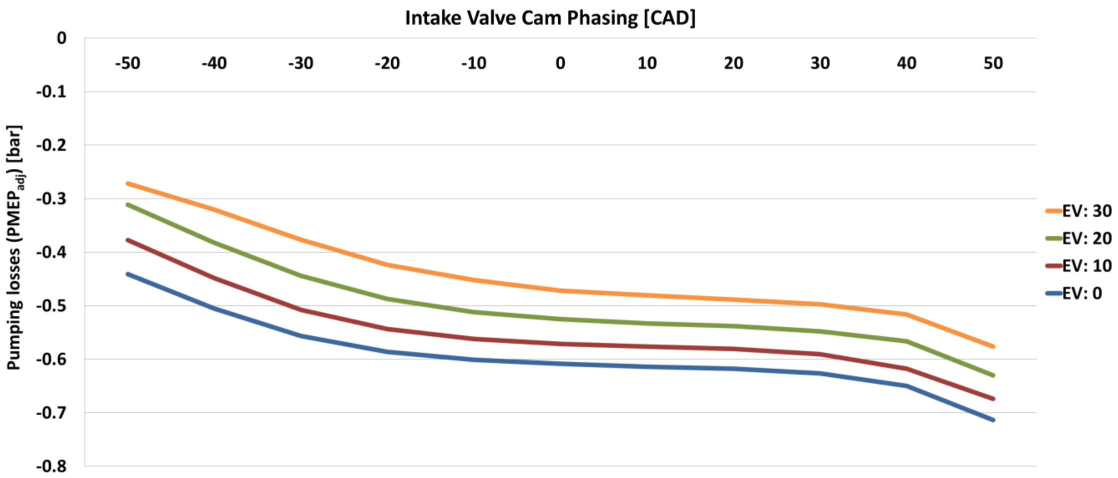

Figure 48 - PMEP$_{adj}$ at 3bar IMEP 2000rpm for different VVT settings

The resulting Intersection Pumping Integrals (Shelby´s Area B) for the part load point is seen in *Figure 49* for each exhaust valve cam phasing with respect to the intake cam phasing. Each curve has similar shapes with global minimum of Area B at maximum overlap and the global maximum of Area B at minimum overlap. There is also a local maximum at IV -20 CAD and local minimum between IV 20-30 CAD.

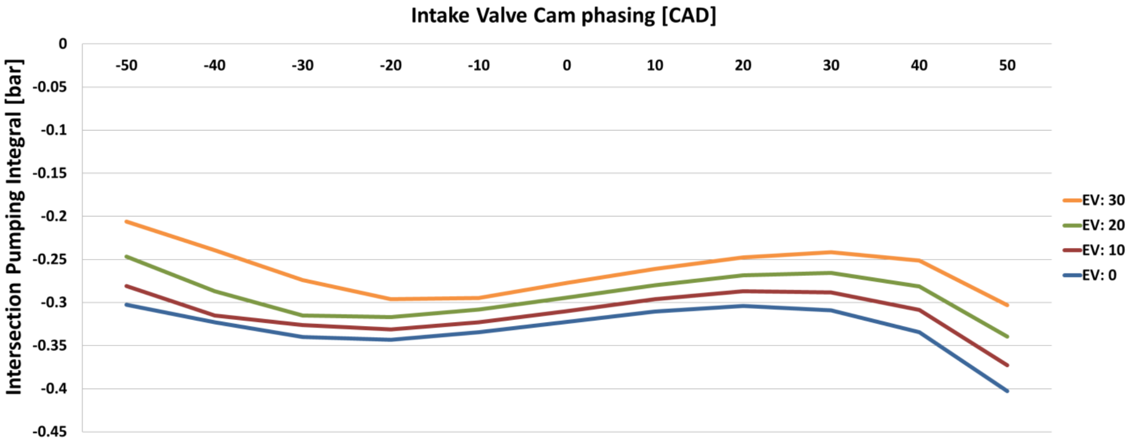

Figure 49 - Intersection Pumping Integral at 3bar IMEP 2000rpm for different VVT settings

5.7 Two-Stage Valve Lift

The duration of the LLC is chosen to 150 CAD, which is a compromise between the operating area and the ability of the cam to reduce the pumping losses at light load. In *Figure 50*, the lift curves of the exhaust cam, LLC and HLC are shown. The LLC is scaled from the HLC with respect to maintain the same valve overlap as the HLC. The lift of the HLC and LLC is 8.6 and 4 mm respectively.

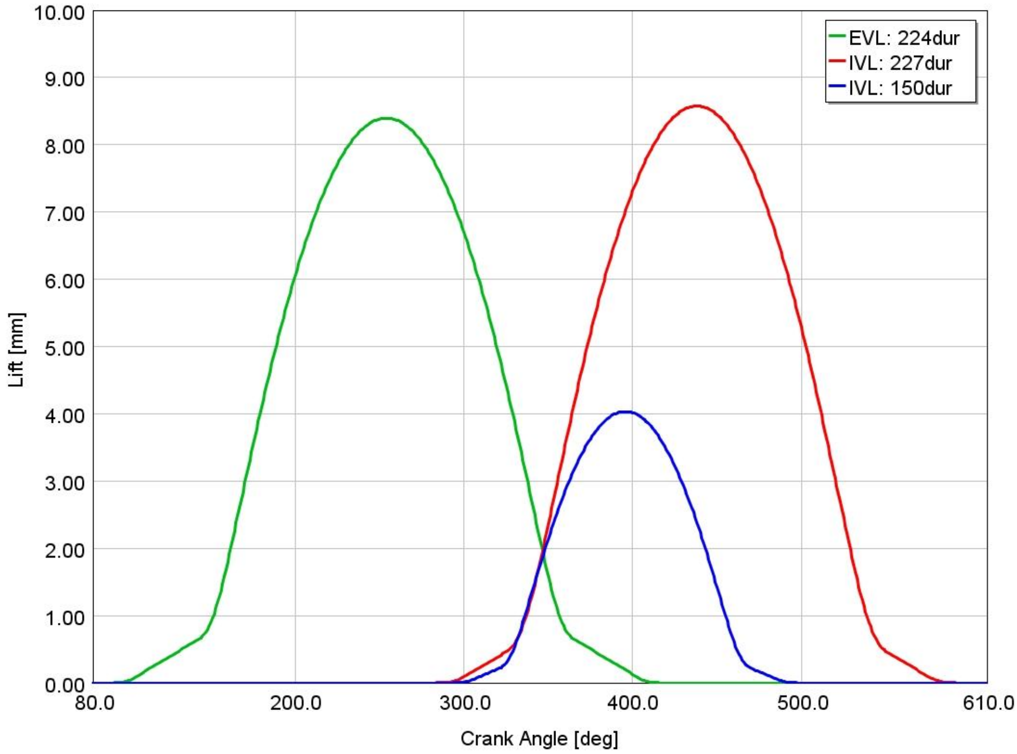

Figure 50 - Lift curve for the 150 and 227 camshafts

In *Table 20*, the LLC and HLC on the intake side are compared regarding BSFC. The comparison is made for six load points for the engine speed of 1000, 2100 and 3000 rpm at 45 and 90 Nm. The BSFC values in *Table 20* are generated with optimized cam phasing settings. The change in BSFC is also shown in the table for the six load points of which the largest improvement is 2.7%.

Table 20 - Results from the six load points for the two camshafts (150 and 227)

Engine Speed [RPM]	Torque [Nm]	BSFC 227 dur [g/kWh]	BSFC 150 dur [g/kWh]	Change of BSFC [%]	Phasing 227 dur: IV/EV	Phasing 150 dur: IV/EV
1000	**45**	319.6	311	2.7	0/20	-40/30
	90	271.5	272	0	-50/30	-20/30
2100	**45**	305.7	300	1.9	-50/10	-40/30
	90	257.4	257.7	0	-50/20	-20/20
3000	**45**	304.8	300.2	1.5	-50/20	-40/30
	90	255.7	255.5	0	-50/10	-10/20

In *Table 21*, the pumping work ($PMEP_{adj}$) is shown for both the LLC and HLC. The difference of the pumping work is clearly correlated to the improvement in BSFC for the LLC. The difference in pumping work and BSFC decreases with increased load and engine speed. Above 90 Nm, there is no gain of using the LLC compared to the HLC regarding BSFC.

Table 21- PMEPadj for the LLC and HLC

Engine Speed [RPM]	[Nm]	$PMEP_{adj}$ 227 dur	$PMEP_{adj}$ 150 dur	Change of PMEP [%]
1000	45	-0.278	-0.1627	41.4
	90	-0.139	-0.12329	11.1
2100	45	-0.314	-0.26708	14.9
	90	-0.195	-0.20398	-4.8
3000	45	-0.354	-0.33275	6.1
	90	-0.349	-0.32343	7.3

The largest difference between the pumping work of the investigated load points is at 1000 rpm at 45 Nm (see *Table 21*). In *Figure 51*, the pumping loop is illustrated for the LLC and HLC for the cam phasing settings with the lowest BSFC. The area of the LLC, which enables EIVC is clearly smaller than the area of the HLC.

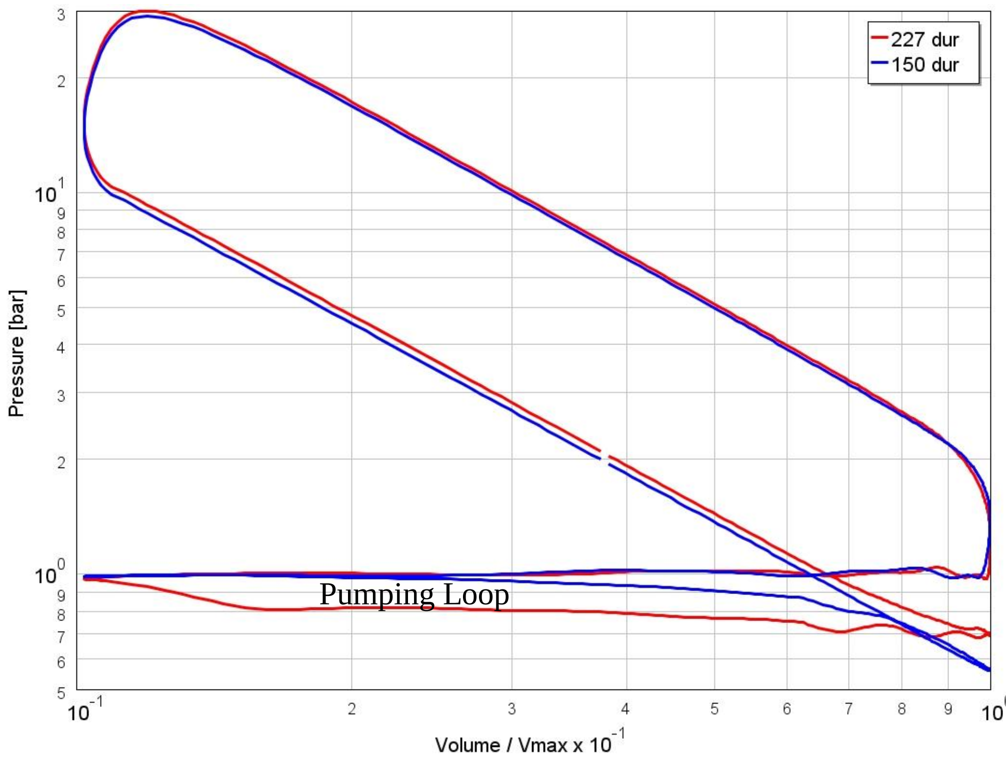

Figure 51 - Pumping loop for the LLC and HLC

At part load and low engine speed, the cam phasing settings are limited for the HLC due to the high amount of residuals. In *Figure 52*, the amount of burned residuals is shown for the various cam phasing settings for the part load point of 45 Nm at 1000 rpm. Due to that the amount of residuals are limited to 30%, the cam phasing is also limited. In *Figure 53*, the BSFC is plotted for the cam phasing settings where the limit of 30% residuals is shown. The cam phasing settings for the best BSFC in *Table 20* are chosen for each load point with the same method as illustrated by *Figure 52* and *Figure 53*.

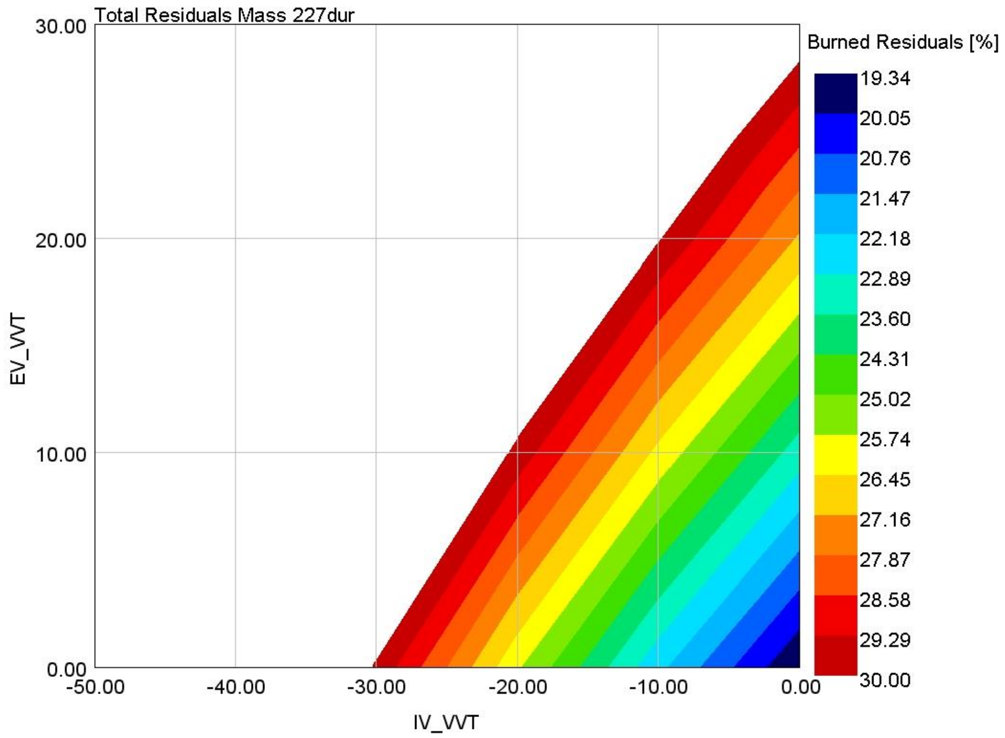

Figure 52 - Burned residuals for the various cam phasing settings (45 Nm at 1000 rpm)

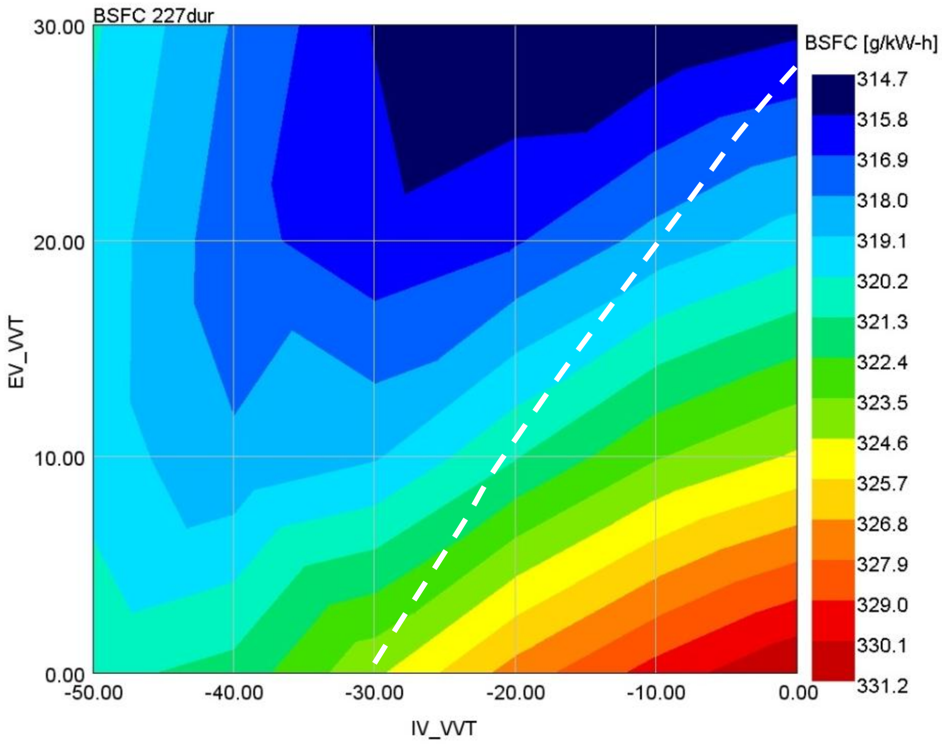

Figure 53 - BSFC for the various cam phasing settings (45 Nm at 1000 rpm)

In *Figure 54* and *55*, the BSFC and the amount of residuals are shown for both the LLC and HLC (45 Nm and 1000 rpm). The amount of residuals is limiting the cam phasing settings for the HLC but not the LLC.

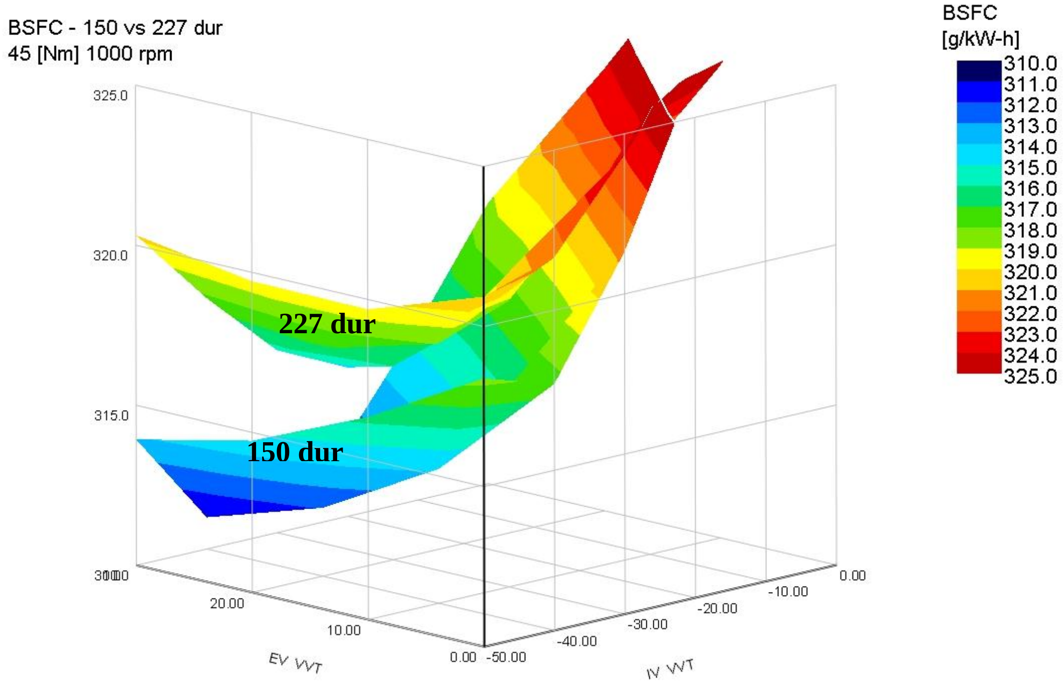

Figure 54 - BSFC for the HLC and LLC at 45 Nm and 1000 rpm

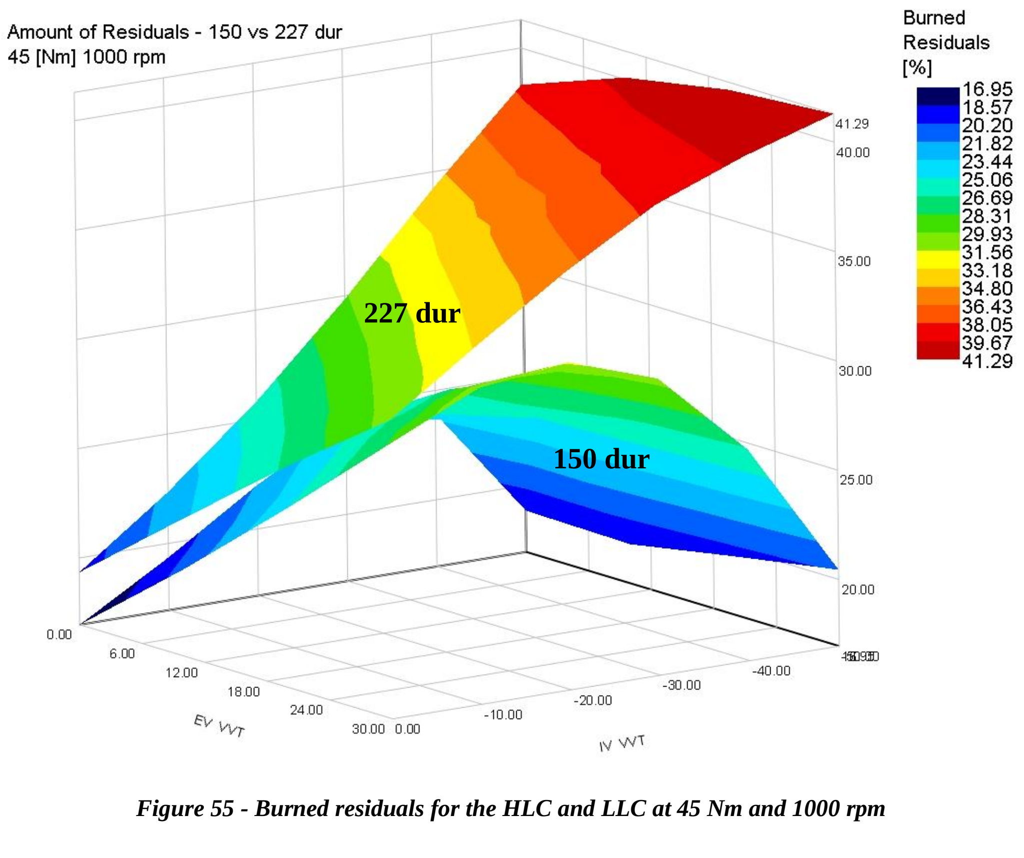

Figure 55 - Burned residuals for the HLC and LLC at 45 Nm and 1000 rpm

5.7.1 Switch Cam

The criterion to succeed with a smooth cam shift is that the same volumetric efficiency is obtained by the cam phasing for both the LLC and HLC. In *Figure 56*, the crossing section of the volumetric efficiency versus cam phasing is shown between the LLC and the HLC at 1000 rpm. *Figure 57* shows the BSFC contour plot of the LLC with the optimal cam phasing settings of both the LLC and HLC. It also shows the crossing section of the volumetric efficiency in the XY-plane of which the cam phasers have to adjust to before switching cam to obtain the same volumetric efficiency.

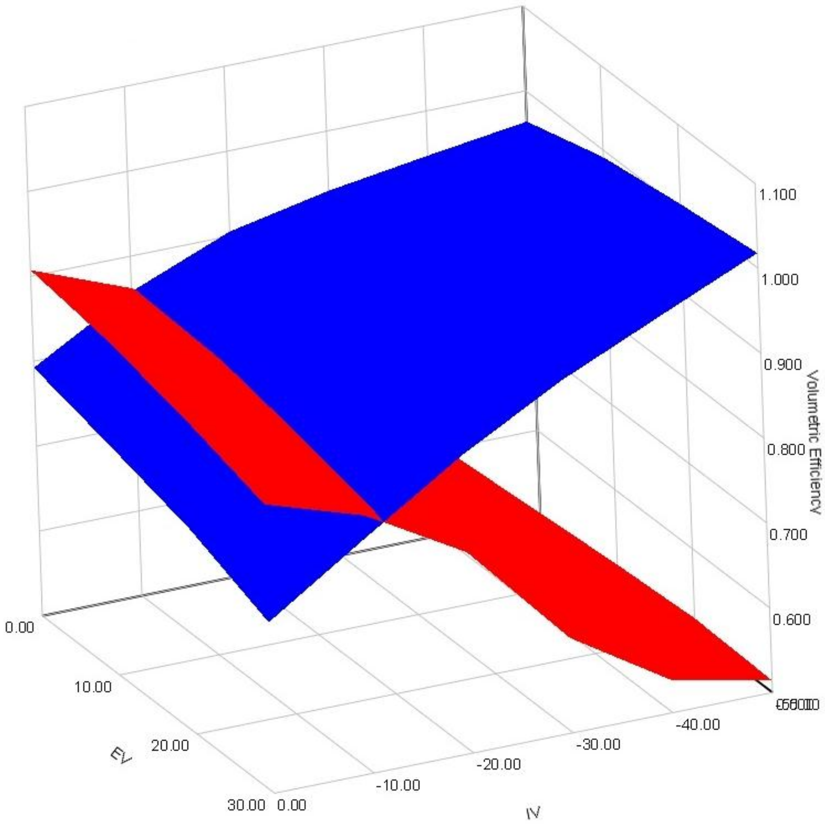

Figure 56 – Volumetric efficiency for the HLC and LLC at 45 Nm and 1000 rpm

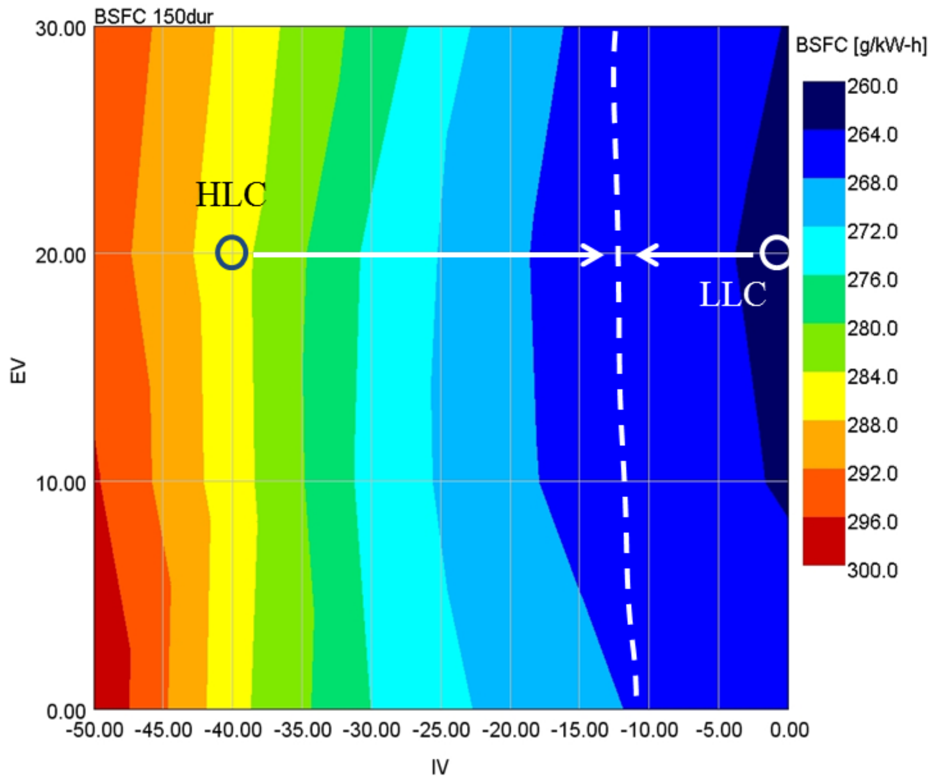

Figure 57 - BSFC for the HLC and LLC at 45 Nm and 1000 rpm

In *Table 22*, the optimal BSFC of both the LLC and HLC are shown where the BSFC of the HLC is better compared to the LLC.

During the event of switching cams, the cam phasers is adjusting the phasing from the optimal settings for best BSFC of each cam, to the phasing of which the same volumetric efficiency is obtained. The phasing of the LLC at 1000 rpm for the switch of cam is from 0 to -12 (interpolated) CAD and from -40 to -12 (interpolated) CAD for the HLC. At the switch event, it is only the intake cam that is adjusted and the exhaust cam is the same as for the optimal BSFC. The maximum torque of the LLC is about 110 Nm when switching cams based on the cam phasing settings from the starting point providing the optimal BSFC.

Table 22 – Table of the optimal BSFC for the LLC and HLC

1000 [rpm]	LLC, 150 dur [CAD]	HLC, 227 dur [CAD]
Optimal BSFC [g/kWh]	263	261
BSFC at Cam Shift [g/kWh]	265	
Torque at Cam Shift [Nm]	~110	
IV [CAD]	0	-40
IV at Cam Shift [CAD]	-12 (interpolated)	
EV [CAD]	20	20

In *Figure 58*, the cross section of the volumetric efficiency versus cam phasing is shown for the LLC and HLC at 1800 rpm. The cross section is almost at the limit of phasing of the intake cam, which means that 1800 rpm is the maximum engine speed of where the switch of cam could be made in order to switch cam with the same volumetric efficiency.

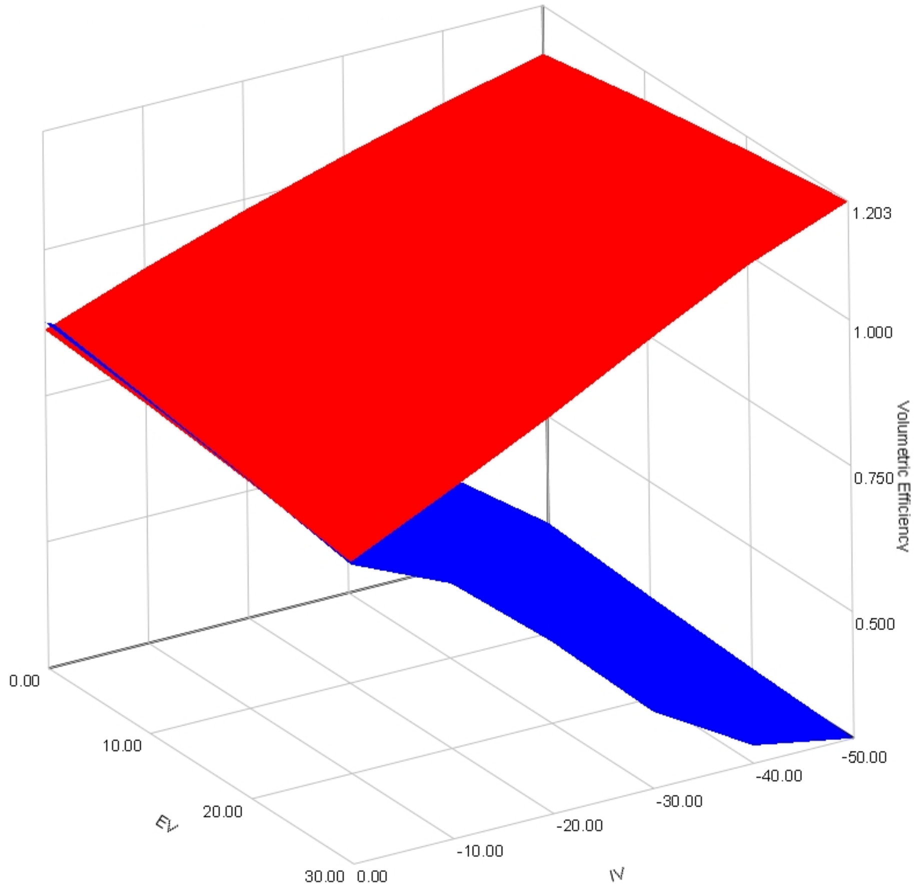

Figure 58 - Cross section of the volumetric efficiency vs. cam phasing for the LLC and HLC at 1800 rpm

Figure 59 shows the contour plot of the BSFC for the LLC for various cam phasing settings at 1800rpm. The cross section where the LLC and HLC have the same volumetric efficienc is also illustrated with the optimal cam phasing settings of the cams.

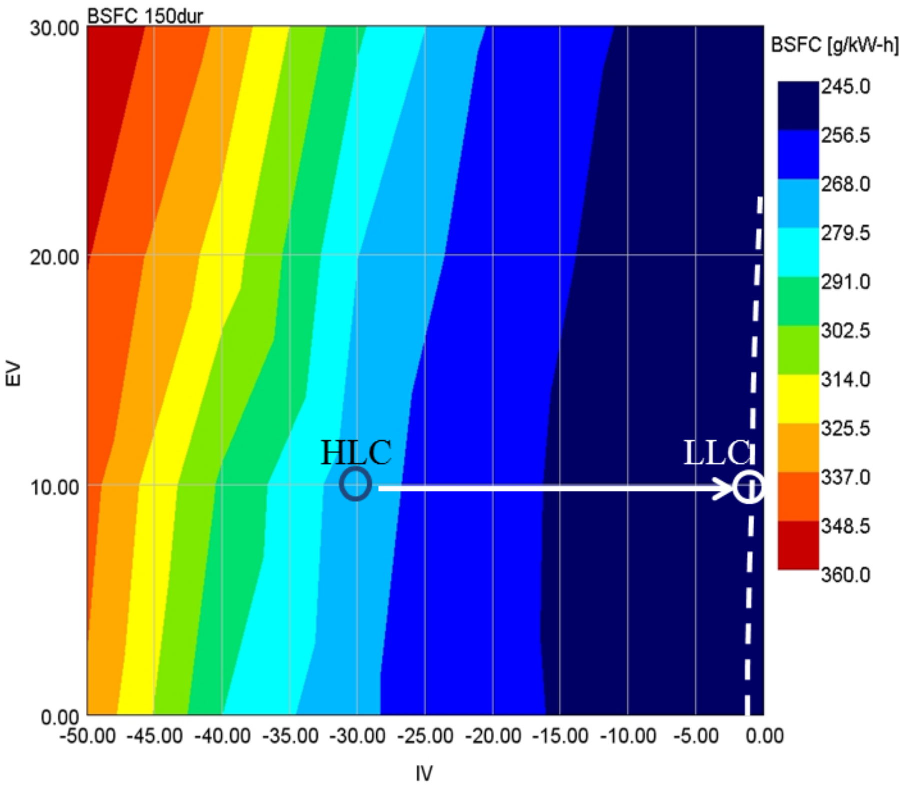

Figure 59 - BSFC for the LLC and HLC for various cam phasing settings at 1800rpm

The cam phasing settings for the optimal BSFC for the LLC and HLC are shown in *Table 23*. The exhaust cam phasing do not change when switching cam but the intake cam have to be adjusted from -30 to -1 (interpolated) CAD for the HLC and from 0 to -1 (interpolated) CAD for the LLC. The maximum torque of the LLC is 122 Nm when the switch of cam occurs.

Table 23 - VVT settings for optimal BSFC for the LLC and HLC at 1800rpm

1800 [rpm]	150dur [CAD]	227dur [CAD]
Optimal BSFC [g/kWh]	249	245
BSFC at Cam Shift [g/kWh]	249	
Torque at Cam Shift [Nm]	122	
IV [CAD]	0	-30
IV at Cam Shift [CAD]	-1 (interpolated)	
EV [CAD]	10	10

It is also possible to shift cam where higher torque is reached by closing the wastegate. A simulation is performed at 1800 rpm with the wastegate diameter set to 10 mm (compared to 20 mm at wide open wastegate). In *Figure 60*, the cross section of the volumetric efficiency is shown which is above one due to the turbocharging.

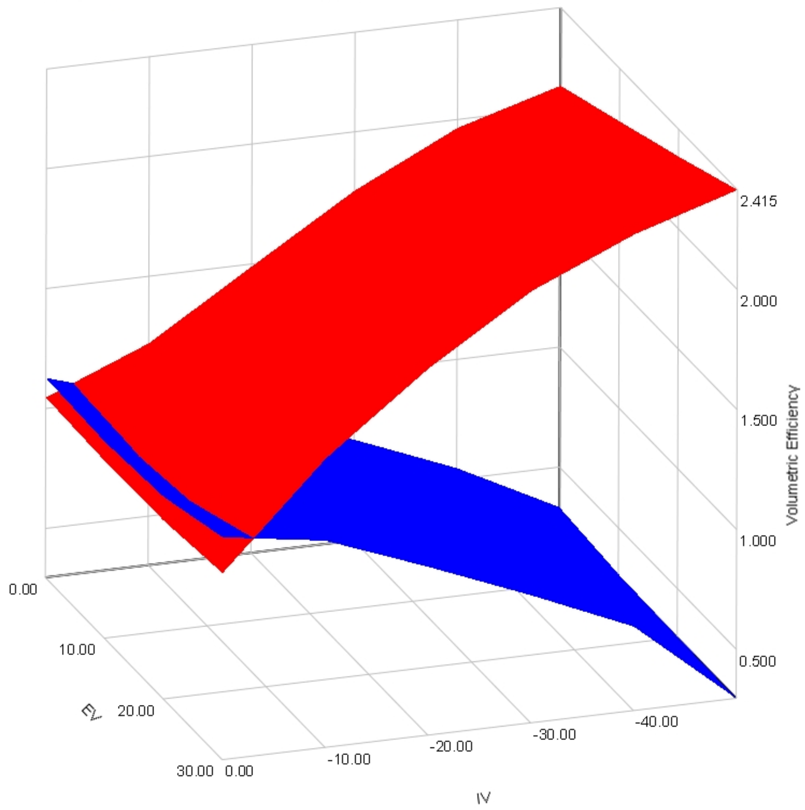

Figure 60 - The cross section of the volumetric efficiency for the HLC and LLC

The difference noticed when using the wastegate to increase the torque is that also the exhaust cam phasing settings is changing for shifting cam from the optimal settings regarding BSFC. In *Figure 61*, the optimal cam phasing settings are shown for both cams and to which cam phasing settings that have to be adjusted to when shifting cam.

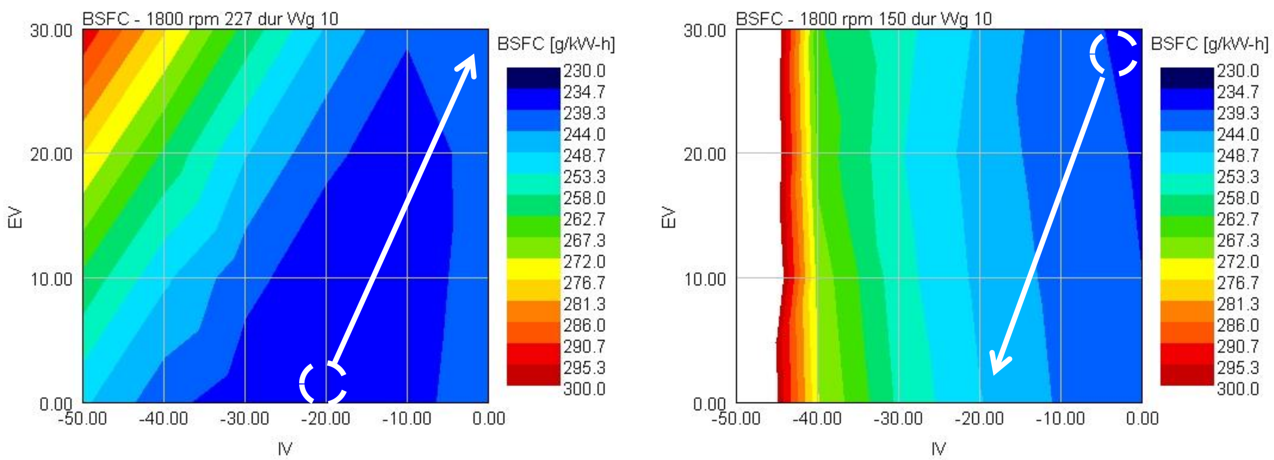

Figure 61 - VVT settings for the switch between HLC to LLC

5.8 Fully Variable Valve Train (FVVT)

The investigation of a FVVT system at 2000 rpm (with variable lift and duration on the intake cam shaft) showed largest improvements on low- and high load. Of the investigated load points from 7 to 19 bar IMEP (see *Table 24*), there is no improvement in BSFC with decreased lift and duration compared to the standard intake cam. The largest improvement of the FVVT system is found at 3 bar IMEP where the difference in BSFC is 6%. At the highest investigated IMEP of 31 bar, the improvement is 3.1%.

Table 24 – BSFC and improvements for different IMEP points at 2000rpm

IMEP [bar]	3	7	11	15	19	23	27	31
Optimal BSFC [g/kWh]	387.17	-	-	-	-	244.84	245.26	250.17
Duration for optimal BSFC [g/kWh]	130	-	-	-	-	170	170	190
BSFC [g/kWh] Std. Lift and Duration (227 dur)	411.89	-	-	-	-	248.91	252.98	258.23
Improvement of BSFC [%]	6.0%	-	-	-	-	1.6%	3.1%	3.1%

In *Figure 62*, the BSFC and PMEP is plotted versus varying duration of the intake cam. *Figure 63* shows the cam phasing settings used in order to optimize the BSFC. The BSFC of the LLC's is quite similar but according to *Figure 63*, the residuals and cam phasing settings differ. For the LLC of 150 CAD, the cam phasing settings are needed to be adjusted in order to limit the residuals. The difference in BSFC between the LLC's and the HLC is mainly due to the increased pumping work which is illustrated in *Figure 62* (see the plots of the other load points in the Appendix A).

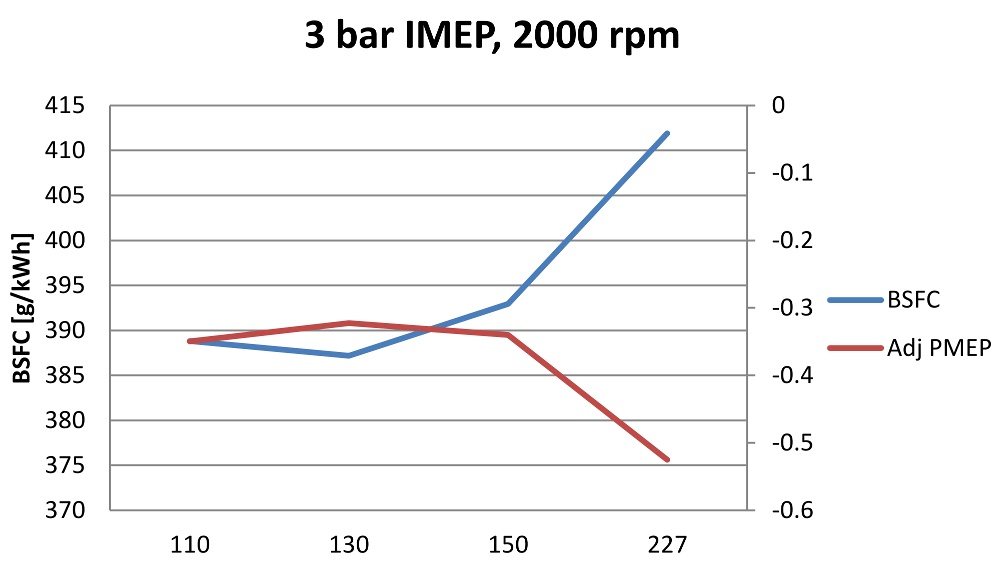

Figure 62 - BSFC and PMEP$_{adj}$ for 3bar IMEP at 2000rpm

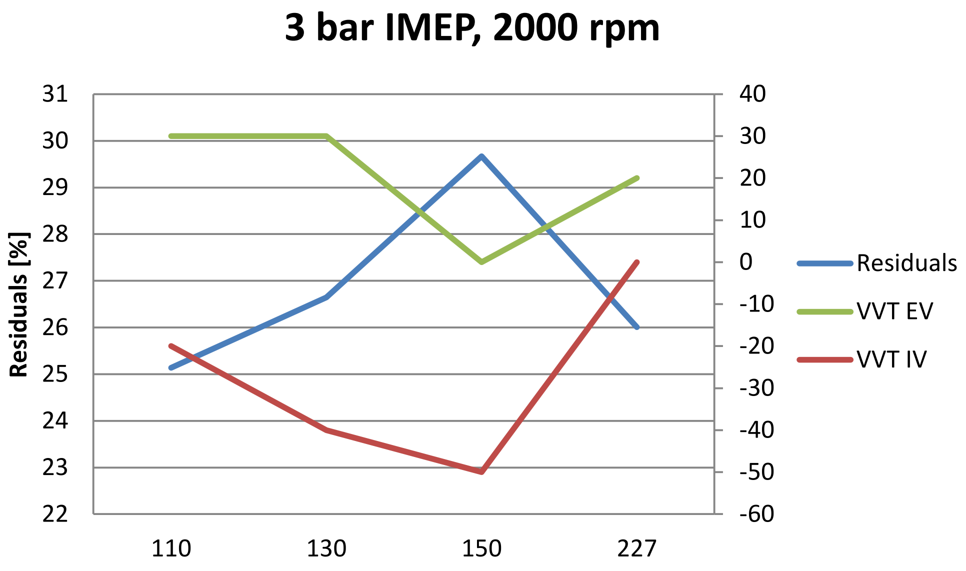

Figure 63 - Residuals and VVT settings for 3bar IMEP at 2000rpm

5.9 Part Load, 3-Cyl vs. 4-Cyl

The results from the different part load points with optimal cam phasing settings for lowest possible ISFC are seen in the *Figure 64-67*. In *Figure 64*, the increase of adjusted IMEP is shown for the 3-cylinder engine compared to the 4-cylinder benchmark engine. The resulting increase of the adjusted IMEP is related to that the BMEP is increased by 33% for the 3-cylinder engine.

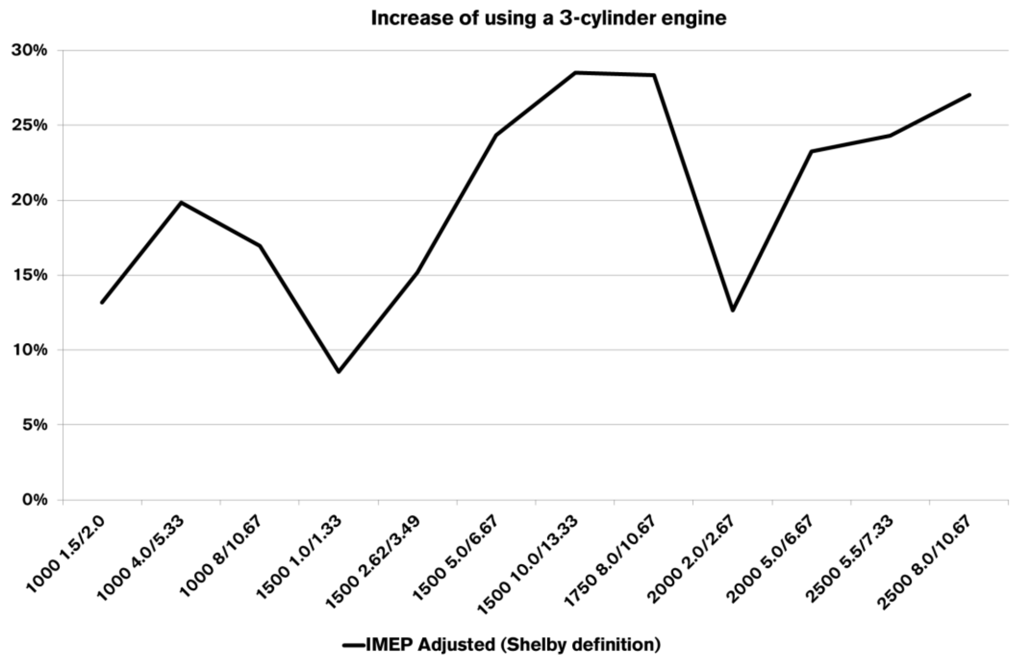

Figure 64 - Increase of $IMEP_{adj}$ at optimum VVT settings for the 3-cylinder compared to the 4-cylinder

According to *Figure 65*, the ISFC is improved for all load points with 5.2 – 14.2% where the improvements are lowest at the highest engine load on each chosen engine speed.

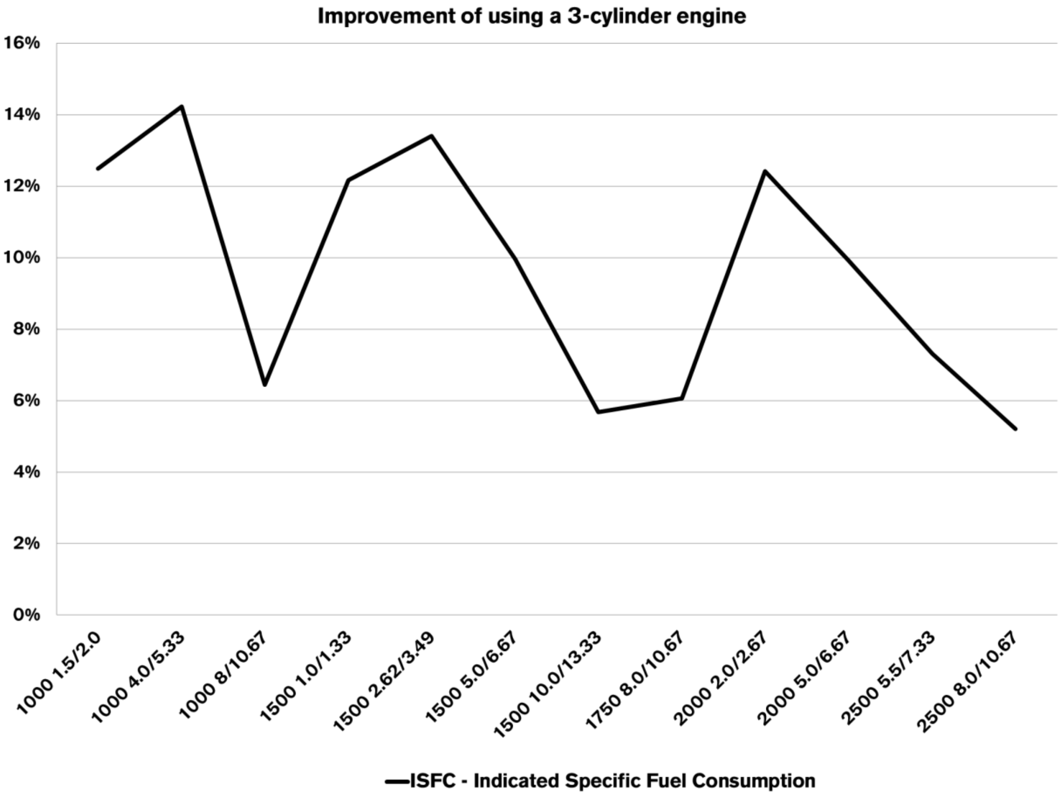

Figure 65 - Improvement in ISFC at optimum VVT settings for the 3-cylinder compared to the 4-cylinder

The improvements in adjusted PMEP are seen in *Figure 66.* The improvement at 1500rpm of 131% is a result of the positive PMEP (0.04bar) on the 3-cylinder engine compared to the 4-cylinder engine (-0.12bar) at the optimum point with respect to ISFC.

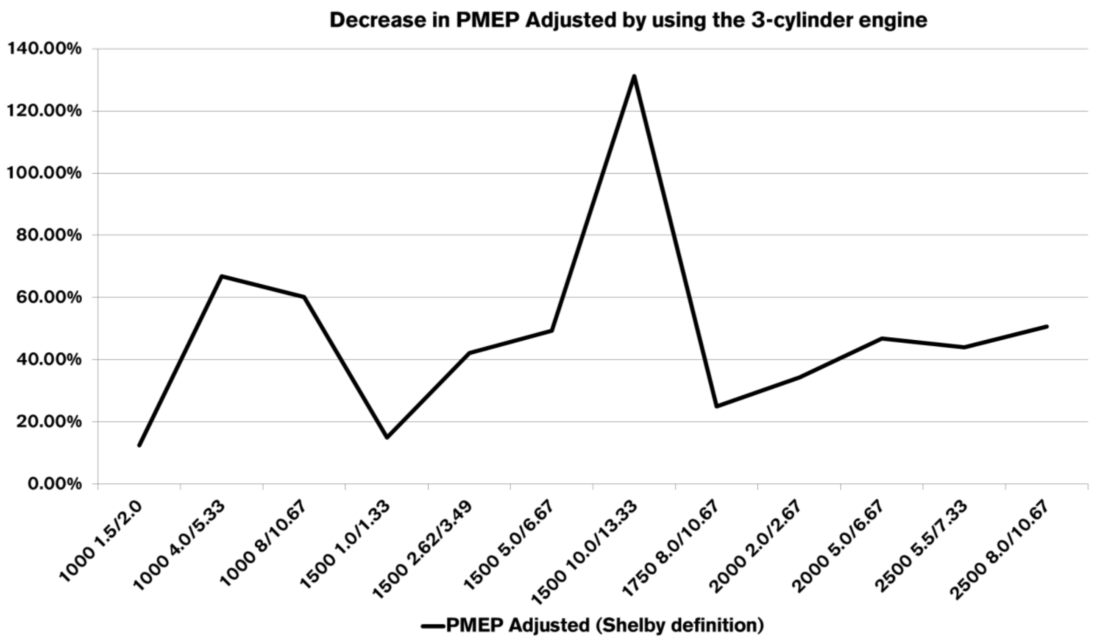

Figure 66 - Decrease in $PMEP_{adj}$ at optimum VVT settings for the 3-cylinder compared to the 4-cylinder

This result is also seen in *Figure 67* where the decrease of the Intersection Pumping Integral (Area B) is plotted for the part load points as a result of the different looks of Area B for the two engines which are seen in *Figure 68* PLP7 (1500rpm and 10.0/13.3bar).

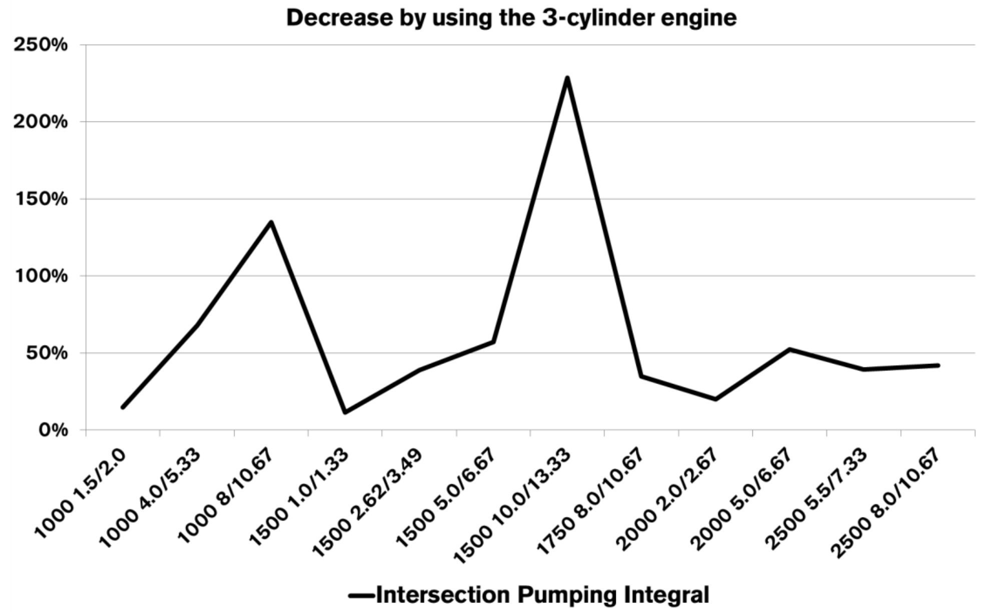

Figure 67 - Decrease of Area B at optimum VVT settings for the 3-cylinder compared to the 4-cylinder

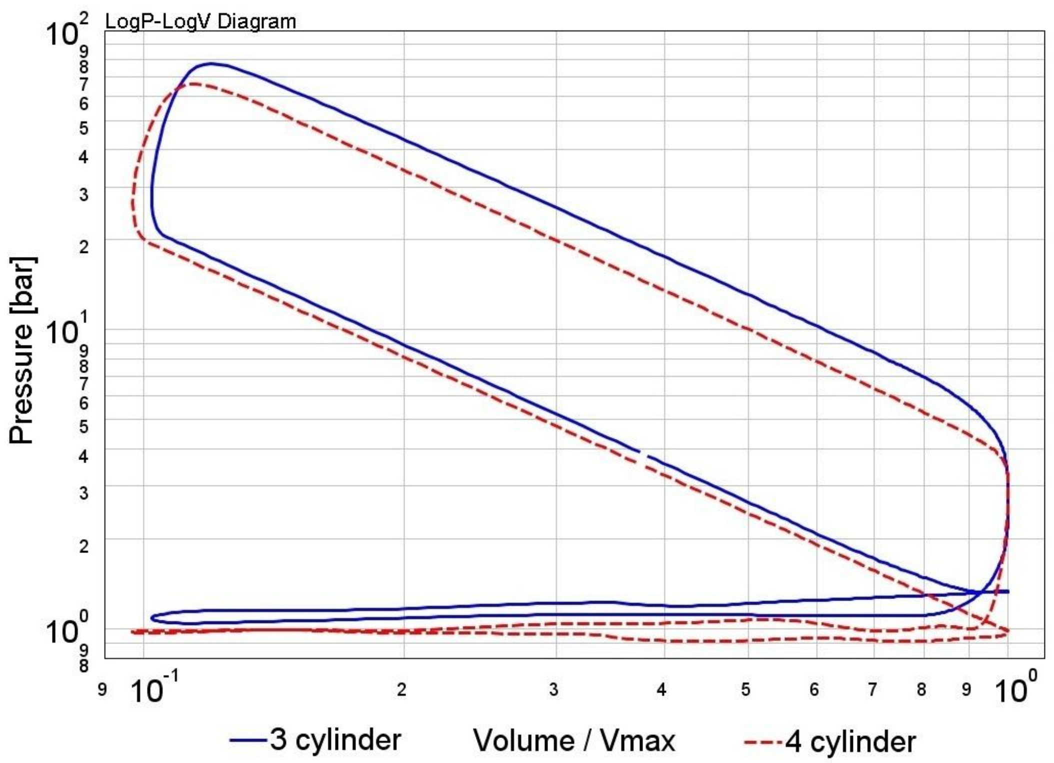

Figure 68 - Pumping loop comparison at PLP7 for the 3- and 4-cylinder engine

The results of the part load point, 3bar IMEP is seen in *Table 25*. By using the 3-cylinder concept, the BSFC and ISFC is reduced by 5.91% and 7.11% respectively and the pumping losses is reduced by 17.13%.

Table 25 - Comparison between the 3- and 4-cylinder engines at 3bar IMEP 2000rpm

3 bar IMEP at 2000rpm	Improvement of 3-Cyl vs. 4-Cyl
BSFC	5.91%
ISFC	7.11%
$PMEP_{Adj}$	17.13%
Intersection Pumping Integral	16.81%

5.10 Cylinder Deactivation

With Cylinder Deactivation (CD), the in-cylinder pressure of the 3-cylinder engine increases by around 49.5% compared with the 3-cylinder engine and around 85% compared to the 4-cylinder engine which is seen in *Table 26-29*. For the evaluated four part load points, the ISFC and adjusted PMEP are reduced by using cylinder deactivation.

For the part load point of 3bar IMEP at 2000rpm (see *Table 26*), the decrease of ISFC for the 3- and 4-cylinder engine is 17.66% and 23.52% respectively as well as a decreased adjusted PMEP of 52.86% and 60.93% respectively.

Table 26 - Cylinder Deactivation for the 3- and 4-cylinder engines at 3bar IMEP 2000rpm

3 bar IMEP @ 2000rpm	3-Cyl CD vs. 3-Cyl	3-Cyl CD vs. 4-Cyl
Orifice Diameter Output	25.02%	5.00%
ISFC	-17.66%	-23.52%
$PMEP_{Adj}$	-52.86%	-60.93%
$IMEP_{Adj}$	34.45%	32.61%
Intersection Pumping Integral	-31.54%	-43.05%

At PLP1seen in *Table 27*, the adjusted PMEP decreased by 64.88% compared with the non-deactivated 3-cylinder engine which resulted in a reduced ISFC of 20.36%. The results compared with the 4-cylinder engine are a decrease in ISFC by 30.31% and Adjusted PMEP by 69.23%.

Table 27 - Cylinder Deactivation for the 3- and 4-cylinder engines at PLP1

1.5/2.0 bar BMEP @ 1000rpm [PLP1]	3-Cyl CD vs. 3-Cyl	3-Cyl CD vs. 4-Cyl
Orifice Diameter Output	32.29%	18.57%
ISFC	-20.36%	-30.31%
$PMEP_{Adj}$	-64.88%	-69.23%
$IMEP_{Adj}$	32.89%	54.55%
Intersection Pumping Integral	-57.00%	-63.33%

The results at PLP5 are seen in *Table 28* and show a decrease in ISFC of 12.65% and 24.36% compared to the 3- and 4-cylinder engines respectively. The reduction in adjusted PMEP was 42.82% and 69.27% respectively.

Table 28 - Cylinder Deactivation for the 3- and 4-cylinder engines at PLP5

2.62/3.49 bar BMEP @ 1500rpm [PLP5]	3-Cyl CD vs. 3-Cyl	3-Cyl CD vs. 4-Cyl
Orifice Diameter Output	99.29%	87.04%
ISFC	-12.65%	-24.36%
$PMEP_{Adj}$	-46.82%	-69.27%
$IMEP_{Adj}$	40.29%	65.01%
Intersection Pumping Integral	-47.45%	-67.82%

The fourth part load point, PLP9 seen in *Table 29* shows that the ISFC is reduced by 14.26% and 24.9% respectively compared to the 3- and 4-cylinder engines. The adjusted PMEP was also decreased compared to both engines by 46.89% and 65.09% respectively.

Table 29 - Cylinder Deactivation for the 3- and 4-cylinder engines at PLP9

2.0/2.67 bar BMEP @ 2000rpm [PLP9]	3-Cyl CD vs. 3-Cyl	3-Cyl CD vs. 4-Cyl
Orifice Diameter Output	32.31%	20.41%
ISFC	-14.26%	-24.90%
$PMEP_{Adj}$	-46.89%	-65.09%
$IMEP_{Adj}$	38.79%	59.00%
Intersection Pumping Integral	42.36%	70.91%

6 Discussion

In this chapter, the results of the investigated areas in the report are discussed.

6.1 Gas Exchange benefits

The results show that the PMEP and $PMEP_{Adj}$ are almost equal at the intake cam phasing from -50 to -10, but from -10 and later cam phasing, the ICW is increased. This means that the $PMEP_{Adj}$ is a better parameter of comparison than PMEP and is therefore used when evaluating different VVT settings. This correlates with the theory written by Shelby, where later IVC causes higher ICW and hence differentiate the $PMEP_{Adj}$ with respect to PMEP.

6.2 Part Load Points

The largest improvements of fuel consumption between the 3- and 4-cylinder engines are seen at low load and engine speed. This is due to the increased load of the 3-cylinder engine to produce the same torque output. The 3-cylinder engine is therefore operated with less throttling which reduces the pumping losses, i.e. downsizing. The 25% downsizing (removing 1-cylinder from the 4-cylinder) gave an improvement of between 6-14% in ISFC which correlates with the Mahle engine concept, where a 30% engine size reduction gave a 20% improvement in fuel consumption.

6.3 Cylinder Deactivation

For the investigated load points with cylinder deactivation, which are 3bar IMEP, PLP1, PLP5 and PLP9 (see Chapter 4.9) the fuel consumption were reduced by 12-20%. This correlates with the literature.

When comparing the cylinder deactivated 3-cylinder engine with the 4-cylinder engine, the cylinder volume is reduced by 50%. This resulted in 23-30% improvement of the fuel consumption compared to the Mahle engine, which reduces the fuel consumption by 30% in the New European Driving Cycle (NEDC).

The pumping losses were also decreased with cylinder deactivation. One contribution to this is that the engine operates with less throttling due to the increased load.

6.4 Maximum Load Curve

Both turbine configurations utilises large valve overlap (scavenging) at low engine speed to increase the mass flow for the turbine, hence helping it to accelerate at lower exhaust gas flow. At higher engine speed the valve overlap is decreased, enabling maximum trapping which is needed to keep the residual gas levels down during the high flow rates associated with high engine speed. With less residuals, the maximum amount of air/fuel mixture can be used and the engine can produce more power at high engine speed.

The 50 mm turbine has less resistance since it has larger inducer/exducer diameter compared to the 45 mm turbine. This means that the same mass flow has to travel through a smaller section on the smaller turbine, resulting in a larger backpressure. With increased backpressure, the gas exchange process is harder to complete. This results in higher amount of residuals left in the cylinder, which reduces the maximum amount air/fuel mixture and results in a lower peak power.

The limitation of peak power for the 45mm turbine is the exhaust temperature which is reaches its limit when the backpressure is not limited. This results in that the fuel injectors deliver maximum allowed amount of fuel ($\lambda = 0.75$). The temperature is then reduced by decreasing the turbine speed which is controlled by the wastegate.

By using an IEM the need for injecting more fuel is reduced at peak power. The maximum elongation of these ports is 70mm without losing performance at lower engine speed. With longer ports, the torque target at 1500rpm is not met, hence limiting the possible improvements of an IEM. Since the total length of the exhaust ports are increased in order to simplify the modelling, the evaluated configuration is not a fully IEM. This could be a contributing factor to the limitation of 70mm elongation since the turbine is located 70mm further away from the engine which reduces the effect of pulse turbocharging. At higher engine speed, a longer pipe helps to reduce the temperature at the exhaust manifold where the thermocouple temperature is measured hence reducing the need for a mixture enrichment to decrease the temperatures. The results of lower levels of backpressure, boost pressure and fuel enrichment indicates that the engine could be enabled to reach a higher peak power than the limited 45mm turbine due to high backpressure without an IEM.

6.5 Time-To-Torque

The Time-To-Torque (TTT) was investigated in order to evaluate which turbine to choose to match the drivability of the 4-cylinder benchmark engine. The results showed that the 50 mm turbine did not provide the desirable engine response, but it would have been preferable to use the 50mm turbine regarding backpressure, residuals, peak power etc. The other alternative was the 45 mm turbine which showed improved engine response as expected with lower inertia. Though, in order to get the same TTT as the benchmark engine, the operating engine speed is forced to be increased by 300 rpm.

The optimal cam phasing strategy to enable the best TTT differed between the two engines. The TTT investigation of the 4-cylinder engine (performed by VCC), showed best results by starting with moderate valve overlap after engaging full throttle in order to utilize the characteristics of a naturally aspirated engine. For the 3-cylinder engine it was best to enable maximum valve overlap as soon as full throttle was requested. Though, at 2400 rpm, the best TTT response with the 45 mm turbine was to retard the intake cam phasing by 10 CAD relative the maximum valve overlap.

Further, a test was performed in order to investigate how much the inertia would have to decrease in order to match the TTT of the 4-cylinder engine at the same operating engine speed. The inertia of the 45 mm turbine was decreased with over 50% and did still not match the TTT of the 4-cylinder engine at 1000 rpm, i.e. the engine speed has to be increased for the 3-cylinder engine.

6.6 Two-Stage Valvelift vs. FVVT

In order to decrease the pumping losses during the gas-exchange process, a two-stage valve lift system was considered. The operating area of the chosen Low Lift Cam (LLC) was restricted to approximately 1800 rpm and 120 Nm in order to obtain the same volumetric efficiency when switching to the High Lift Cam (HLC). The operating area of the LLC was obtained by simulating the engine model with WOT and WOW.

Mats Morén at Volvo Cars, made an investigation of the load and engine speed required to propel a passenger car of 1590 kg in the NEDC. The investigation showed that the torque and engine speed was approximately 125 Nm and 1800 rpm during the cycle. The investigation was made for the 4-cylinder engine architecture which means that the engine speed required for the 3-cylinder concept engine would have to be 2100 rpm for the LLC due to TTT.

It is not a requirement that the two-stage valve lift system should only use the LLC during the NEDC, but the efficiency might decrease if several cam shifts during the cycle are required. This is e.g. for the deviations from the optimal cam phasing settings needed to prepare the cam shift (see Chapter 5.7.1). The operating area of the LLC could be increased regarding torque by closing the wastegate. Though, the cam phasing settings needs to be adjusted more in order to obtain the same volumetric efficiency for the cam shift, specially the exhaust cam.

The benefit of a FVVT system compared to a two stage valve lift system is that the operating area is not limited. According to the investigation of the FVVT system, it is able to reduce the fuel consumption by about 6% at 3 bar IMEP at 2000 rpm which is about 1.5% better compared to the two-stage valve lift system. With a FVVT system, the cost and complexity is increasing compared to a two-stage valve lift system that has to be compensated for a reduction in fuel consumption. How much the winning has to be in terms of fuel consumption to overcome the cost and complexity is not considered in this report.

6.7 Knock

Knock is most likely prevented by the decreased compression ratio and manually set 50% burn point. The knock probability data from the 4-cylinder benchmark engine was not used due to the high uncertainties if weather the 3-cylinder concept engine would behave likewise.

6.8 Compression ratio vs. Combustion Efficiency

The Combustion Efficiency (CE) in the engine model was set to 95% which is expected to vary with engine speed and load. The Compression Ratio (CR) was decreased after the evaluation of the knock probability data from the 4-cylinder benchmark engine. The investigation made by varying the CE and CR for the load point of 3 bar IMEP at 2000 rpm indicates the potential of improvements. The largest deviation of the results regarding fuel consumption by increased CE and CR was 3%.

6.9 Reflections on Sustainable Development

The 3-cylinder concept engine is developed to investigate if it is possible to replace a 4-cylinder engine with larger displacement, i.e. downsizing. Downsizing is an acknowledged method in the automotive industry to decrease the fuel consumption, which is a step further to sustainable development. By enable downsizing, the engine operates at higher load which is beneficial since the combustion efficiency increases with load. This result in lower specific fuel consumption, i.e. less fuel is needed to produce the same work. A downsized engine with less cylinders (or decreased displacement) also reduces overall weight. A lighter engine results in a lighter vehicle which reduces the vehicle resistance and the fuel consumption decreases. Also, a downsized engine uses less material which reduces the efforts on nature resources.

7 Conclusion

The master thesis was performed on request by Volvo Car Corporation (VCC) with focus on evaluating if a three cylinder engine could be used for a mid-high performance application. The developed concept is compared to a benchmark 4-cylinder engine provided by VCC with respect to steady state performance and fuel efficiency as well as transient response (Time-To-Torque). The model is developed, tested and evaluated using GT-Suite.

The engine concepts is developed from a 2.0liter 4-cylinder engine of which one cylinder has been removed, resulting in a 1.5liter 3-cylinder. A single-scroll turbocharger was fitted to the 3-cylinder concept of which several alternatives of turbocharger configurations were presented. A recommendation of a turbocharger was made, based on engine response, required boost pressure, backpressure, temperature and the amount of residuals at the max load curve. Due to the high specific power output (kW/l), a relatively large turbocharger was needed. In order to match the engine response of the benchmark engine with the chosen turbocharger, an alternative operating engine speed of the 3-cylinder engine is suggested.

Several technologies were investigated based on the literature study with the aim of reducing the fuel consumption and utilize synergistic effects, i.e. the investigated technologies are meant to have the possibility of being combined. Technologies that have been evaluated are different turbocharger set-ups, Fully Variable Valve Train, Two-Stage Valve Lift, Dual Individual Cam Phasing, Integrated Exhaust Manifold and Cylinder Deactivation.

8 Future Work

The GT-Power model has not been fully validated for the 3-cylinder engine concept since the load and engine speed has not been evaluated in a test-rig which is something that needs to be done in the future. A knock target table for the load and engine speed corresponding to the max load curve of the 3-cylinder concept engine is desirable. Then the compression ratio and the ignition timing could be optimized for preventing knock with higher accuracy.

The turbocharger configuration consists of a single-stage mono-scroll turbocharger which has proven to almost meet all performance targets but with some limitations. The transient response is reached with increased engine speed of 300 rpm and the peak power reaches 98% of the target with limited backpressure with the 45 mm turbine. There are more advanced and expensive turbocharging configurations which has better response with maintained peak power. A Variable Geometry Turbine (used by BMW) or a two-stage turbo system (used by Mahle) are two alternatives to reach peak power and improve the transient response, but the cost will increase. Another alternative is to use a mechanically driven compressor in combination with a turbocharger which is a more cost efficient system compared to the previous mentioned alternatives. An investigation whether it is possible to reduce the inertia of the 50 mm turbine to levels of the 45 mm turbine would be interesting since this would help meet the performance targets.

The TTT and the torque-knee are reached 300rpm later compared to the benchmarked 4-cylinder engine. The part load points are performed at the same engine speed with corresponding load. An investigation of how the increased engine speed of the 3-cylinder engine will affect the combustion and fuel consumption for the same power is of interest.

An analysis of the possibilities of using an IEM with kept total length between the exhaust valve and turbine would be interesting since the results and theory about the subject can improve the fuel consumption. Since the tests resulted in reduced back pressure and boost pressure it would be interesting to evaluate if the actual power target could bet met with the 45mm turbine with levels of back pressure below 4bar. An investigation of how the engine would operate at part load with an IEM would be interesting since the engine reaches working temperature faster as well as igniting the catalyst earlier, hence reducing more emissions.

The concept of cylinder deactivation on a 3-cylinder engine has to be studied further since balancing is an issue with this cylinder arrangement. Strategies how the cylinders could be deactivated separately in a certain pattern to limit engine vibrations is an important subject since the results on fuel consumption reductions are substantial compared to the engine running at 3- or 4-cylinders.

Regarding the two-stage valvelift system, an investigation of how large the losses are when shifting cam would be needed to take into account in order to investigate the trade of between operating area and number of cam shift for the investigated driving cycle. If the losses are large, the number of shifts during a driving cycle has to be minimised.

9 References

9.1 Written References

Becker, N. (2011), *The New 1.0-l Three-Cylinder MPI Engine for the up!*, ATZ extra, September 2011

Brüstle, C., Schwarzenthal, D. (2001) VarioCam Plus – A Highlight of the Porsche 911 Turbo Engine. SAE International

Coltman, D., Turner, J., Curtis, R., Blake, D. et al. (2009), *Project Sabre: A Close-Spaced Direct Injection 3-Cylinder Engine with Synergistic Technologies to Achieve Low CO2 Output*, SAE Int. J. Engines 1(1):129-146

Davis, M. (2013), *BMW THREE-CYLINDER*, Engine Technology International, January 2013

Flierl. R. et al (2011) *Univalve – A Fully Variable Mechanical Valve Lift System for Future Internal Combustion Engines.* ATZ-Online

Friedfeldt, R., Zenner, T., Ernst, R., Fraser, A. (2012), *Three-Cylinder Gasoline Engine With Direct Injection,* ATZ autotechnology, 02-2012, Volume 12

Heisler, H., *Vehicle and Engine Technology*, Second Edition, Butterworth-Heinemann, Oxford, UK, 1999

Heywood, J.B. (1988) *Internal Combustion Engines Fundamentals*. Singapore: McGraw-Hill.

Hiereth, H., Prenninger, P. (2007), *Charging the Internal Combustion Engine*, Springer-Verlag Wien, Austria (Translated from the German by Drexl, K.W.)

Huber, R., Klumpp, P., Ulbrich, H., (2010) *Dynamic Analysis of the Audi Valvelift System.* SAE International

Kirwan, J., Shost, M., Roth, G., Zizelman, J., (2010) *3-Cylinder Turbocharged Gasoline Direct Injection: A High Value Solution for Low CO2 and NOx Emissions*. SAE International

Korte, V., Lumsden, G., Fraser, N., Hall, J. (2010), *30 % Higher Efficiency with 50 % Less Displacement*, MTZ worldwide Edition: 2010-03, Volume 71

Kramer, U., Philips, P., (2002), *Phasing Strategy for an Engine with Twin Variable Cam Timing,* SAE Technical Paper 2002-01-1101

Kuberczyk, R., Berner, H.J., Bargende, M., (2009) *Differences in Efficiency between SI Engine and Diesel Engine,* ATZ-Online

Lefebvre, A., Guilain, S. (2005) *Modelling and Measurement of the Transient Response of a Turbocharged SI Engine*, SAE International

Leroy, T., Alix, G., Chauvin, J., Duparchy, A., et al (2008) *Modeling Fresh Air Charge and Residual Gas Fraction on a Dual Independent Variable Valve Timing SI Engine.* SAE International

Grill, M., Billinger, T., Bargende, M., (2006) *Quasi-Dimensional Modeling of Spark Ignition Engine Combustion with Variable Valve Train.* SAE International

Oswaldo M.F., (2009) *Impact of the Miller cycle in the efficiency of an FVVT*. SAE International

Research Institute of Automotive Engineering and Vehicle Engines Stuttgart (2013) *Operating instructions for the GT-Power expansion*

Robert Bosch GmbH. (2011) *Bosch Automotive Handbook* (8th edition), Cambridge: John Wiley & Sons

Schernus, C., Dieterich, C., Nebbia, C., Sehr, A. et al., *Turbocharging of Downsized Gasoline DI Engines with 2 and 3 Cylinders*, SAE Technical Paper 2011-24-0138, 2011

Shelby, M.H., Stein, R.A., Warren, C.C. (2004), *A New Analysis Method for Accurate Accounting of IC Engine Pumping Work and Indicated Work*, SAE Technical Paper 2004-01-1262

Stephenson, M., (2009), *Engine Downsizing - An Analysis Perspective*, Article for the 2009 SIMULIA Customer Conference May 18-21, 2009, London, England

9.2 Internet Sources

3K-Warner-1 (2013), Design and Function of a Turbocharger: Turbine, BorgWarner Turbo Systems, http://www.3k-warner.de/products/turbochargerTurbine.aspx [Accessed 13.02.20]

3K-Warner-2 (2013), Design and Function of a Turbocharger: Compressor, BorgWarner Turbo Systems, http://www.3k-warner.de/products/turbochargerCompressor.aspx [Accessed 13.02.20]

3K-Warner-3 (2013), Turbo Facts, BorgWarner Turbo Systems, http://www.3k-warner.de/products/default.aspx [Accessed 13.02.20]

AutoZine (2013), Engine Smoothness, AutoZine Technical School, http://www.autozine.org/technical_school/engine/smooth1.htm [Accessed 13.01.25]

Garrett-1 (2013), Turbine housing A/R and sizing, Honeywell International Inc, http://www.turbobygarrett.com/turbobygarrett/turbine_housing_AR_and_housing_sizing [Accessed 13.02.20]

Garrett-2 (2013), Surge Line, http://www.turbobygarrett.com/turbobygarrett/surge_line [Accessed 13.02.20]

Garrett-3 (2013), Wastegates http://www.turbobygarrett.com/turbobygarrett/wastegates [Accessed 13.02.20]

Green Car Congress (2012) *New Volkswagen Polo BlueGT with cylinder deactivation offers gasoline engine fuel economy of up to 52 mpg US*. Available at Internet: http://www.greencarcongress.com/2012/03/new-volkswagen-polo-bluegt-with-cylinder-deactivation-offers-gasoline-engine-fuel-economy-of-up-to-5.html [Accessed 2013-01-25]

Knowling, M., (2005), *Mountain of MIVECs*, AutoSpeed, Available at Internet: http://autospeed.com.au/cms/article.html?&A=2651 [Accessed 2013-01-25]

Mahle (2012), *Downsizing*, MAHLE Powertrain, Available at Internet: http://www.mahle-powertrain.com/MAHLE_Powertrain/en/Engineering/Gasoline-Systems/Downsizing [Accessed 13.05.29]

Mechadyne (2012), *Intake Valve Closing Strategies*, Available at Internet: http://www.mechadyne-int.com/vva-reference/intake-valve-closing-strategies [Accessed 13.02.20]

9.3 Pictures

[Figure 1] AutoZine (2013), Engine Smoothness, AutoZine Technical School, http://www.autozine.org/technical_school/engine/smooth1.htm (2013-01-25)

[Figure 2] Garrett-4 (2013), Honeywell International Inc, http://www.turbobygarrett.com/turbobygarrett/basic

[Figure 3] Garrett-1 (2013), Turbine housing A/R and sizing, Honeywell International Inc, http://www.turbobygarrett.com/turbobygarrett/turbine_housing_AR_and_housing_sizing [Accessed 13.02.20]

[Figure 4] 3K-Warner-1 (2013), Design and Function of a Turbocharger: Turbine, BorgWarner Turbo Systems, http://www.3k-warner.de/products/turbochargerTurbine.aspx [Accessed 13.02.20]

[Figure 5, 6, 7] Hiereth, H., Prenninger, P., *Charging the Internal Combustion Engine*, Springer-Verlag Wien, Austria, 2007 (Translated from the German by Drexl, K.W.)

[Figure 8] Kuberczyk, R., Berner, H.J., Bargende, M., (2009) *Differences in Efficiency between SI Engine and Diesel Engine.* ATZ-Online

[Figure 9] Mechadyne (2012), *Intake Valve Closing Strategies*, Available at Internet: http://www.mechadyne-int.com/vva-reference/intake-valve-closing-strategies [Accessed 13.02.20]

[Figure 10, 11, 12] Shelby, M.H., Stein, R.A., Warren, C.C. (2004), *A New Analysis Method for Accurate Accounting of IC Engine Pumping Work and Indicated Work*, SAE Technical Paper 2004-01-1262

[Figure 13, 14] Kramer, U., Philips, P., (2002), *Phasing Strategy for an Engine with Twin Variable Cam Timing*, SAE Technical Paper 2002-01-1101

[Figure 15] Flierl. R. et al (2011) *Univalve – A Fully Variable Mechanical Valve Lift System for Future Internal Combustion Engines.* ATZ-Online

[Figure 16] Lefebvre, A., Guilain, S. (2005) *Modelling and Measurement of the Transient Response of a Turbocharged SI Engine,* SAE International

10 Appendix A - Plots of Different Load Points for FVVT

The plots below shows the BSFC, pumping work, the amount of residuals and the optimal cam phasing settings to obtain the optimal BSFC of each evaluated cam duration.

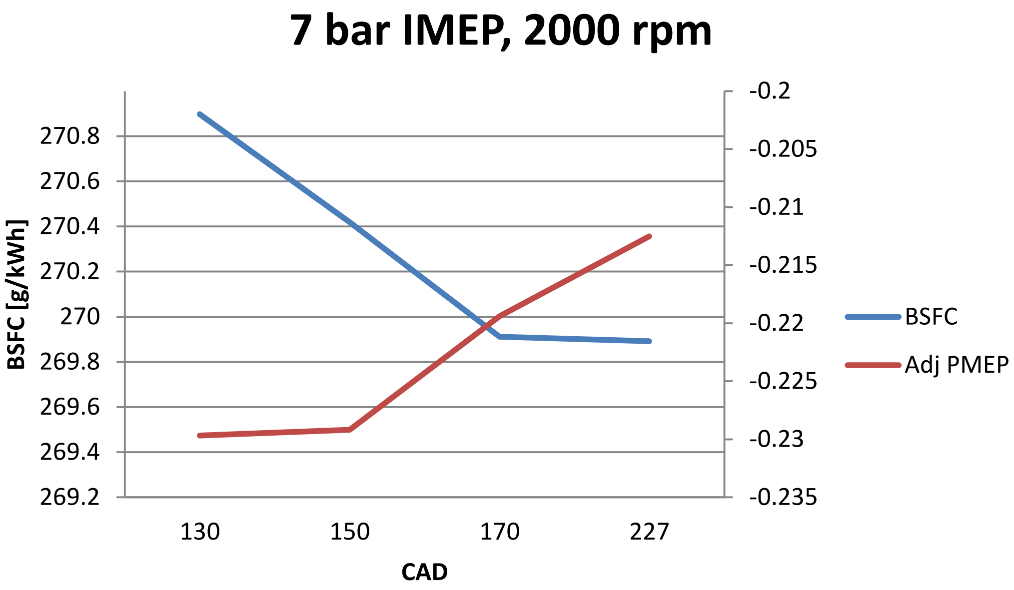

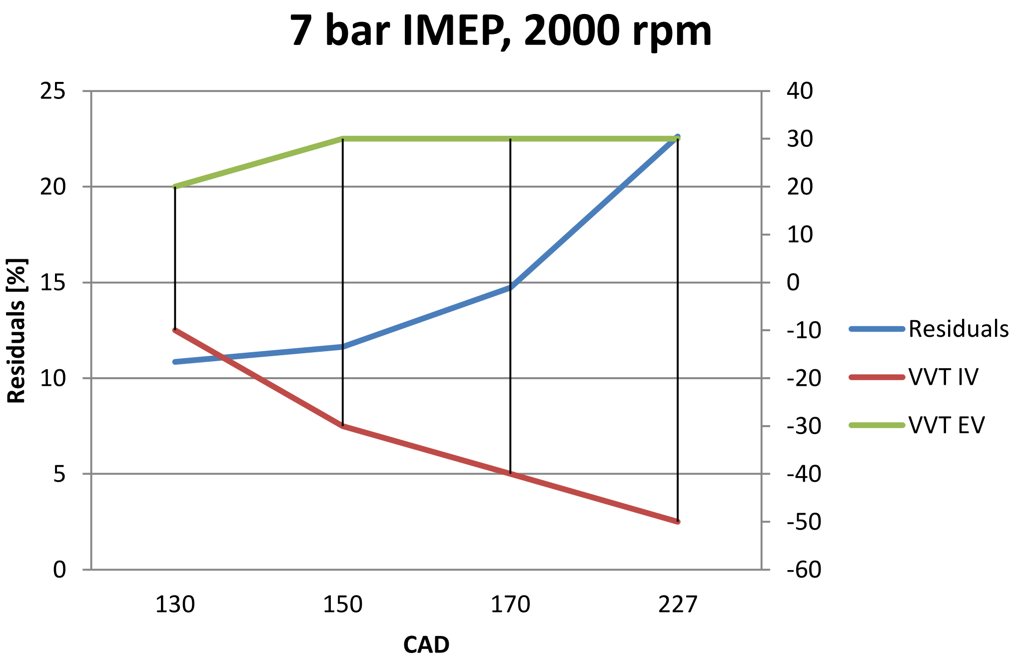

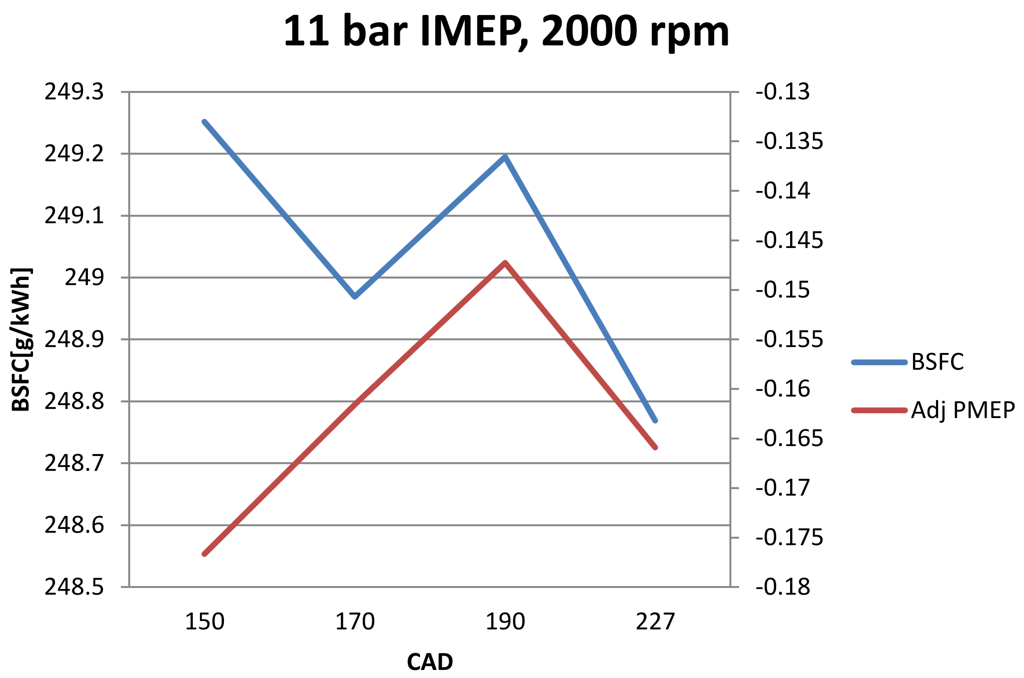

11 bar IMEP, 2000 rpm
249.3
249.2
249.1
249
248.9
248.8
248.7
248.6
248.5
BSFC[g/kWh]
-0.13
-0.135
-0.14
-0.145
-0.15
-0.155
-0.16
-0.165
-0.17
-0.175
-0.18
150
170
190
227
CAD
BSFC
Adj PMEP

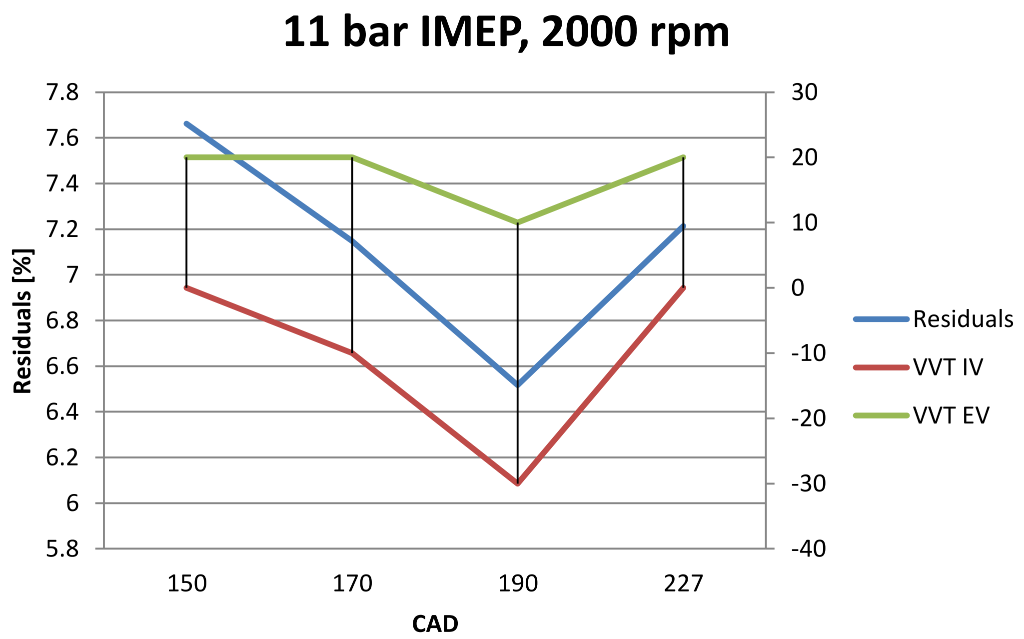

11 bar IMEP, 2000 rpm
7.8
7.6
7.4
7.2
7
6.8
6.6
6.4
6.2
6
5.8
Residuals [%]
30
20
10
0
-10
-20
-30
-40
150
170
190
227
CAD
Residuals
VVT IV
VVT EV

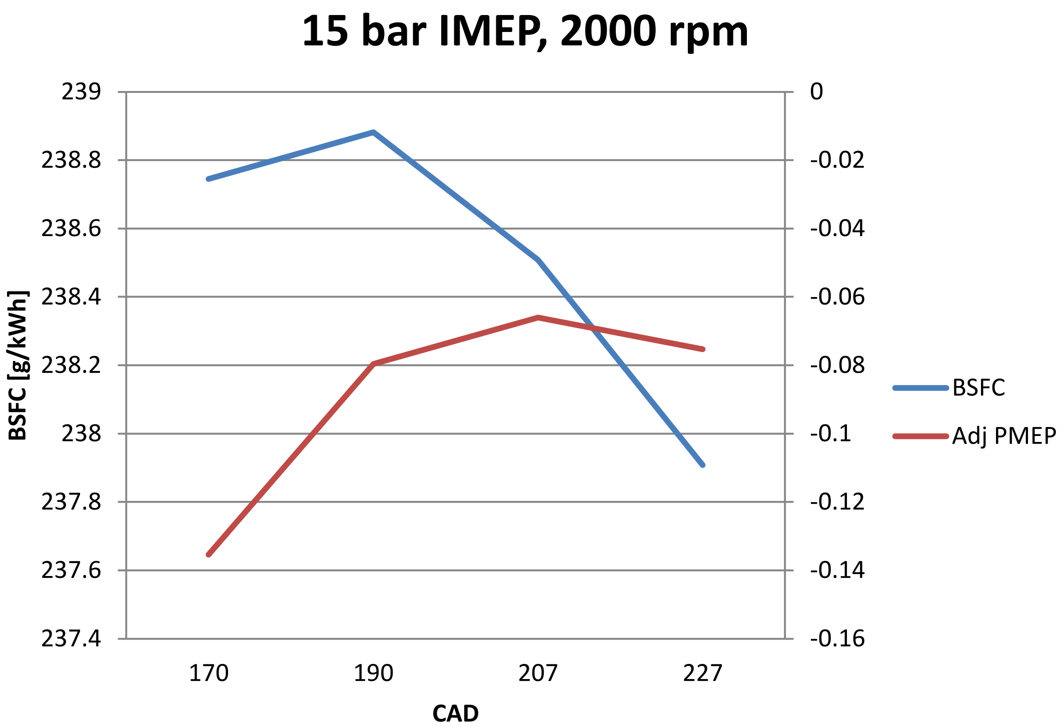
15 bar IMEP, 2000 rpm
239
238.8
238.6
238.4
238.2
238
237.8
237.6
237.4
0
-0.02
-0.04
-0.06
-0.08
-0.1
-0.12
-0.14
-0.16
BSFC [g/kWh]
170
190
207
227
CAD
BSFC
Adj PMEP

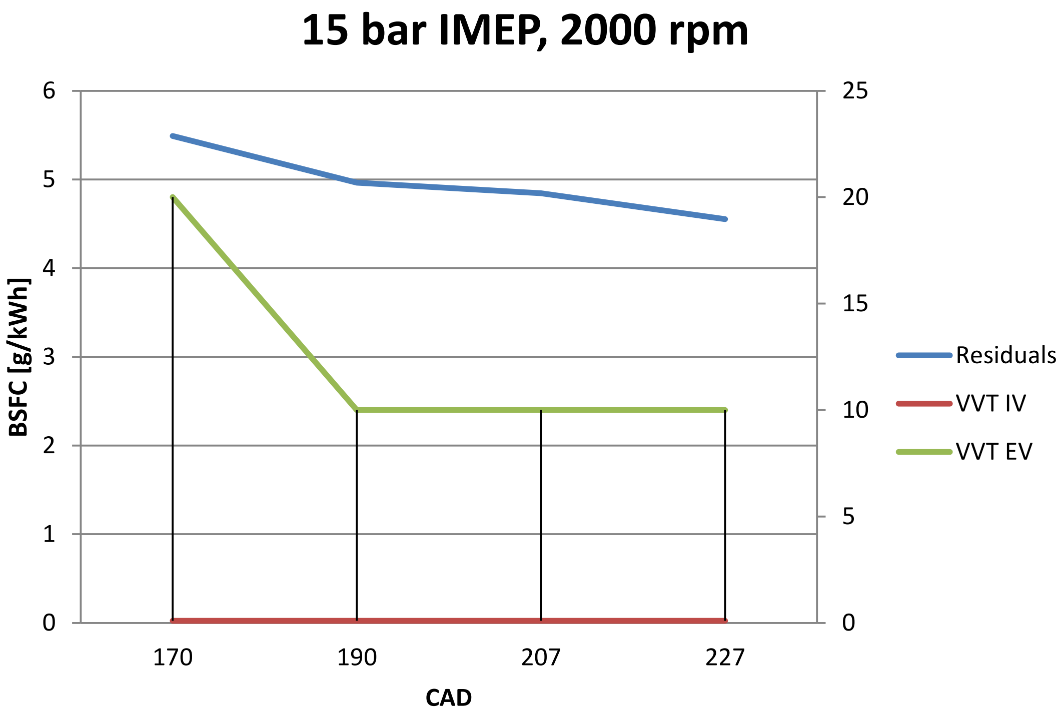
15 bar IMEP, 2000 rpm
6
5
4
3
2
1
0
25
20
15
10
5
0
BSFC [g/kWh]
170
190
207
227
CAD
Residuals
VVT IV
VVT EV

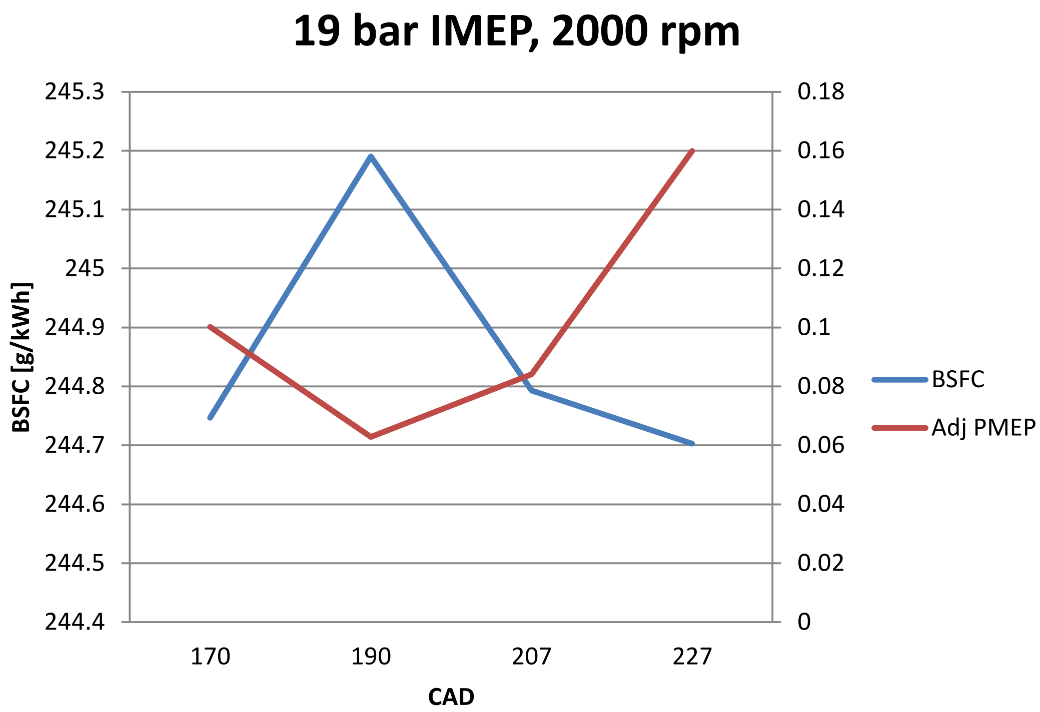
19 bar IMEP, 2000 rpm
245.3
245.2
245.1
245
244.9
244.8
244.7
244.6
244.5
244.4
BSFC [g/kWh]
0.18
0.16
0.14
0.12
0.1
0.08
0.06
0.04
0.02
0
170
190
207
227
CAD
BSFC
Adj PMEP

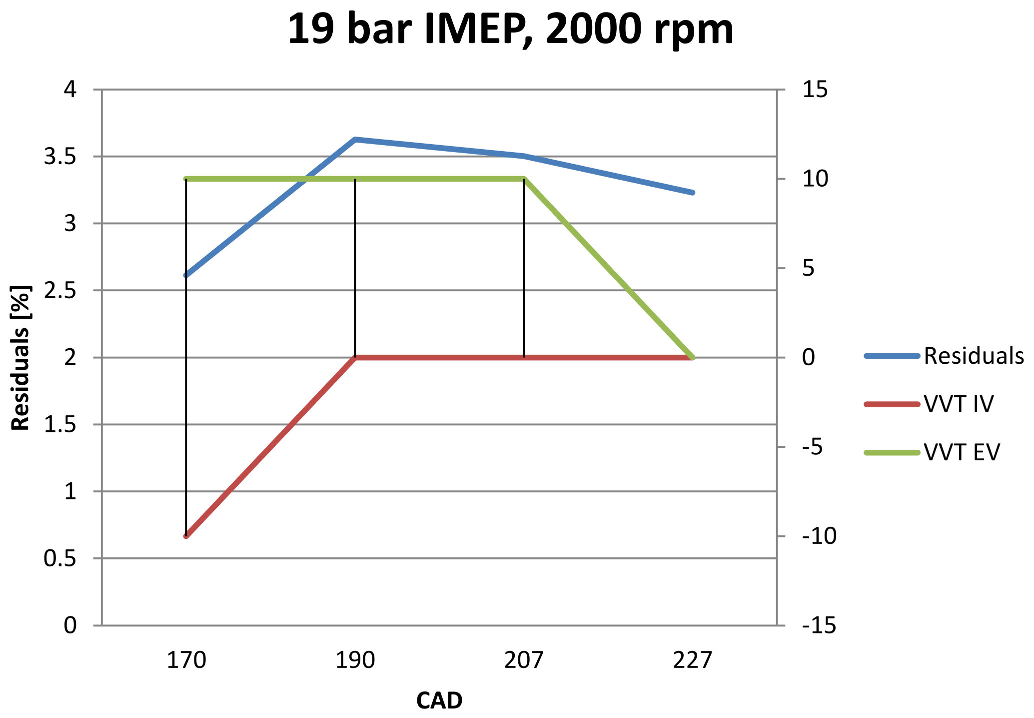
19 bar IMEP, 2000 rpm
4
3.5
3
2.5
2
1.5
1
0.5
0
Residuals [%]
15
10
5
0
-5
-10
-15
170
190
207
227
CAD
Residuals
VVT IV
VVT EV

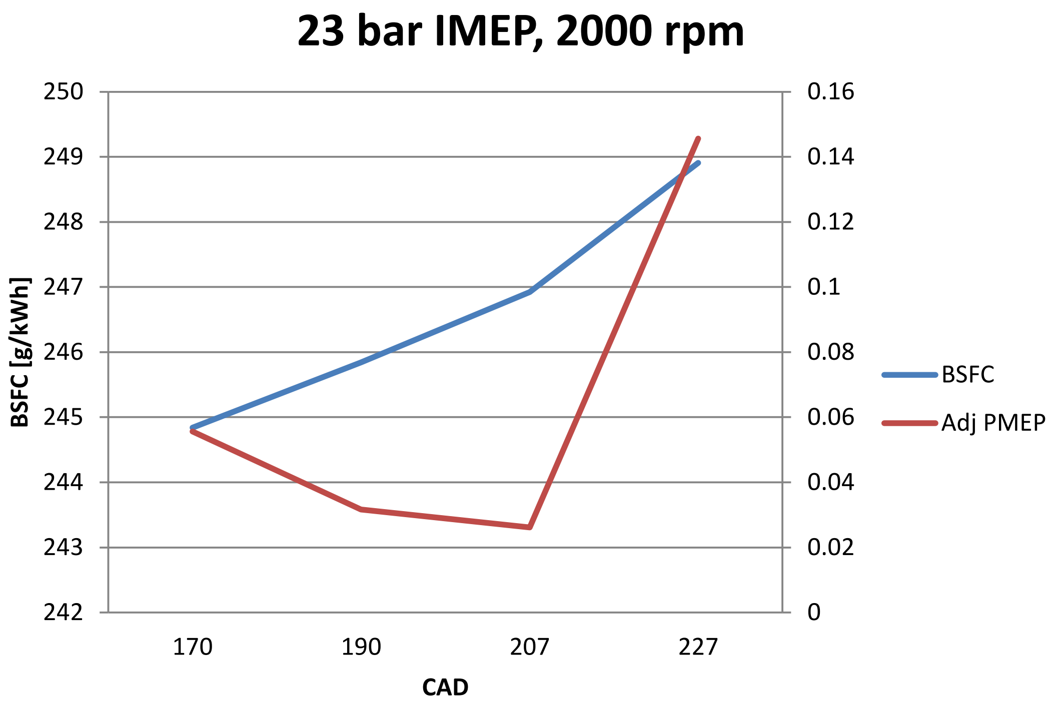
23 bar IMEP, 2000 rpm
BSFC [g/kWh]
250
249
248
247
246
245
244
243
242
0.16
0.14
0.12
0.1
0.08
0.06
0.04
0.02
0
170
190
207
227
CAD
BSFC
Adj PMEP

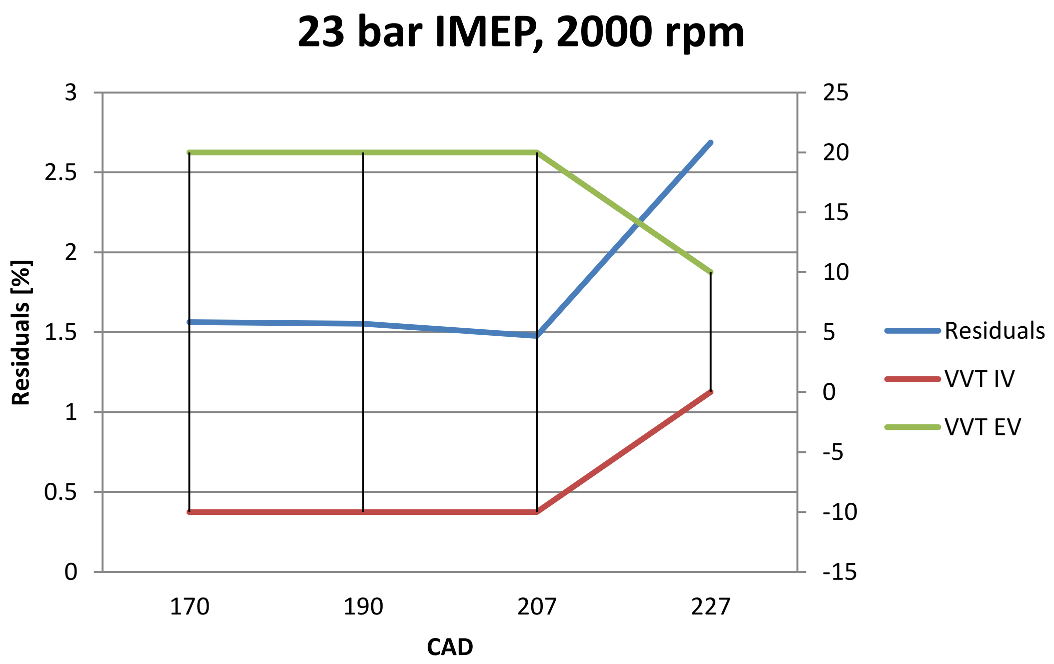
23 bar IMEP, 2000 rpm
Residuals [%]
3
2.5
2
1.5
1
0.5
0
25
20
15
10
5
0
-5
-10
-15
170
190
207
227
CAD
Residuals
VVT IV
VVT EV

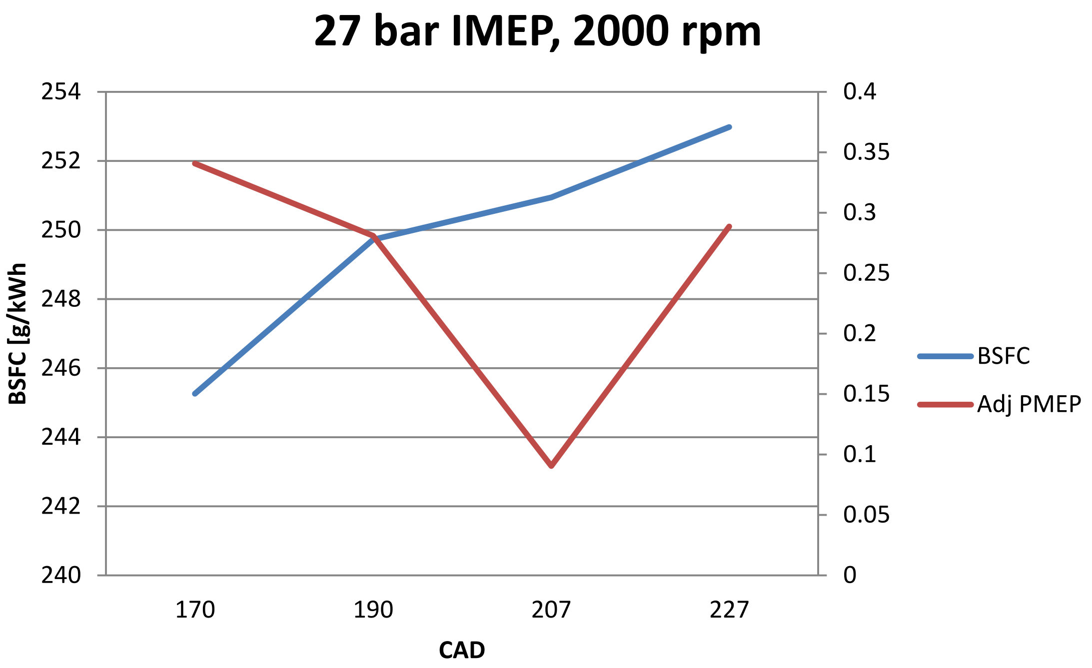
27 bar IMEP, 2000 rpm
254
252
250
248
246
244
242
240
0.4
0.35
0.3
0.25
0.2
0.15
0.1
0.05
0
170
190
207
227
CAD
BSFC [g/kWh
BSFC
Adj PMEP

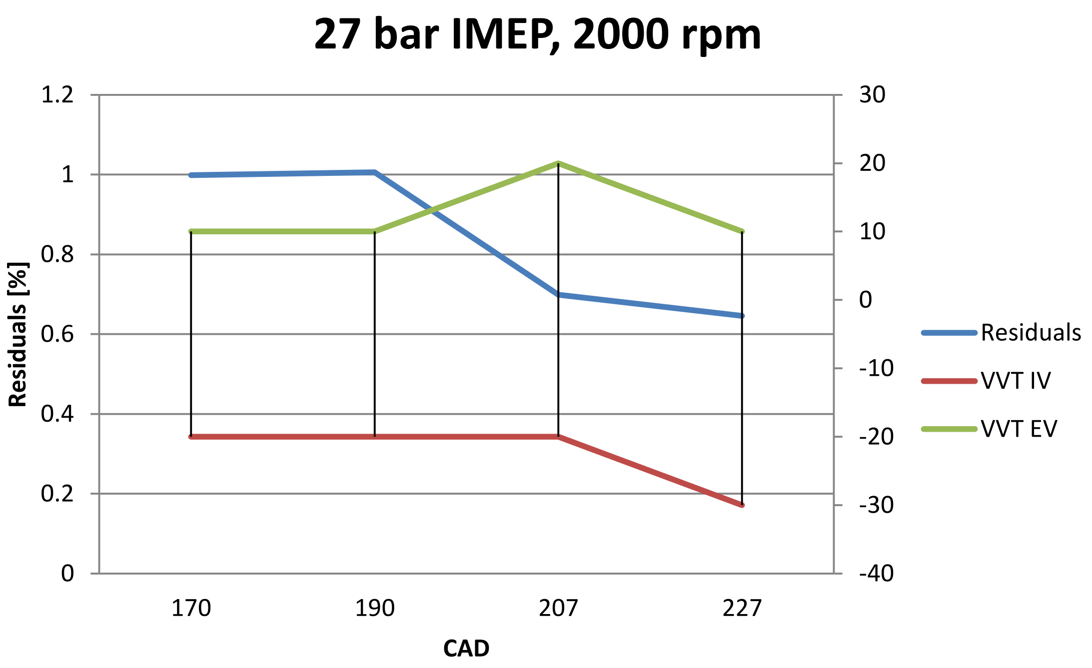
27 bar IMEP, 2000 rpm
1.2
1
0.8
0.6
0.4
0.2
0
30
20
10
0
-10
-20
-30
-40
170
190
207
227
CAD
Residuals [%]
Residuals
VVT IV
VVT EV

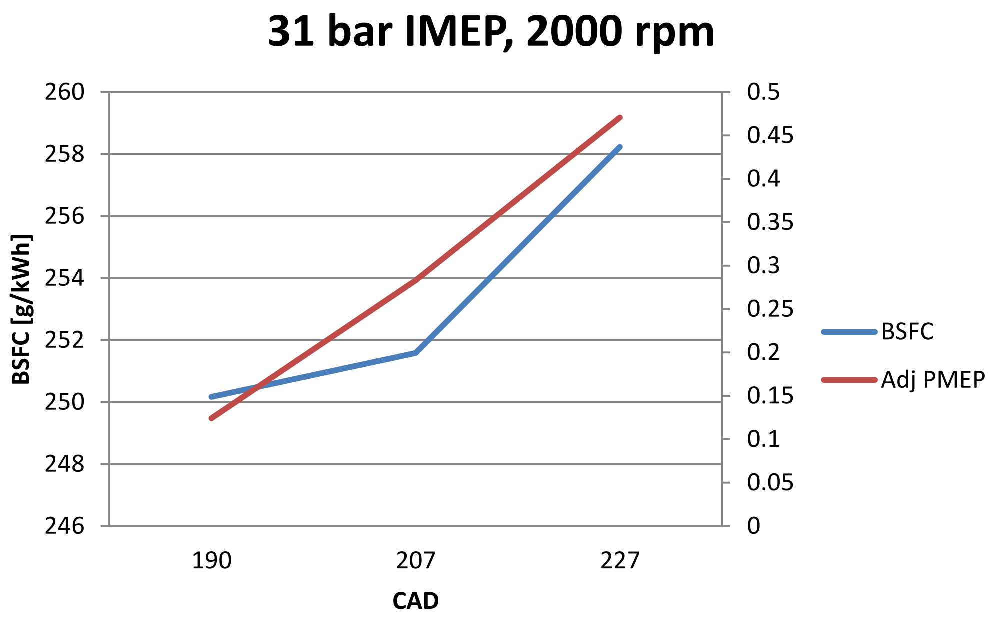
31 bar IMEP, 2000 rpm
BSFC [g/kWh]
260
258
256
254
252
250
248
246
0.5
0.45
0.4
0.35
0.3
0.25
0.2
0.15
0.1
0.05
0
190
207
227
CAD
BSFC
Adj PMEP

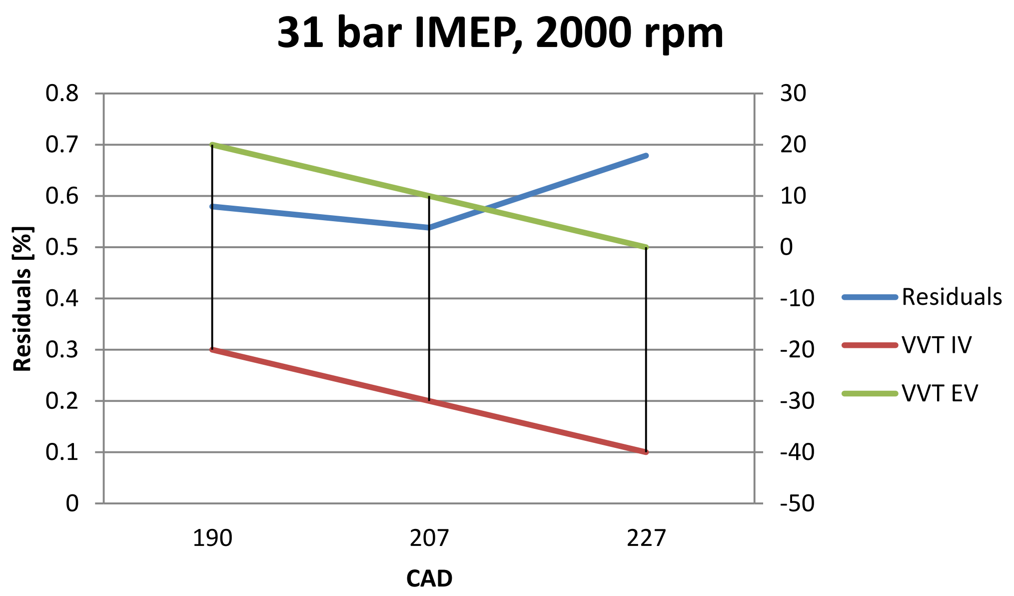
31 bar IMEP, 2000 rpm
Residuals [%]
0.8
0.7
0.6
0.5
0.4
0.3
0.2
0.1
0
30
20
10
0
-10
-20
-30
-40
-50
190
207
227
CAD
Residuals
VVT IV
VVT EV